RadCom plus

RADIO SOCIETY OF GREAT BRITAIN
ADVANCING AMATEUR RADIO SINCE 1913

May 2015
Volume 01 ◆ Number 01 ◆ £4.95

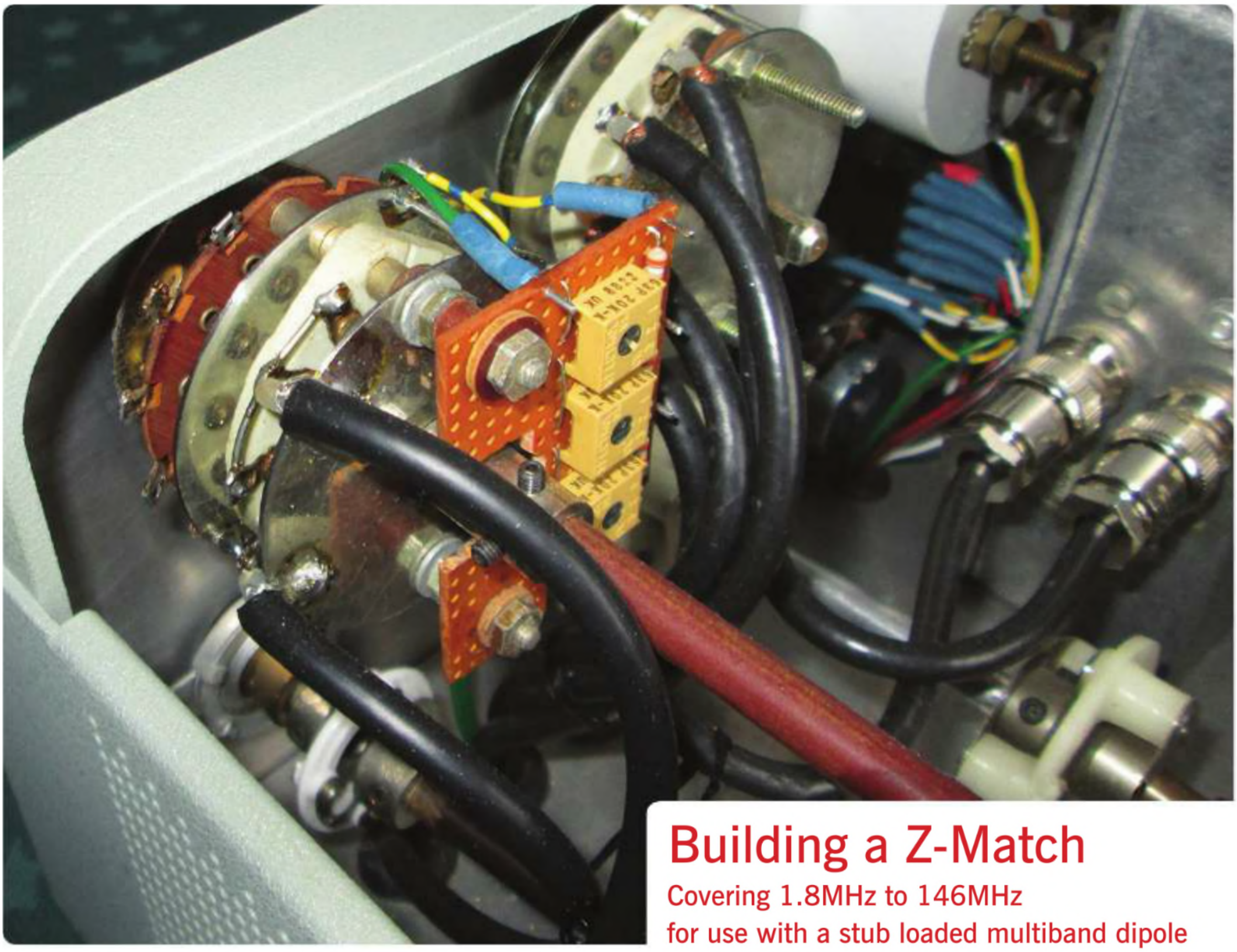

Building a Z-Match

Covering 1.8MHz to 146MHz
for use with a stub loaded multiband dipole

The DG8 preamplifier

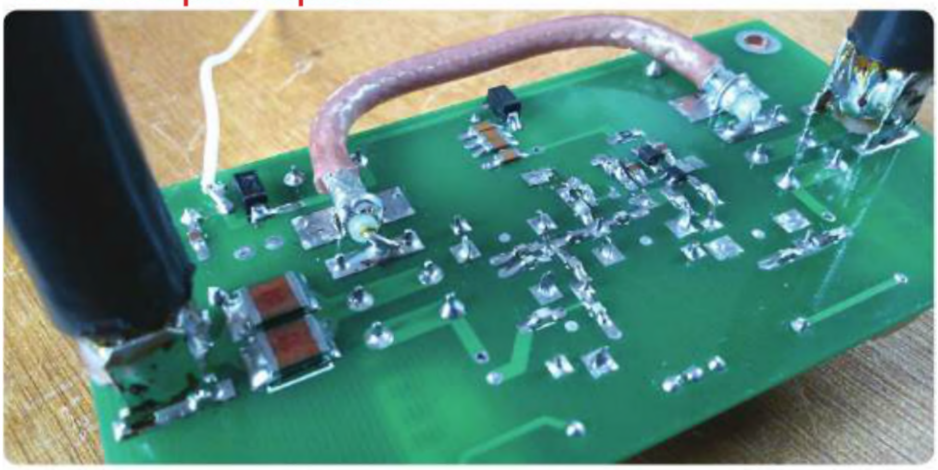

A low-cost, high performance masthead preamp for 2m with integral T/R switching

A look at chokes

High performance common-mode chokes

FROM P&P FREE OVER £30

E&OE **All prices shown plus p&p**

Novel Antennas

Compiled and edited by Steve Telenius-Lowe, PJ4DX

Radio Amateurs to one extent or another all experiment with antennas to get the best performance they can. But few have ever considered anything beyond the basic antenna designs – this book tries to set that right with a myriad of 'novel' antenna designs from around the world.

What is a 'novel' antenna anyway? This book does **not** include designs for standard Yagis, quads, quarter-wave verticals, horizontal loops, delta loops, magnetic loops, off-centre-fed dipoles or any of the more standard antenna designs that are found elsewhere. Although you won't find a standard dipole in this book, you will find the choke dipole; magnetic loops tuned by a variable inductance or a novel home-made capacitor rather than the usual vacuum variable; the 'Super Moxon', which adds a pair of directors to the standard Moxon Rectangle design; an orthoganally steered receive antenna that provides incredible levels of rejection of interfering signals; the home-made 'Wonder Whip' for QRP portable operation; a mobile antenna that can double as a car roof rack and, yes, the original Spiderbeam construction project described by its designer. Probably the most novel antenna in *Novel Antennas* is the 'PICaYAGI' by Peter Rhodes, G3XJP. This is a major constructional project in which the physical length of the elements are automatically adjusted to provide not just monoband but mono-frequency performance. Originally published in the Radio Society of Great Britain's journal *RadCom* this is the first time it has appeared in print, in full.

Novel Antennas ensures novel commercially made antennas are not excluded either, and independent reviews can be found of the unusual-looking Bilal Isotron antennas; the OptiBeam OBW10-5, which combines a five-element driver cell with both Moxon and Yagi-type elements in a novel hybrid design; InnovAntennas' new Opposing Phase Driven Element System ('OP-DES') and Loop Fed Array (LFA) designs, and several others.

With material included from no less than 57 different authors it shows the ingenuity of radio amateurs around the world knows no bounds. With designs from the UK, USA, Canada, France, Germany, Italy, Sweden and even El Salvador there will be something of interest to all antenna experimenters.

Size: 174x240, 192 pages,
ISBN: 9781 9101 9310 5
Non Members' Price: £14.99
RSGB Members' Price: £12.74

Contents

RadCom plus

THE RADIO SOCIETY OF GREAT BRITAIN'S MEMBERS' MAGAZINE

MANAGING EDITOR:
Elaine Richards, G4LFM
E-mail elaine.richards@rsgb.org.uk

TECHNICAL EDITOR:
Giles Read, G1MFG
E-mail giles.read@rsgb.org.uk

All contributions and correspondence concerning the content of *RadCom Plus* should be sent to: The Editor, *RadCom*, 3 Abbey Court, Fraser Road, Priory Business Park, Bedford MK44 3WH Telephone 01234 832 700 Facsimile 01234 831 496 E-mail radcom@rsgb.org.uk

Notices to readers concerning errors and omissions and advertisments can be found at www.rsgb.org/radcomplus

RadCom Plus is published by the Radio Society of Great Britain as an addition to its official journal, *RadCom*, and is avaiable free to all Members of the Society via the RSGB website at www.rsgb.org

All material in *RadCom Plus* is subject to editing for length, clarity, style, punctuation, grammar, legality and taste. No responsibility can be assumed for the return of unsolicited material (if in doubt, call us first!)

Technical Features

Cover image: The Dual Z-match for 1.8 to 146MHz

Photo courtesy of Bob, G3OOU

Welcome

to the inaugural edition of *RadCom Plus*!

I have been Chairman of the RSGB Board for two years and when talking to people at clubs, rallies, on the telephone and other face to face opportunities I have been hearing a consistent message. 25% of members believe that *RadCom* is too technical, 50% think it is about right and 25% think it is not technical enough. Other members of the Board have been told the same.

Two years ago the Society launched the Newcomers' Newsletter (soon to be renamed *RadCom Basics*) to address the concern that *RadCom* is too technical. Today we have launched *RadCom Plus* which addresses the opposite view. *RadCom Plus* will be available only in electronic form and will be free to all RSGB Members via the RSGB website. If you wish to receive an email reminder of when future editions are published, please sign up by logging into the RSGB website, www.rsgb.org

This magazine is for RSGB Members only and is being funded from Members' subscriptions. You can print out articles but we ask you not to forward electronic copies to non-Members. If others ask you for a copy then please encourage them to join the Society – this will mean that there is one less excuse not to do so!

A number of people have been key to making this happen – in particular, our thanks to Phillip Brooks, G4NZQ, for his initial work and Ian White, GM3SEK, who has, over the last six months, guided this project and approached potential contributors personally. Thanks also to Elaine Richards, G4LFM and Giles Read, G1MFG who have taken *RadCom Plus* into the wider *RadCom* 'stable' and will be responsible for the regular production of the publication.

As ever, we are reliant on content and we know there are plenty of people out there who are more than capable of producing excellent quality articles of the appropriate technical standard. If you feel that you have an article that you would like to see in print then don't worry too much about getting the presentation 'spot on' as the editorial team will help you – better that the frontiers are stretched rather than something is not published! We are aiming to make *RadCom Plus* the best and most technically advanced e-magazine in the world for radio amateurs.

We are targeting three or four copies a year but the frequency is dependent on YOU – send in the articles and embarrass the editorial team with quantity!

Graham Murchie, G4FSG
RSGB Board Chairman

Ian White, GM3SEK • gm3sek@ifwtech.co.uk

The DG8

A low-cost, high-performance masthead preamp for 2m

A masthead preamplifier is the greatest single improvement you can make to your receiving performance for VHF/UHF DX and contesting. But the preamp MUST be at the masthead for optimum performance, and unfortunately many preamp designs leave the user to provide the necessary RF switching and weatherproofing. As a result, the preamp tends to remain in the shack where it cannot deliver the optimum performance. Meanwhile, many commercial masthead preamps seem expensive for what you get, and the weatherproofing still leaves much to be desired.

The DG8 Masthead Preamp for 2m is designed specifically for outdoor use, close to the antenna. The integrated single-board design avoids the expense of coaxial relays without any significant impact on performance (see later). The weatherproof packaging uses simple low-cost plastic enclosures and waterproof cable glands. As well as coping with the weather on the West Coast of Scotland, this method of construction offers better RF performance by eliminating unnecessary connectors.

The complete DG8 design is the fusion of three different strands of ideas which the rest of this article will explore in more detail.

(1) The heart of the DG8 preamp is the 144-147MHz RF front end from the highly successful Anglian transverter by G4DDK, G4SWX and G7OCD (and this part of the circuit is, of course, being used with their kind permission **[1]**). The Anglian RF front end begins with a simple bandpass input filter that protects against all but the strongest signals in the FM and TV broadcast bands. The RF amplifier device is a SPF5043, chosen for its low noise figure (0.8dB), gain of 22dB and very good strong signal handling. That is followed by a much narrower 3-pole bandpass filter covering 144-147MHz. I also added a variable attenuator, so that each individual user can optimise the preamp gain for the best overall system performance.

(2) A masthead preamplifier also requires RF input and output switching, capable of handling several hundred watts on transmit but also providing low losses and good RF isolation on receive. But a low-cost masthead preamp doesn't use expensive coaxial relays when they aren't actually necessary. With careful design and the use of VHF stripline techniques, compact PCB-mounted mains power relays can handle high RF power at 144MHz with low loss and low VSWR. These power relays are backed up by miniature SMD relays for improved RF isolation. The use of PCB-mounted relays for high power RF switching was pioneered by Chris Bartram, GW4DGU in his muTek designs. This work was carried forward more recently by Gyula Nagy, HA8ET, who identified relays that can handle at least the German power limit of 750W **[2]**, and many thousands of similar relays have proved themselves capable of carrying 1.5kW at HF with excellent reliability.

The only minor problem is that the large contacts and close spacing provide relatively poor isolation to the open-circuit port, especially at VHF. HA8ET solved that problem by using compact SMD relays at the input and output of the receiving preamp to provide the additional isolation, and that idea has also worked very well here.

(3) To all this, I added my own experience about performance priorities and the overall system design **[3, 4]** along with some proven techniques for low-cost, lightweight and thoroughly weatherproof packaging.

This article takes a 'top-down' design approach. First we are going to identify everything that the preamp will need to accomplish. Then we'll set about designing and building it.

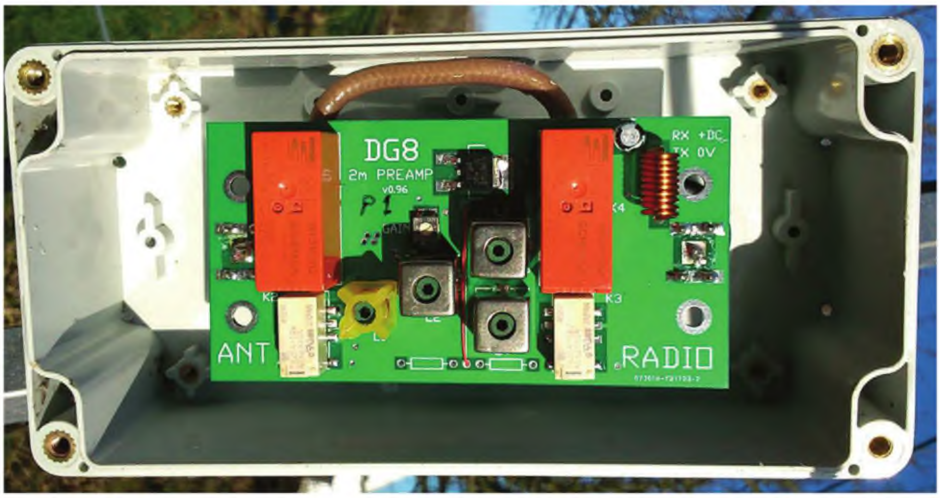

PHOTO 1: The completed DG8 preamplifier is a very neat construction.

TABLE 1: Performance data for the DG8 2m preamp.

Frequency range	144–147MHz
Noise figure	1.2-1.3dB typical (including relay losses)
Gain	adjustable, 18dB to 11dB
Tx power handling	500–750W (full carrier, JT65 Tx cycle)
Tx VSWR	<1.1

PERFORMANCE PRIORITIES. The first priority for VHF/UHF DXers and contesters is to be able to copy weak signals. That requires a low noise figure (NF) for the receiving system as a whole. But we also need to maintain that good weak-signal performance when extremely strong local signals appear on the band.

There is always some conflict between those two performance priorities – as we shall see, preamplifier gain can be both your best friend and your worst enemy. An optimised receiving system design will always need to find the best balance.

Our ability to copy a weak signal is measured by its signal-to-noise ratio (SNR). For any given signal level, the SNR will be determined by the competing level of noise, which is the sum of two separate components: the internal noise generated within the receiver itself, plus external background noise picked up by the antenna. If we aim for the receiver's internal noise level to be the same as the minimum likely level of external noise at a quiet site, then the receiver will be about as sensitive as it needs to be for terrestrial DXing and contesting. There is no point in striving to reduce receiver noise much further because (a) the SNR will still be limited by external noise, and (b) the strong-signal handling will rapidly become worse.

For the 2m band, a NF of around 2dB is well established as a good design target for the receiving system as a whole [3, 4]. Relatively few people except moonbounce and satellite operators can make practical use of a NF lower than this; many urban dwellers may find 2dB is lower than they need.

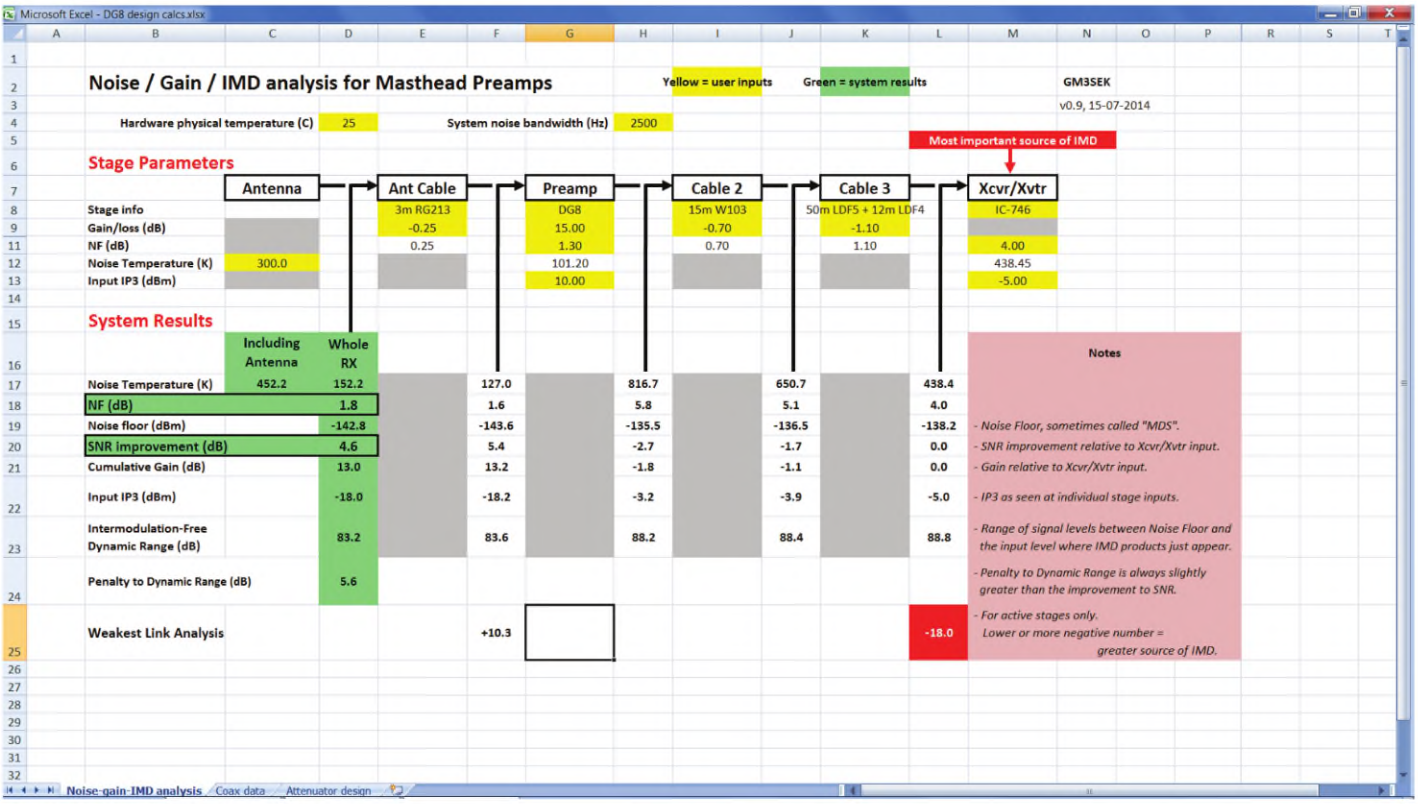

FIGURE 1: Spreadsheet to calculate receiving system NF and strong-signal performance. For more detail, zoom into this PDF image and/or download the Excel spreadsheet from www.ifwtech.co.uk/g3sek/vhfdx/dg8-design-calcs.xls.

To achieve the goal of 2dB for the complete receiving system, the NF of the preamplifier will need to be lower than 2dB; and the NF of the RF amplifier device inside the preamp will need to be lower still. With that in mind, the DG8 preamp uses an SPF5043 RF amplifier device with a NF of 0.8dB, giving a NF of about 1.2-1.3dB for the complete preamp (including the RF switching relays). The gain is adjustable between about 11dB and 18dB, which will be enough to meet the target of a 2dB NF for the complete receiving system.

But meanwhile, don't forget our other major priority: to be able to copy weak signals without overloading by strong signals. The main causes of receiver overload are:

- **Third-order intermodulation** – spurious signals generated within the receiver caused by two strong signals that are not on the receiving frequency. Typically these strong signals would be either inside the 2m amateur band or just outside the band. A defining feature of 'intermod' problems is that if either one of the two stations stops transmitting, the spurious signal disappears completely.

- **Blocking, limiting or gain compression** – three names for essentially the same problem, where one extremely strong signal drives an amplifier or mixer device within the receiver to the physical limit of its available output. Any further increase in input level can cause no further increase in output from the affected stage, which corresponds to a reduction in gain – and that will be for *all* signals, including the one you're trying to copy. In extreme cases of limiting, a strong carrier makes the whole receiver fall quiet (which is what FM receivers are specifically designed to do, but SSB/CW receivers definitely are not!). Blocking can be caused either by strong signals inside the amateur band or by extremely strong out-of-band signals from nearby commercial transmitters.

- **Phase noise, noise sidebands and reciprocal mixing** are all problems connected mainly with the local oscillator of your transceiver so they are not the main focus of this article.

All of that interference is being **created within your own receiving system** when other strong stations appear on the band, and is **entirely your problem** – you can't blame other stations merely for being there, and being strong! Other stations certainly do transmit spurious signals as well, but you won't be able to resolve those problems unless you first understand the performance and limitations of your own receiving system.

HOW MUCH GAIN DO I REALLY NEED?

Gain in a preamplifier is your best friend and your worst enemy. Low-noise amplification is a necessary part of achieving a low system NF; but too much amplification will make all signals stronger, which plays havoc with the strong-signal handling. That is why we always need to think about finding the optimum balance – enough gain, but not too much. This is where a preamp at the masthead allows us to find a better optimum.

A preamp in the shack is the perfect example of a 'lose-lose' strategy. The losses in the long run of feedline will add directly to the system NF, and that degradation in weak-signal performance cannot be completely recovered by a preamp in the shack. Worse still, recovering even part of that lost performance will require high levels of preamp gain, so we have lost performance on both weak signals and strong signals.

But that same preamp at the masthead will avoid the feedline losses on receive, and so will give us a lower system NF using less preamp gain. Simply by moving the preamp to the masthead, we have transformed a 'lose-lose' situation into a 'win-win'.

Optimisation is a numbers game, which is why I have included a downloadable Excel spreadsheet **(Figure 1)** that you can use to analyse your own station. Simply overtype my cable losses with estimates of your own, and then you can then calculate the effects on your receiving system NF. Further technical details are beyond the scope of this article but the whole spreadsheet is based on information from *The VHF/UHF DX Book* [3, 4].

The spreadsheet also estimates the effects of gains and losses on strong-signal performance, and the highlighted red box shows that the **'weakest link' in strong-signal performance is always the transceiver** –

Ian White, GM3SEK • gm3sek@ifwtech.co.uk

PHOTO 2: Prototype preamplifier weatherproofed and mounted on the Yagi itself.

not the preamp. The point where overload takes place is probably quite deep inside the transceiver, at the output of an amplifier or mixer stage where signal levels have built up to a substantial fraction of a volt. An external preamplifier makes all incoming signals even stronger, which causes that stage inside the transceiver to overload more readily. It is actually quite difficult to overload the preamp itself, especially a design like the DG8 that uses a high dynamic range RF amplifier device and good filtering for out-of-band signals (which is why I adopted those proven features straight from the Anglian transverter).

If you are using a preamp ahead of a VHF/UHF transverter followed by an HF transceiver, the transverter will provide even more gain for all in-band signals, so most likely point of overload will then become the HF transceiver.

This is why it is vital to use **the minimum possible amount of preamp gain**... which can only be achieved by mounting the preamp **at the masthead** and then carefully adjusting its RF gain with an aim to reduce it even further if possible. And having done all that...

- **Switch OFF the internal preamp in the transceiver! You only need ONE preamp – the one at the masthead.**

RF SWITCHING AND SEQUENCING.

Enough now about receiving. A masthead

WEATHERPROOFING

Another major priority for a masthead preamp is to keep it working in all weathers.

Many people avoid using masthead preamps because of poor reliability – but here is some good news. A home-built masthead preamp can have far better long-term reliability than a commercial product, because we have freedom to do things that commercial manufacturers can't.

What's wrong with bulkhead connectors? Most commercial preamps and antenna switches use metal enclosures with ordinary N or 'UHF' flanged sockets that were never designed for outdoor use. Water can easily get underneath the bolted flanges and a connector mounted on a flat surface is very difficult to seal by wrapping with tape. Bulkhead sockets also bring technical problems inside the enclosure, either requiring internal connectors and jumper cables or else encouraging poor RF termination techniques. So why do commercial manufacturers use bulkhead connectors at all? The only reason is marketability – so that the product can be packaged neatly for shipping and sale. Bulkhead connectors are not used for any reason related to performance.

DIY is better. If you choose to build your own preamp, none of those problems need affect you. As a home constructor, you can build a masthead preamp with much better weatherproofing, with better performance due to eliminating unnecessary connectors – and all at a much lower cost.

My Prime Directive for weatherproofing is: no exposed metal parts! No metal cases, no bulkhead coax sockets, no metal power connectors and no fixing bolts penetrating the enclosure. This is very easy to achieve as shown here, using an inexpensive IP65 waterproof plastic box, with 'tails' of coax and control cable coming out through waterproof plastic cable glands. All connections are made using inline plugs and jacks – your choice – to eliminate all unnecessary back-to-back adapters or jumpers. These inline connections can then be easily and completely waterproofed by wrapping with tape.

But sealing against rainwater is not enough! Even an IP65 enclosure is not gas-tight, so the daily cycle of atmospheric warming and cooling can draw water vapour into the enclosure where it condenses – and then accumulates because it cannot get out. For that reason, it is much better to drill small vent holes in the enclosure to allow the pressure to equalise and any liquid water to escape. To provide additional protection for the internal electronics, use a conformal coating spray (see the construction notes section in the main text).

Use custom cables for minimum RF losses. To reduce RF losses even further, use the exact lengths of coax that YOU need for your particular installation. Photo 2 shows how the input cable for my own DG8 preamp is just long enough to connect with the short length of RG213 coming from the antenna feedpoint. RG213 was chosen for flexibility and reliability, so the output cable is a longer continuous length of RG213 that also includes the rotator loop, ending with the correct connector to mate with the lower-loss but less flexible cable coming up the tower.

Proven performance. These techniques for cable termination and waterproofing have proved 100% reliable over several years, at a location that experiences frequent driving rain and wind-driven salt spray. They work where other techniques have failed.

Ian White, GM3SEK • gm3sek@ifwtech.co.uk

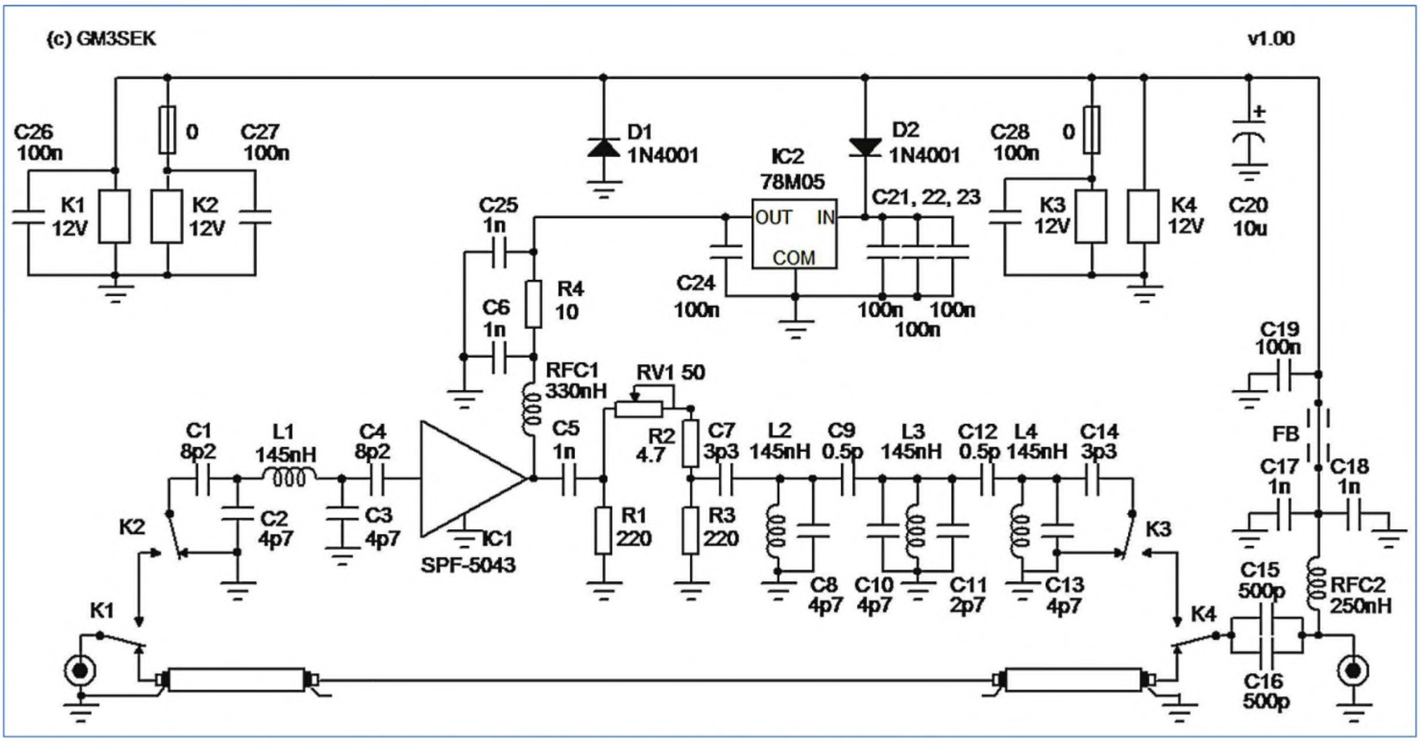

FIGURE 2: Circuit diagram of the DG8 preamplifier. Relays are shown in the NON-energised (Tx/bypass) state.

preamp must also provide switching for the transmitted signal. This requires relays that have a low VSWR at VHF/UHF and are capable of carrying full legal power. Digital modes like JT65 also require that everything is rated for alternating 60-second periods of full carrier.

As mentioned earlier, we're using low-cost mains relays for switching. The only minor problem is that the large contacts and close spacing provide relatively poor isolation to the open-circuit port, especially at VHF. HA8ET solved that problem by using compact SMD relays at the input and output of the receiving preamp to provide additional isolation, and that idea has also worked very well here.

To make the DG8 preamp as easy as possible to install at the masthead, I decided that no additional cables should be required – no DC power/control cables, and no separate coax downlead for the receive signal either. Instead, the DG8 is simply connected into the existing coax feedline, as close as possible to the antenna, and the switched DC power for the preamp and the relays arrives on the centre conductor of the main feedline from the shack. When no DC power is applied, the preamp reverts to a 'safe' state with the RF amplifier fully isolated and a direct RF connection from input to output.

Because the DC power is fed through the coax, the DG8 has to include an onboard 'bias tee' to separate the DC supply from the RF. You will also need a similar bias tee in the shack to inject the switched DC power onto the centre conductor of the coax. The DC blocking capacitors at both ends of the line have to carry the full transmit power, so these are special SMD mica components. Only one capacitor is required for power levels up to about 500W, but the DG8 board makes provision to use two in parallel for higher power levels.

All preamplifiers require a sequenced Tx/Rx changeover system to avoid transmitting before all the relays have changed over. Tx/Rx sequencing is another topic that would need a full-length article on its own, but fortunately there are some good articles on the web. The DG8 is fully compatible with a number of modern Tx/Rx sequencers that also include the bias tee, such as the SSB Electronic DCW 2004B and many lower-cost and DIY alternatives such as the boards from W6PQL and W1GHZ.

If Tx/Rx sequencing is new to you, the web pages by those two US authors make an excellent introduction, along with Chapter 11 (Transmit/Receive Control) in *The VHF/UHF DX Book* [3].

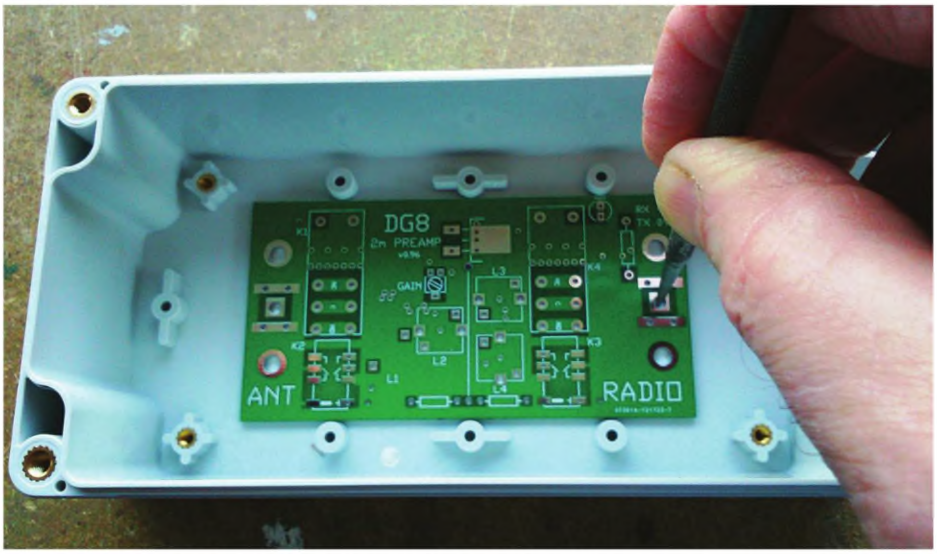

PHOTO 3: Using the PCB as a template to mark the cable gland holes.

CONSTRUCTION NOTES. Construction of the DG8 Masthead Preamplifier is very straightforward. Experienced constructors can probably 'just do it', though you may still find it easier to follow this sequence.

Figure 2 shows the circuit diagram and the complete components list is in **Table 2**.

ENCLOSURE PREPARATION. Use the bare PC board to mark the hole centres for the cable glands (**Photo 3**). Drill pilot holes at the marked locations and then open out the holes in several careful steps to 16mm diameter. Also drill four 2mm weep holes near the corners of the box to equalize the air pressure and allow drainage of any

Ian White, GM3SEK • gm3sek@ifwtech.co.uk

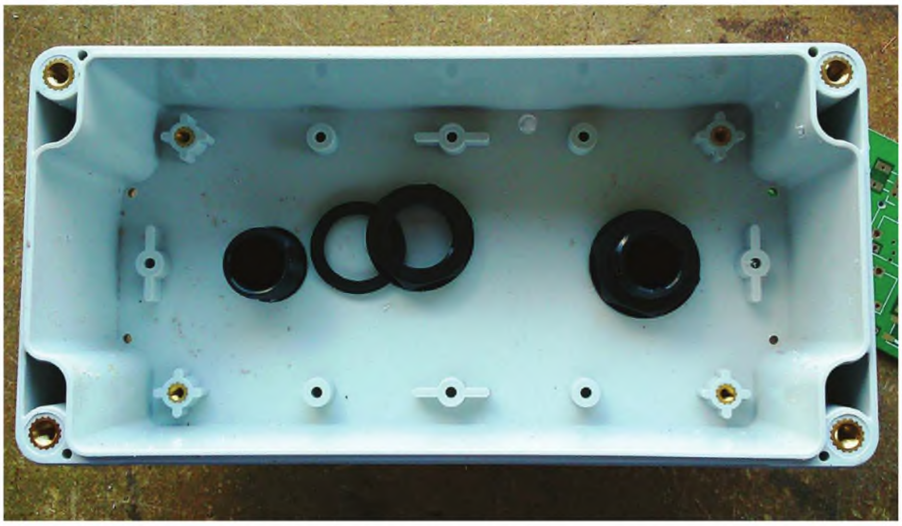

PHOTO 4: Installing the cable glands. Note the four small drainage holes drilled at the widest points of the box.

condensation. **Photo 4** shows the four holes and installation of the cable glands. Fit the rubber washers inside the box (no further sealant is required) and tighten the 16mm plastic nuts down very firmly. The completed enclosure can be seen in the lead photograph.

CIRCUIT BOARD ASSEMBLY. Begin with the underside of the board, see **Photo 5**.

1. Install the coax bypass link between K1 and K3, underneath the board. This coax has to carry 400W or more, so the recommended cable is a 6mm OD, PTFE insulated type such as RG306 or RG142.

   (a) The overall length of cable is 110mm. Remove 12mm of jacket from each end and prepare as shownin **Figure 3**. (Tip: pre-tin the whole 12mm of bared shield, score around at 6mm and snap off the unwanted end by bending back and forth.) Carefully remove any loose strands of braid.

   (b) Bend the cable into a parallel-sided U shape as shown in the photograph. To avoid kinking the cable, make the bends around a solid former. Tie each bared end of the shield to the board using loops of 1mm tinned copper wire, threaded through the holes in the large rectangular solder pads (see Photo 5). Tighten each loop by twisting the wires on the topside of the board.

   (c) Solder the coax shield onto the solder pads and the U-shaped tie wires. (Only solder the tie wires on the underside of the board, not the topside.) When cool, turn the board over and cut the wires off flush to the topside. Use a craft knife to make a really flush cut, so that K1 and K3 can sit tight down onto the board.

   (d) Finally, bend each end of the centre conductor down to touch the pad between the relay pins, and solder.

2. Install components on underside of board. Install all of the underside SMD components shown in Photo 5, except for IC1 and the ferrite bead.

3. Install components on topside of board. For ease of access with a hot soldering iron, follow this sequence:

   (a) Wire link W1 (Kynar or PTFE insulated wire is recommended)

   (b) IC2 (78M05)

   (c) K2, K4 and RV1. (Do not install K1 and K3 yet.)

   (d) L1-L4: Pull off the screening cans so you can see which is the upper end of each winding (furthest away from the groundplane). Upper end of L1 goes nearest to L2. Upper ends of L2, L3 and L4 connect down to the groundplane.

   (e) Screening cans for L2, L3 and L4 (no screening can for L1). Solder from underside of board, and fill the holes with solder.

   (f) K1 and K3: Press these relays tight down onto the board (see earlier). When soldering close to the coax bridge, avoid melting the coax jacket.

   (g) RFC2: 10 turns 1mm enameled copper wire, close wound on 5.5mm drill. Mount with 3mm spacing above the board. RFC2 is part of the VSWR compensation, so make it exactly as specified.

   (h) C20, the wire-ended electrolytic capacitor.

All of the topside components should now be in place.

4. Install IC1 and test voltages/currents

   (a) On the underside, install IC1. Take great care to install this IC the correct way around – one of the pins is broader than the other three, and that goes onto the broad PC pad connected to the grounded area nearest the centre of the board.

   (b) Connect a current-limited +12V DC supply to the positive side of C20. You should hear all four relays click, and the total current draw should be close to 130mA. The voltage at the junction of C24 and R4 should be very close to 5.0V and the voltage drop across R4 (10R) should be about 0.45V.

Correct any faults before proceeding further!

5. RG213 coax terminations. Photo 5 shows how the cable shields are soldered between two large solder tags (listed in catalogues as "6.3mm/¼in blade connectors"). This DIY termination method doesn't look pretty but don't let that fool you – it has excellent RF performance.

   (a) Solder the large tags into place on the underside of the board (two tags per termination). Re-tin the inside facing surfaces of the tags.

   (b) Decide what lengths of RG213 you wish to attach to the input and output. Remember, this is your chance to eliminate unnecessary adapters and jumpers. Measure the lengths of cable and cut the ends accurately square.

   (c) Remove 15mm of the RG213 outer jacket, then lightly solder-tin the outer shield braid to prevent any loose strands. Cut through the braid (but not the centre insulation) to leave 10mm of bare tinned shield exposed beyond the end of the jacket.

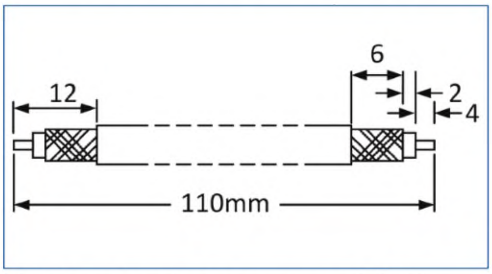

FIGURE 3: Preparing the coax bypass link. All dimensions are in mm.

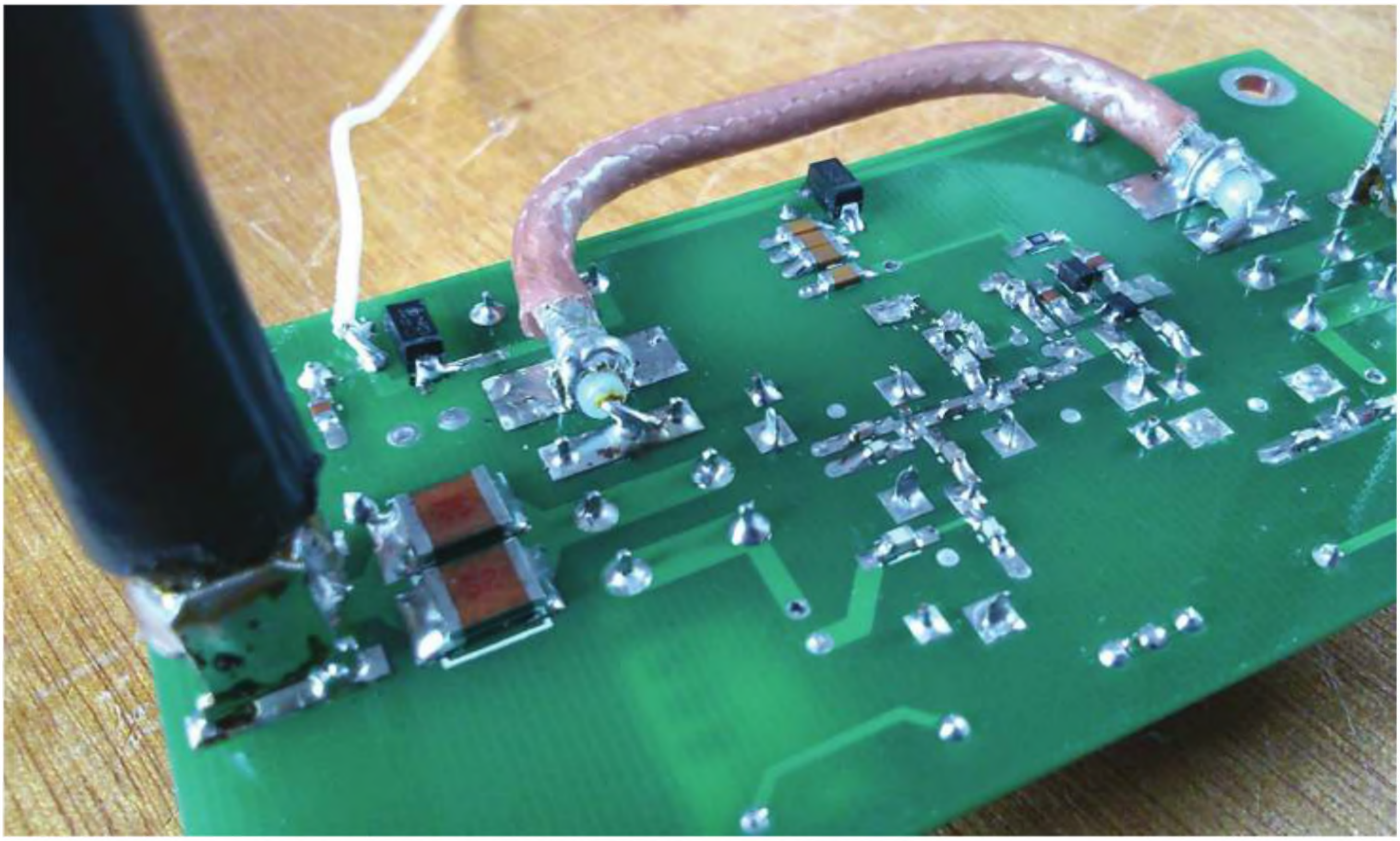

PHOTO 5: Underside component layout. Production boards have printed component markings.

(d) Leave 2-3mm of bared centre insulator beyond the end of the shield, and then remove the remaining insulation to leave a final 3mm of centre conductor. Check again for loose strands.

(e) Now is the moment to pass the prepared ends of the cable through the cable glands and through the holes in the waterproof box. Don't forget to do this!

(f) Feed the prepared end of the cable between the solder tags and push the centre conductor through the board. Make sure the end of the insulation presses firmly against the underside of the board, and make a final check for loose strands of braid. Then solder the centre conductor on the topside of the board and trim off any excess length.

(g) Use pliers to squeeze the two solder tags inward so they grip the coax, and then quickly solder the braid to the tags using a large iron. Aim for a solid line of solder along both edges of each tag – see **Photo 5**.

6. Final cleanup. Before alignment, clean up the board with flux solvent. Rinse at least two times until the board no longer feels sticky. Take care not to allow solvent inside the screening cans of L2, L3 and L4.

POWER-UP AND ALIGNMENT. If you have followed the instructions listed earlier, you already completed all the DC tests in step 4(b).

Alignment consists only of optimising the bandpass filter L2-3-4 followed by a very small adjustment of L1 for minimum NF. Use the correct plastic trimming tool to avoid breaking the fragile ferrite cores!

1. The best way to power the preamp board for these tests is to remove the SMD ferrite bead and connect a +12V DC supply directly to the board (the white wire in Photo 5).

2. Connect the input of the preamp to a 2m antenna, and the output to a receiver tuned to 145.0MHz SSB with the AGC switched OFF. You may also find it useful to set up three quick-access memory channels at 144.0, 145.0 and 146.0MHz (all SSB).

3. When you apply power, the noise in the receiver should increase (it may still be quite low level at this stage). Rotate the trimpot RV1 fully clockwise to maximise the noise level.

4. Set the cores of L2, L3 and L4 exactly one turn below the top of the screening can. The noise level should increase slightly. Adjust the core of L3 inward by about one more turn. The noise level should increase noticeably.

5. Adjust L2 and L4 to increase the noise level. Re-adjust L3 if necessary.

6. By careful setting of the cores of these three inductors it should be possible to equalise the noise levels as you flick between the memory channels on 144.0, 145.0 and 146.0MHz. (If you have access to a spectrum analyser and tracking generator, then of course use it; but remember to keep the RF input level well below 0dBm.)

7. With the receiver manually tuned to 144.30MHz, carefully adjust the core of L1 to maximize the noise. Do this as accurately as you possibly can, and then adjust the core of L1 inward by exactly a quarter-turn.

8. Where we go next will depend on your access to test equipment.

   (a) If you have no test equipment at all, don't worry – if you were careful and accurate when carrying out step 7, you are already very close to the optimum NF.

   (b) Another simple method is to switch to FM and find a very weak and 'noisy' FM signal that is right at the threshold of demodulation. Now very carefully adjust L1 for the clearest possible modulation relative to the noise, in other words for the best possible SNR.

TABLE 2: Components List.
Unless otherwise noted, all SMD are 0805 and order codes are from Farnell. A list that can be pasted directly into the Farnell ordering system is at www.ifwtech.co.uk/g3sek/vhfdx/dg8-farnell-order.xls but some items are only available in larger quantities, so the system automatically increases the numbers. Try to share with a friend!

Capacitors	Ref	Notes	Supplier and Order Code
0p5	C9, C12	Close tolerance +/- 0.5pF	Farnell 1740744
2p7	C11		Farnell 2332766
3p3	C7, C14		Farnell 1856217
4p7	C2, C3, C8, C10, C13	Farnell 1855762	
8p2	C1, C4		Farnell 2332712
1000p 1kV	C16, C17	CDE mica (use one capacitor for 500W, two for 750W+)	Farnell 2112927
1n0 50V	C6, C17, C18, C25	Use C0G ceramic *only*	Farnell 317457 or similar
100n 50V	C19, C21, C22, C23, C24, C27, C28, C29		Farnell 1759266 or similar
10µ 35V	C20	Wire ended radial electrolytic	Farnell 9451242 or similar
Resistors	**Ref**	**Notes**	**Supplier and Order Code**
4R7	R2		Farnell 2447677 or similar
10R	R4		Farnell 2447556 or similar
220R	R1, R3		Farnell 2447606 or similar
50R	RV1	Trimpot	Farnell 2321831
Other components	**Ref**	**Notes**	**Supplier and Order Code**
L1-L4	Coilcraft 10K series inductors , 142-04SL		G4DDK
330nH	RFC1		Farnell 2286428
RFC2	Hand made		See construction notes
FB		SMD ferrite bead	Farnell 1651723
K1, K3		Schrack/TE RTC31C012	Farnell 1770612
K2, K4		PANASONIC EW - TX2SA-12V	Farnell 910480
S1M	D1, D2	1A, 1000PIV	Farnell 1791846 or similar
78M05	IC2		Farnell 2323452 or similar
SPF-5043 IC1			G4DDK
Coax cable		110mm of RG306 or RG142 PTFE cable	See construction notes
Hardware			**Supplier and Order Code**
PC Board			G4DDK
2-pin PCB blade terminals (4 required)			Farnell 1870759
Enclosure, HITALTECH - SE-226-0-0-D-0			CPC EN82698
Cable glands, Hellermann Tyton - NGM16-BK (2 required)			CPC CB15745
Conformal coating spray, Electrolube APL400H			Farnell 3026838

(c) If you have access to a noise figure meter, it should be possible to optimize the noise figure to around 1.3dB at 144.3MHz.

By any of those methods, the core of L1 should still be very close to where it was at the end of step 7.

9. Rotate RV1 fully counter-clockwise and notice that the noise level decreases. Then advance RV1 clockwise until you hear a clear increase in noise level; but no further. In most stations this will be close to the optimum balance between good sensitivity and good dynamic range.

10. Connect a 2m antenna and switch on the receiver AGC. The noise level arriving from the preamp must not be high enough to activate the AGC – that would be a sure sign of too much preamp gain. If there is any movement of the S-meter due to background noise (apart from intermittent impulse noise) then return to step 9 and reduce the preamp gain.

11. Remove the temporary +12V DC connection, replace the ferrite bead (FB) so that the preamp can be powered through the coax, and check for correct operation with your Tx/Rx sequencer.

FINAL WEATHERPROOFING AND INSTALLATION. When everything is OK, apply an acrylic conformal coating for weatherproofing (see Table 2). Mask off the adjusting screws of L1, L2, L3, L4 and RV1 with small pieces of tape, and then lightly spray both sides of the board including the ends of the RG213 coax. Allow to dry in a well ventilated area.

Slide the preamp board back into the enclosure and hand-tighten the cable glands to make them fully waterproof. Your completed DG8 preamp should look like Photo 1.

Finally, tighten down the lid that seals the enclosure, making sure that the gasket is correctly seated into its groove.... and your preamp is ready to install. As you see from Photo 2, I simply taped mine to the boom of the Yagi, close to the feedpoint.

WEBSEARCH

[1] http://www.g4ddk.com/
[2] Mast-Mounted EXTRA-2 144MHz Contest Preamplifier by Gyula Nagy, HA8ET, http://www.ha8et.hu/Mast_Mounted_EXTRA_2/Mast_Mounted.htm
[3] The VHF/UHF DX Book edited by Ian White, G3SEK (out of print, occasionally available on eBay or from dealers)
[4] Modern VHF/UHF Front-end Design by Ian White, G3SEK. Parts 1–4, *Radio Communication* April–July 1985

RSGB shop

FROM P&P FREE OVER £30

E&OE **All prices shown plus p&p**

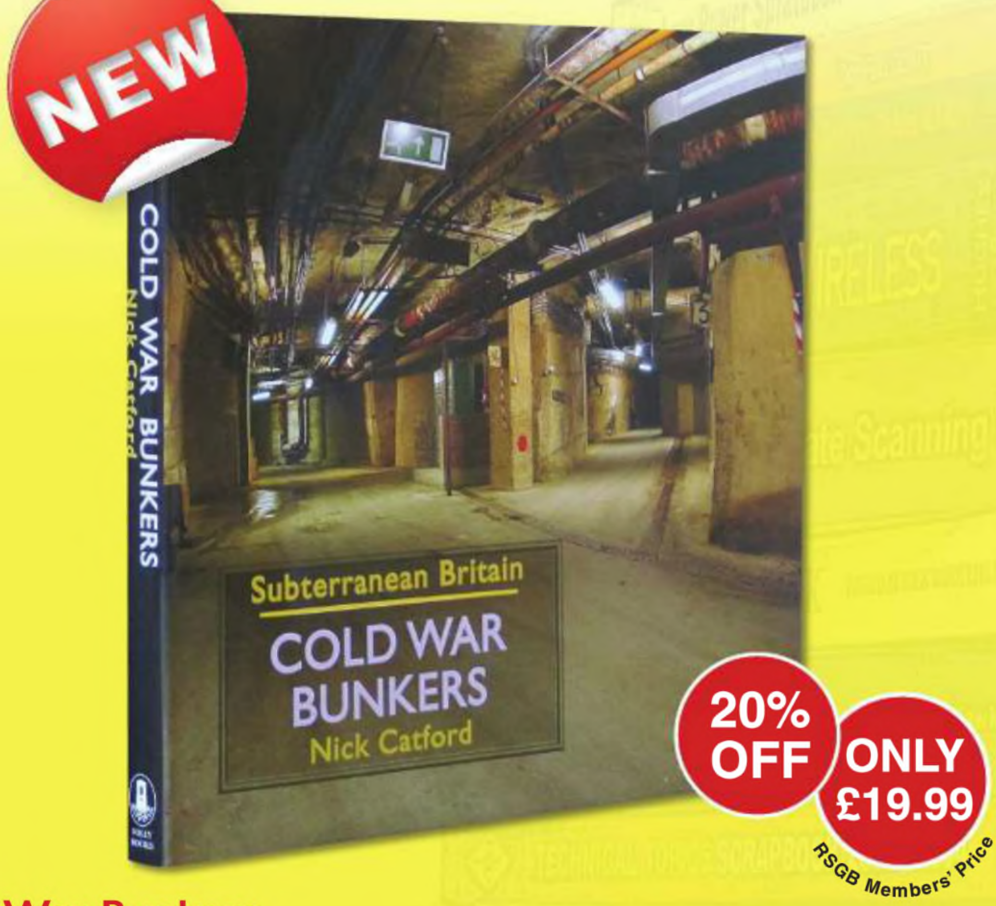

Cold War Bunkers

By Nick Catford

Cold War Bunkers is a comprehensive overview of all the underground, semi-underground and surface-built cold-war atomic and nuclear bunkers built in the British Isles. Lavishly illustrated on a high quality paper, this book provides over 450 photographs accompanied by comprehensive captions and an authoritative text of the structures built to protect central, regional and local government, military organizations, the Civil Defence organization, the Royal Observer Corps, UKWMO and the public utilities against nuclear attack by the Soviet Union between 1946 and 1989.

In many instances, Nick Catford has been granted unprecedented access to many highly sensitive sites in order to compile the collection of high quality images reproduced in this *Cold War Bunkers*. Readers will find details of The Corsham Central Government War Headquarters (Burlington); The Regional War Rooms built during the early 1950s and the network of Civil Defence bunkers that supported them; The Regional Seats of Government (RSGs) of the 1960s, the SRHQs that were built at the end of that decade and into the 1970s, and the highly sophisticated and hugely expensive Regional Government Headquarters of the 1980s. Also covered are the huge range of Royal Observer Corps bunkers from the very large Sector Controls to the tiny 3-man observation posts; the often complex and sometimes Spartan County and District council bunkers, bunkers built by the water companies, and the deep underground emergency telephone exchanges built by the GPO and BT. *Cold War Bunkers* also goes in great detail into the underground radar control rooms established as part of the RAF's `Rotor' radar system and also the hardened anti-aircraft gun control rooms which were integrated with `Rotor' in the early 1950s. Considerable coverage is also given to the cruise missile site at Greenham Common, the specialist hardened structures at RAF Bentley Priory and elsewhere, along with many other sites and structures too numerous to mention.

Cold War Bunkers is a fascinating and comprehensive view of all the British cold-war structures and is thoroughly recommended for everyone who has an interest in this topic.

Hardback Size 162x240mm, 288 pages
ISBN: 9780 9564 4052 5
Non Members' Price: £24.99
RSGB Members' Price: £19.99 (20% off)

May 2015 • RadCom Plus
Bob F Burns, G3OOU, C Eng FIET MSE • g3oou@aol.com

Building a Dual Z-Match

Covering 1.8 to 146MHz

INTRODUCTION. Since gaining his licence in 1960 and also regularly operating on HF National Field Days with a range of wire aerials, the author has built and used a number of Z-Matches. This article discusses the latest development and construction of a wide frequency range dual Z-Match for use with his stub loaded multiband dipole [1] and built in the style of the Heathkit SB-Line ('green') units to match his other homebuilt radio equipment.

The finished Z-Match project that has been in use for several years with no problems to date.

REQUIREMENTS. An aerial with balanced open wire feeders requires a suitable aerial matching unit that will work over the entire frequency range of the aerial for which there are at least three conceptual solutions:

- An unbalanced matching unit followed by a balun. The issue here is that baluns will not give optimal performance over wide ranges of frequency and impedance
- A fully balanced matching unit with the balun on the 50Ω side that is connected to the transceiver. This would allow the balun to operate in a constant 50Ω environment but the matching unit would be more complex
- The classic Z-Match

This article addresses the last of these three options, although the reader may wish to research the alternative designs and variants of the Z-Match that are easily found in modern amateur radio publications and on the internet. The function of an aerial matching unit is to communicate the transmitter power to the aerial as efficiently as possible – it should never be relied on to provide any significant selectivity for reduction of spurious responses.

Detailed mechanical drawing have not been provided as individual constructors' layouts will be determined by the components that they have chosen to use and the dual Z-Match approach could, of course, be implemented in two separate cases if that is more convenient. However, careful thought should always be given to the front panel layout with respect to access to the controls and ease of use.

ORIGIN OF THE Z-MATCH. The original concept of the multiband switchless tank circuit is thought to have been developed before WWII although it has not been possible to determine the exact date. The design was intended to remove the need for expensive high power bandswitches in transmitter drivers and final amplifiers. However, the first amateur radio 'Z-Match' articles using this technique appeared after WWII with one commercially made product from the Harvey Wells company being reviewed by Allen W. King, W1CJL in the May 1955 edition of *QST*. The original 80m - 10m Z-Match is shown in **Figure 1**.

This was designed to cover 3.5 - 7.3MHz and 14 - 29.7MHz and therefore only required a minimum to maximum variable capacitance ratio of 4.5:1, which was easily achieved. The more recent addition of the 10MHz band significantly increases the required capacitance ratio as will be discussed later in this article.

How does it work? As the circuit is an arrangement of two variable capacitors and two inductors there will always be two resonant frequencies at any one time. The lower frequency will be provided by L2 in parallel with C2a and C2b and the higher frequency by L3 in parallel with the series combination of C2a and C2b. This is based on the assumption that the inductance of L3 is small enough to be ignored on the 3.5 – 7MHz range and the inductance of L2 is large enough to be ignored on the 14 – 30MHz range. Technically this is not quite correct but it is close enough to understand how it works.

There will always be some interaction between the two resonant circuits so some 'cut and try' may be required during construction to obtain the correct frequency coverage on each range. The author has noted that an alternative match can be obtained on the 14-30MHz range by connecting the aerial to the 3.5 – 7MHz

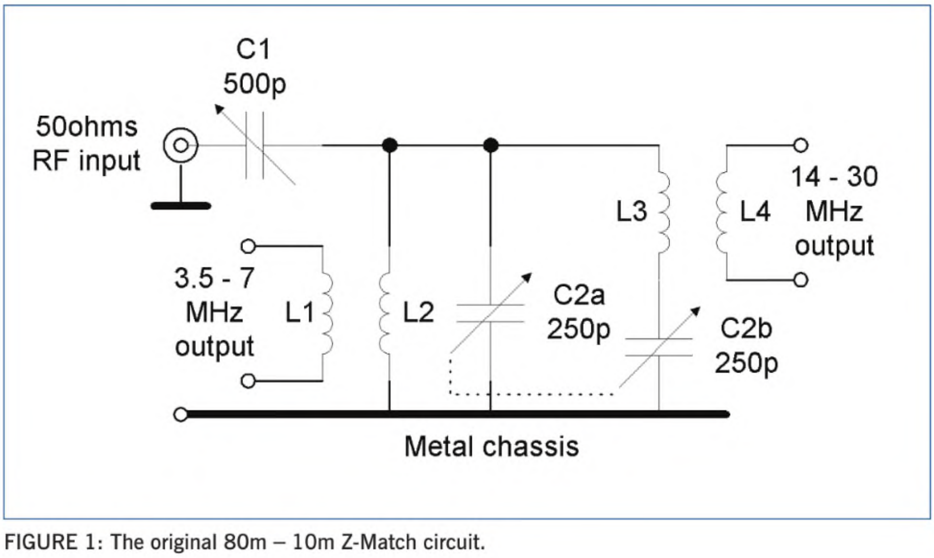

FIGURE 1: The original 80m – 10m Z-Match circuit.

Bob F Burns, G3OOU, C Eng FIET MSE • g3oou@aol.com

output and vice versa and the design in this article allows for that option in the case of a really 'difficult' aerial impedance. However, the overall efficiency may be worse.

More commercially manufactured examples appeared in the 1970s followed by variants in the design including those with toroidal cores or a single RF tuned circuit instead of the original two tuned circuit concept as used in this article.

MODIFICATIONS FOR TOP BAND AND 30m. The author originally developed and constructed a separate single transformer Z-Match for Top Band (1.8MHz) that was published in *RSGB Bulletin* **[2]**. The conventional solution to extend the frequency coverage of an HF bands Z-Match is to switch in an extra inductor in series with the inductor for the 3.5 - 7MHz range. Depending on the aerial impedance, an additional secondary winding may or may not be required for Top Band. If the aerial impedance is low then the 3.5 - 7MHz output may provide an adequate match otherwise an additional secondary winding for Top Band will be necessary as is the case in this design.

To cover the frequency ranges of 3.5 - 10.15MHz and 10.0MHz - 29.7MHz a minimum to maximum capacitance ratio of 8.82:1 is required plus some contingency for stray capacitance and interaction between the two halves of the circuit. During tests on the previous version of this Z-Match it was noted that the frequency coverage did not provide sufficient overlap to reliably cover 3.5 - 10.15MHz. This was probably due to the limited minimum to maximum variable capacitance ratio, so an extra band position in addition to Top Band was included as shown in **Figure 2**. Using the 3.5 - 5MHz link winding did not provide an adequate match on Top Band so the Top Band inductor L6 has its own secondary winding.

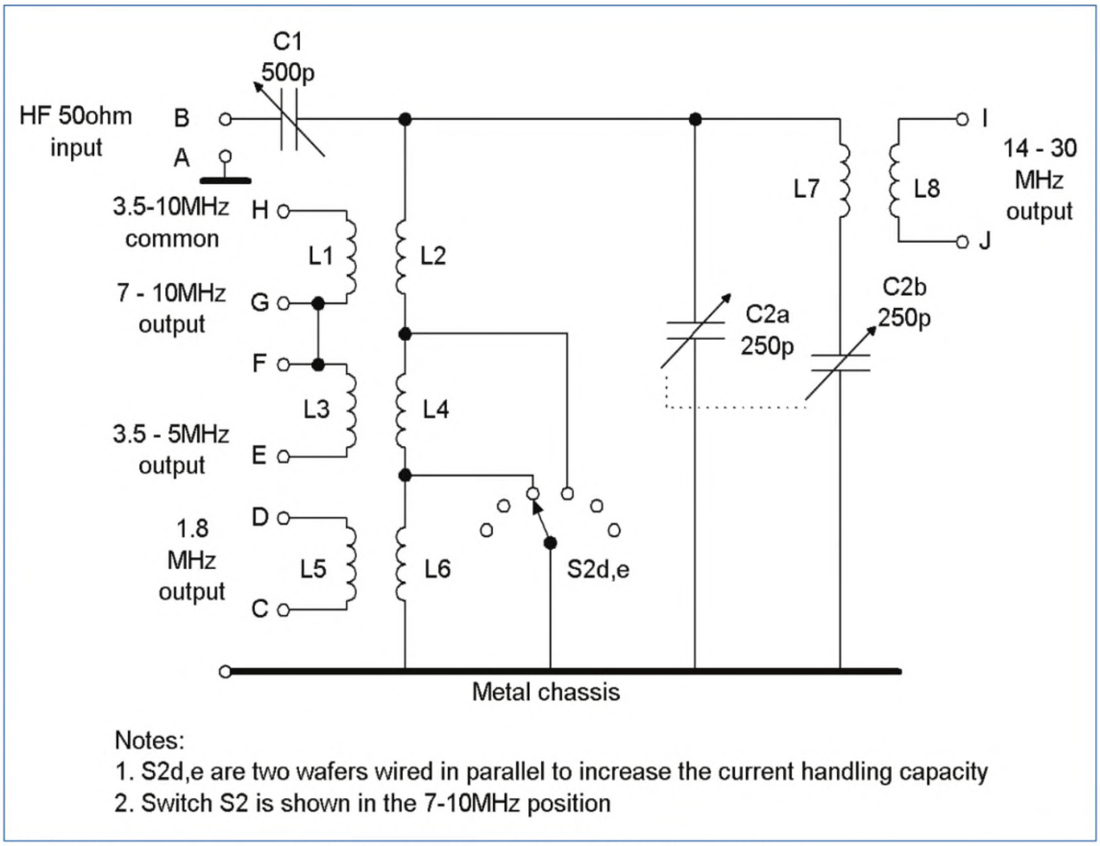

FIGURE 2: An extra band position in addition to Top Band was included in this design.

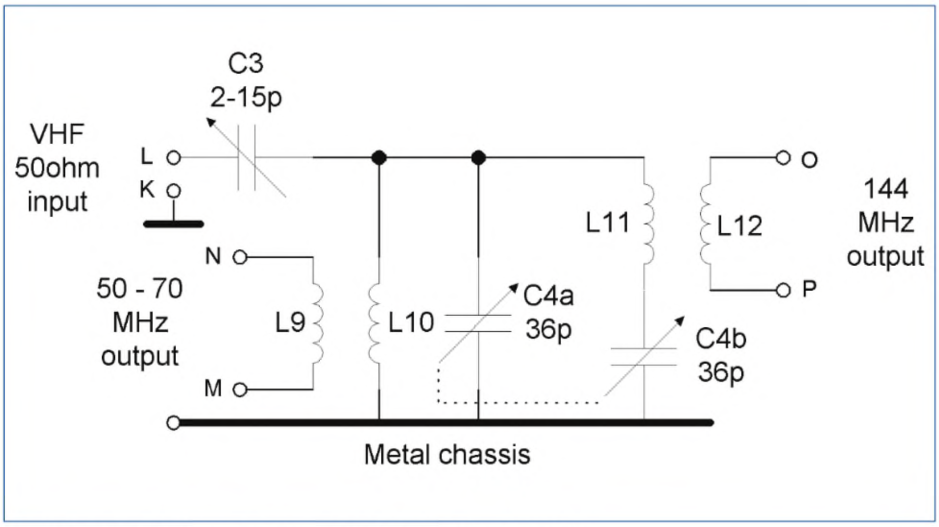

FIGURE 3: The basic, scaled-down, Z-Match for 50 – 146MHz.

MODIFICATIONS FOR VHF. The basic HF Z-Match components may be scaled down in value for operation from 50 - 146MHz. The only difference that was noted compared to the HF version was that there was more interaction between the two tuned circuits because of the smaller frequency spacing ratio.

The minimum capacitance of C3 in **Figure 3** is fairly critical and a search was made for a suitable component with wide spaced vanes. This capacitor is mounted on the diagonal rather then parallel to the sides in order to minimise the lengths of the connecting wires and insulated flexible shaft couplers are used to ease any alignment issues.

CIRCUIT DIAGRAM - RF WIRING. The individual matching circuits are shown as boxes to simplify the circuit with unique circuit references to each connection. Please refer to each matching unit already shown in the respective drawings.

All coaxial cable screening braids are connected to their respective sockets and metal screening plates on the switches. To facilitate soldering, the coax braiding very close to the centre insulating material without it melting, a PTFE coax cable like RG142 **[9]** is preferred. However, it is possible to use a conventional polythene insulated coaxial cable like RG58 with minimal damage. Loosen the braiding and slip a short length of high temperature silicon rubber sleeving over the centre conductor insulator and under the braiding at the soldering point and keep soldering time to a minimum.

May 2015 • RadCom Plus
Bob F Burns, G3OOU, C Eng FIET MSE • g3oou@aol.com

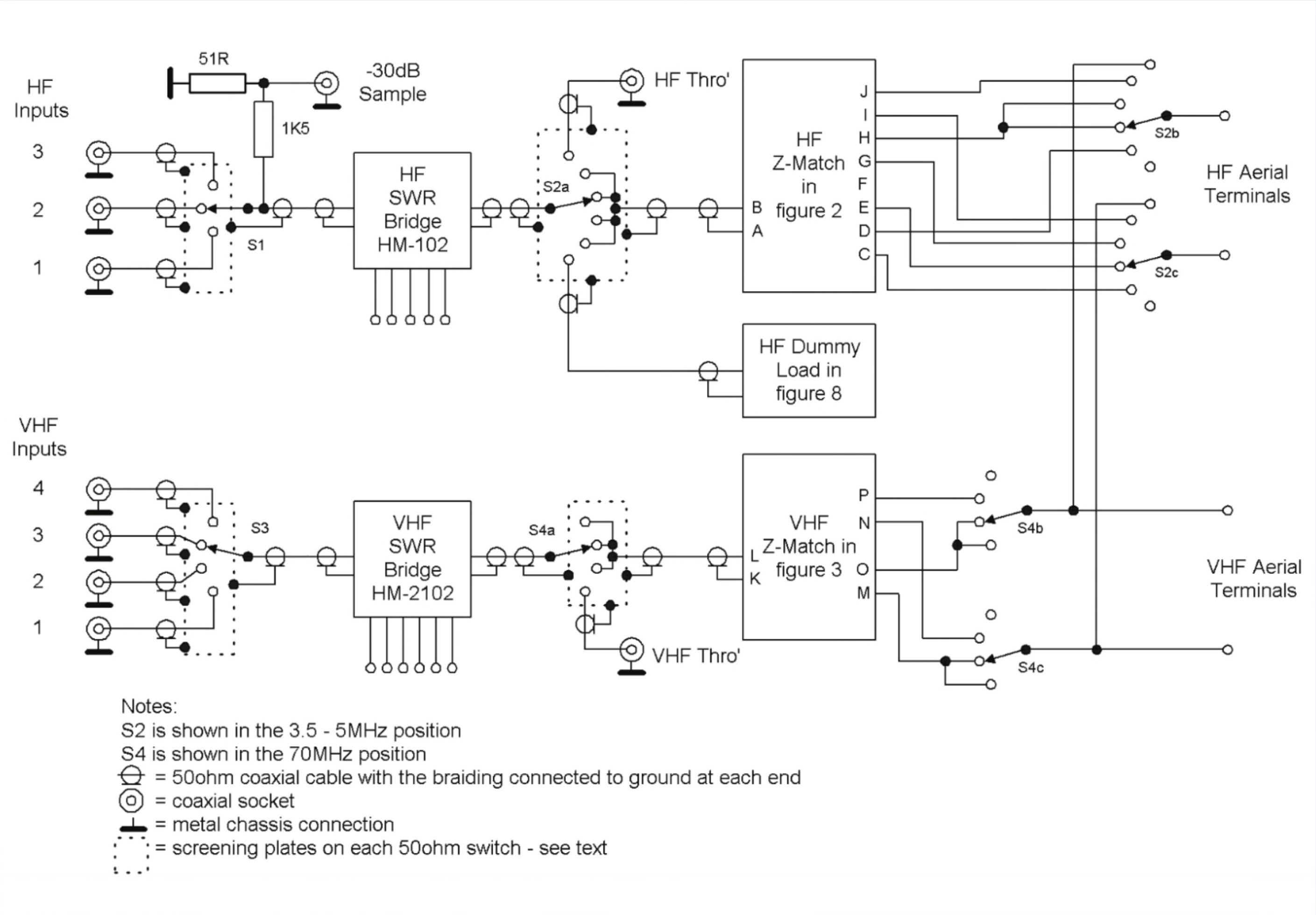

FIGURE 4: The inter-module RF wiring.

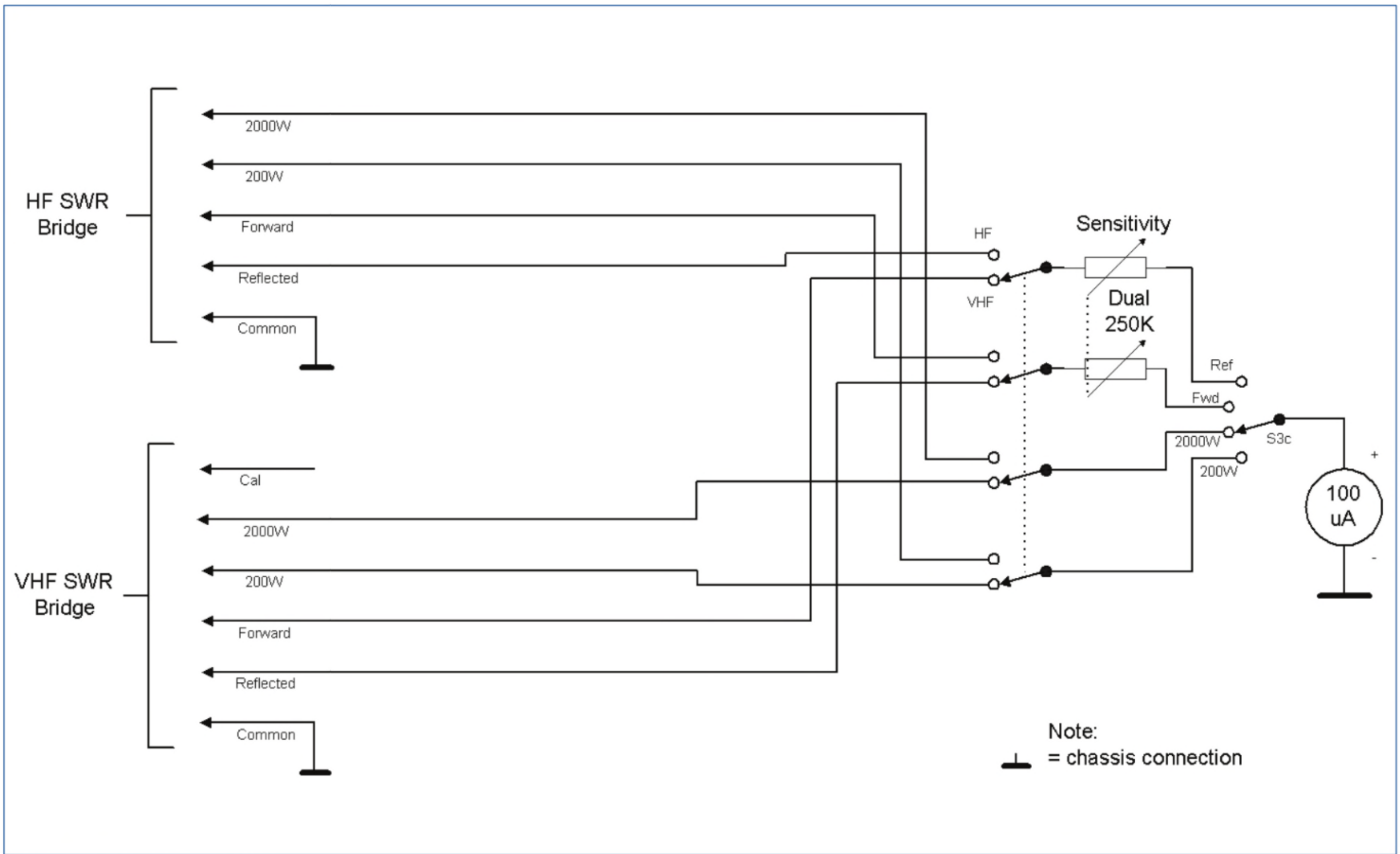

FIGURE 5: The SWR circuit.

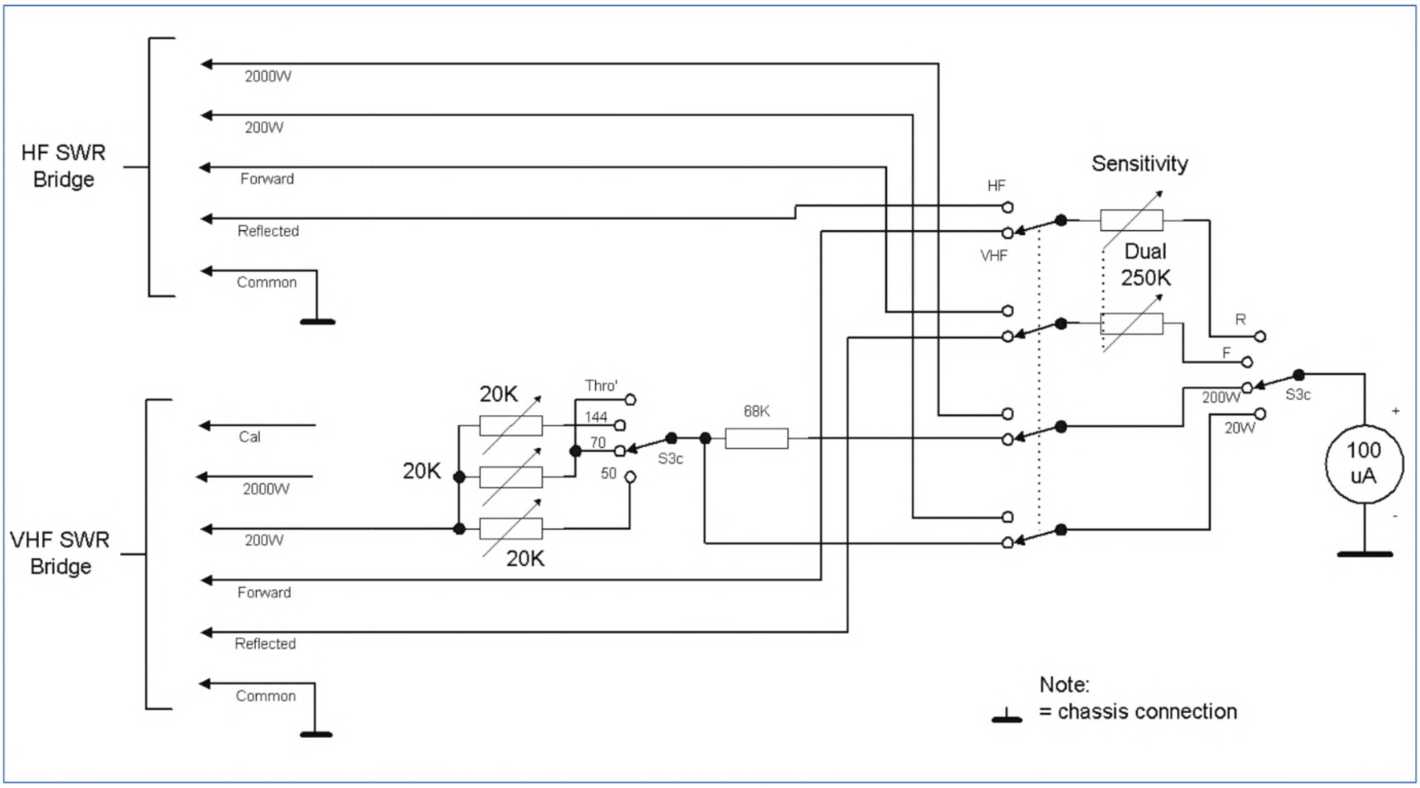

FIGURE 6: My own modification to convert the full scale power reading to 20W to 200W.

Switch wafers S2d and S2e are located in Figure 2. See **Figure 5** and **Figure 6** for SWR and power measurement circuits.

CIRCUIT DIAGRAM – SWR AND POWER MEASUREMENT WIRING. Two wiring circuits are shown. **Figure 5** shows the metering arrangements as suggested for both of the Heathkit SWR bridges giving full scale deflections of 200W and 2000W on the power ranges with the 100μA meter.

Figure 6 shows my own modifications to convert the full scale power readings to 20W and 200W and also to provide individual band calibrations on VHF. Initial tests showed some minor differences in the forward power meter readings for a given constant power output between 6m, 4m and 2m that the additional preset potentiometers allow to be corrected. The constructor will see some increase in non-linearity of readings on the 20W range.

BAND SWITCHES. The original Z-Match design for 3.5 - 30MHz did not contain any form of band switching but with the additional HF bands now available some form of band switching is required. The frequency coverage of each range will be determined by the ratio of the maximum to minimum values of the tuning capacitors, stray capacitance of the switches and wiring and the value of each inductor.

The final HF design uses a six position band switch to provide the functions shown in **Table 1**. The final VHF design uses a four position band switch to provide the functions in **Table 2**.

Once a switch is introduced into an RF environment, including a tuned circuit, the properties of the switch and its contacts must be considered – this includes the inductance, stray capacitance and voltage ratings of the conducting parts and the current carrying rating of the contacts. Note that there is no intent to move the switch while energised so ratings for making and breaking the contacts do not need to be considered.

With respect to the tuned circuit, the rule of thumb is that the circulating current at resonance is approximately Q times the energising current where Q is the loaded value, typically about ten. So for 100W of RF in the 50Ω incoming transmission line, the current will be 1.414 amps and the circulating current in the impedance matching tuned circuit will be about 14A

TABLE 1: The six position band switch functions for the HF design.

S2 Position	Function	Description
1	Straight Through	Connects the selected incoming 50Ω line via the HF SWR bridge direct to an outgoing 50Ω line
2	1.8MHz	Connects the incoming line via the HF SWR bridge to the HF matching circuits and selects the required inductor and secondary output winding
3	3.5 - 5MHz	
4	7 - 10MHz	
5	10 - 30MHz	
6	VHF	Connects the HF open wire feeder to the VHF matching network and the incoming HF 50Ω line via the HF SWR bridge to the internal dummy load

TABLE 2: The six position band switch functions for the VHF design.

S4 Position	Function	Description
1	50MHz	Connects the selected incoming 50Ω line via the VHF SWR bridge to the VHF matching circuits and selects the required secondary output winding.
2	70MHz	A single aerial may be used on VHF by connecting it to
3	144MHz	the HF output terminals and selecting position 6 on the HF function switch
4	Straight Through	Connects the incoming 50Ω line via the VHF SWR bridge direct to an outgoing 50Ω line

Bob F Burns, G3OOU, C Eng FIET MSE • g3oou@aol.com

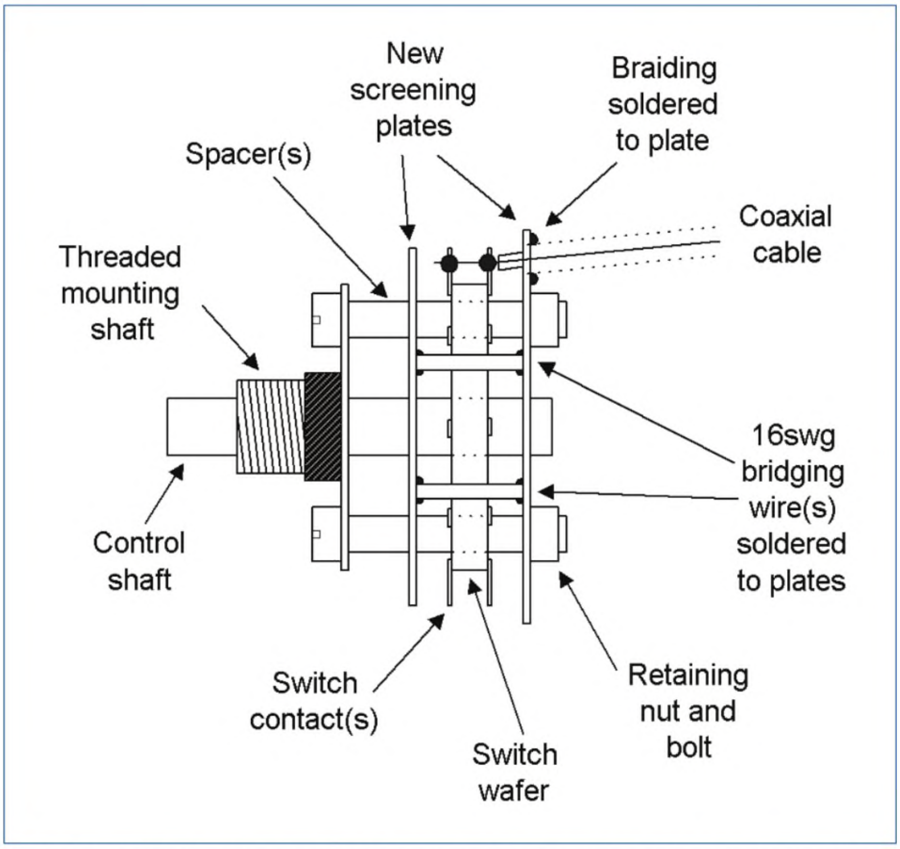

FIGURE 7: The latest wafer arrangement with contacts and screening plates on both sides of the wafer.

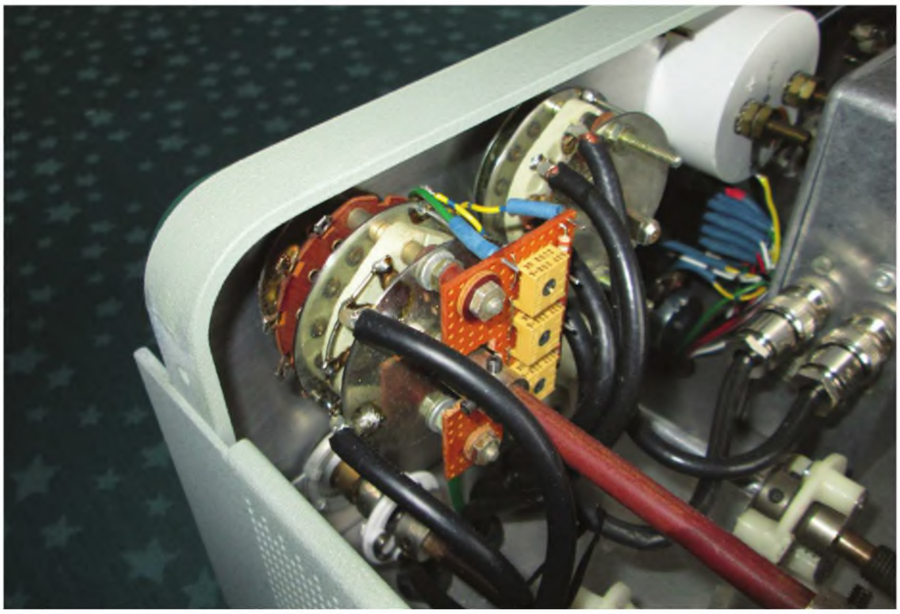

Photo 1: The original VHF band swtich with the range correction presets.

(or 28A for 400W). This is a significant current level so miniature switches are not an option. The switches used in this article have proved adequate for 100W with no signs of overheating or flashover but more robust wafers and contacts will almost certainly be required for full UK licence powers.

Following regular visits to radio rallies over the years the author has amassed a collection of 1 9/16inch (39.7mm) diameter ceramic wafer switches with silver plated contacts, probably military or commercial surplus. These may have originated from one or more manufacturers but have a common set of dimensions so it is possible to mix and match component parts.

Older switch wafers that have become oxidised can be removed from the detent unit, washed clean in a mild detergent solution, rinsed well, immersed in a silver dip **[5]** for a minute or two to remove the oxide, rinsed well and dried. A soft toothbrush may be used to remove any stubborn dirt during the washing process and drying may be completed in a warm area – an abrasive cleaner should not be used as it will remove some of the silver plating. The same cleaning process may be applied to most solid silver or silver plated items, if capable of immersion in a liquid, including for example, the variable capacitors from RF27 units. On completion, any previously lubricated moving metal parts should be sparingly re-lubricated, preferably with a light grease but not a light oil like '3 in 1' that tends to spread out over adjacent surfaces and evaporate much more rapidly.

In this Z-Match, two ceramic wafer switches were wired in parallel to share the circulating current in the switched part of the HF matching tuned circuit. However, in a later designed RF switch box the author determined that a dual parallel connected switch could be constructed using a single ceramic wafer with contacts on the front and rear surfaces of both the wafer and the rotor. This requires somewhat more work and patience to complete the disassembly and re-assembly but results in a smaller wafer assembly.

The drawing in **Figure 7** shows the latest wafer arrangement with contacts on both sides of the wafer. However, the single sided contact arrangement may still be used. **Photo 1** shows the original VHF band switch with the range correction presets.

Each wafer has a metal plate on each side to simulate a double sided 'micro-strip' like environment. This is not perfect but does result in significantly lower losses than without it and eases connection issues with the braiding.

The screening plates are placed as close as possible to the front and rear of each wafer but there must be sufficient space for the voltages involved, movement of contacts during switch rotation and access to the contacts during construction. The bridging wires are positioned between each switch contact position and soldered to the inside of each screening plate.

Calculations suggest that the completed switch assembly exhibits a characteristic impedance in the region of 70 - 80Ω but the physical length of the enclosed transmission line is extremely short so this will be seen as a small discontinuity in the 50Ω environment.

INTERNAL 100W HF DUMMY LOAD. This dummy load is intended for intermittent use and is constructed from two 100Ω 50W surface mount resistors connected in parallel to produce a 50Ω 100W load. **Figure 8** shows the circuit diagram. The internal construction of the resistors results in a low self inductance but a significant amount of parallel capacitance which is

Bob F Burns, G3OOU, C Eng FIET MSE • g3oou@aol.com

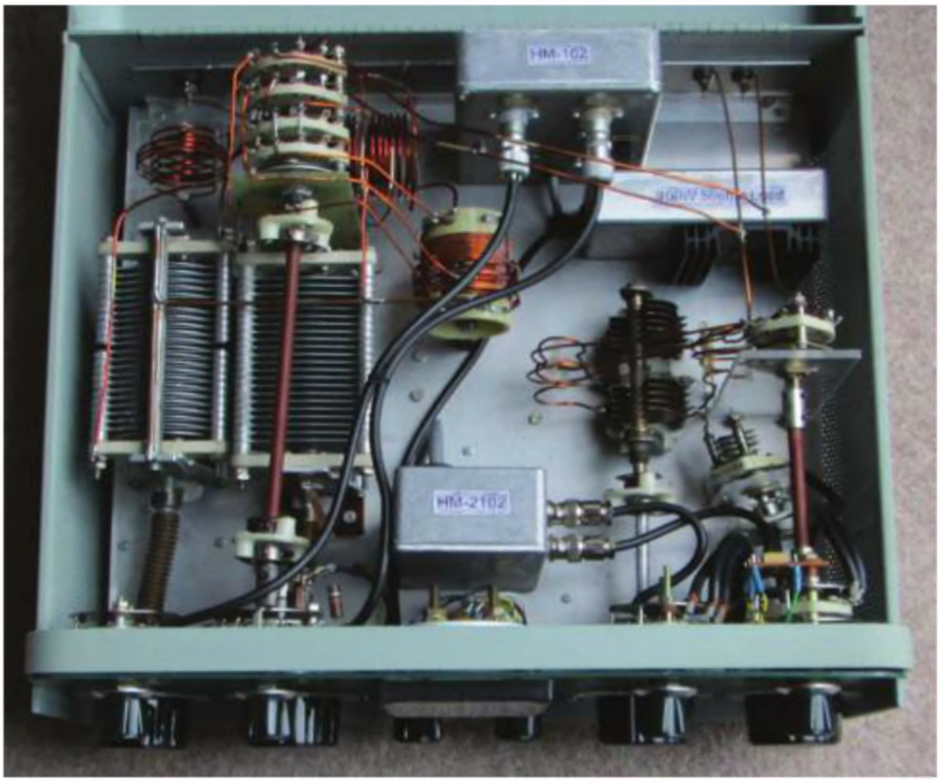

PHOTO 2: Top view of chassis layout showing the modifications to the HF tuning capacitor C2.

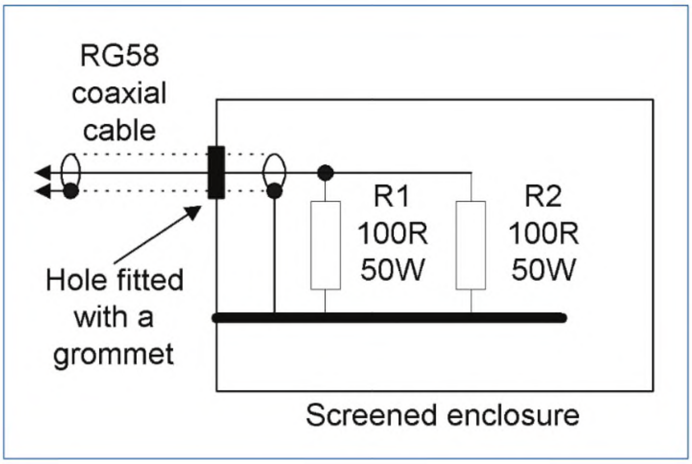

FIGURE 8. Internal 100W HF dummy load constructed from two 100Ω 50W surface mount resistors.

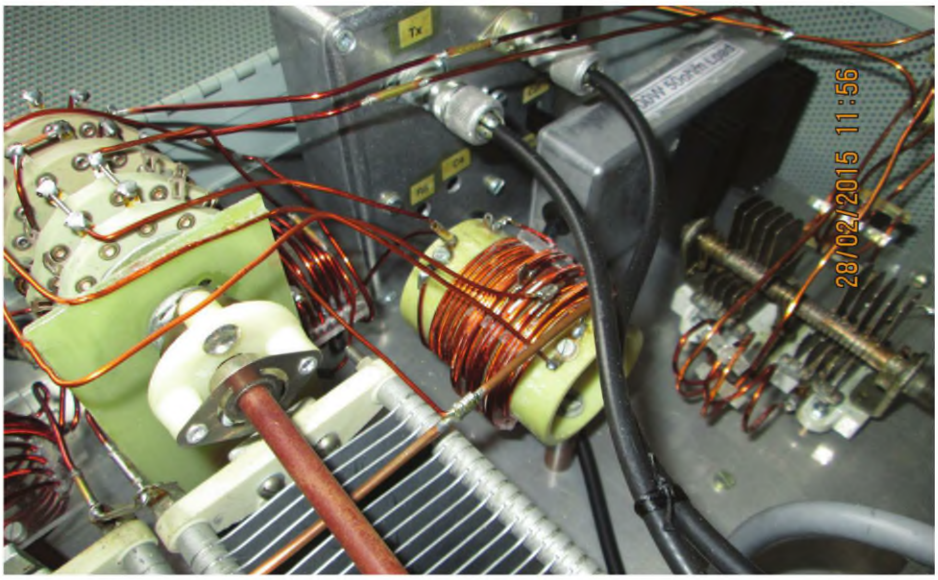

PHOTO 3: More of the details of the Top band transformer.

not an issue on the HF bands but does result in some 25% of the incoming RF energy being reflected back on 144MHz. TO-220 encapsulated high power resistors **[3]** are available which should have a reduced stray capacitance as they are physically smaller but these have not been tried by the author.

The resistors are mounted close together in a small, aluminium die cast case with an external heatsink to aid cooling and a 50Ω flying coaxial lead for connection to switch S2a.

CONVERSION OF THE HEATHKIT HM102 (HF) AND HM-2102 (VHF) SWR BRIDGES. Both SWR bridges were re-housed in smaller die cast boxes to ease fitting into the available space and BNC connectors used on the VHF unit. Access holes for all internal preset controls were provided together with a removable cover to gain access to the two solder joints on the BNC connectors on the VHF unit. The circuits of both of these units were left unchanged but the solid carbon resistors had aged high in value and were replaced with modern equivalent parts.

The internal circuits of both items have not been reproduced here because of copyright rules but they are easily available on the Internet by searching for the model number.

Both units were designed for the North American amateur radio market with its higher license powers but modifications are possible for use with UK licence powers by reducing the internal range setting resistors.

MECHANICAL CONSTRUCTION. The original version of this matching unit, built with the same chassis and case, used two ganged SB-401 PA tuning capacitors and displayed problems of flash-over on the lower bands when used with a 100W transmitter and high impedance aerials. This revised version uses tuning capacitors from a TU5B WWII tuning unit which have wider spaced vanes and do not show any signs of flash-over but being physically larger they do look a little squashed into place. HF tuning capacitor C2 has had its stator carefully divided into two using a hacksaw as is visible in the internal view in **Photo 2**. The stator is securely mounted on each ceramic cheek and does not appear to need any additional mechanical support.

New appropriately rated variable capacitors are available.

The chassis and front and rear panels are made from one sixteenth inch (1.6mm) thick NS4 half hard aluminium sheet. This is an imperial specification material for which there is a metric equivalent and is very strong, drills and punches well but cannot be bent without annealing. The chassis is about one inch (25mm) deep.

The layout of the HF section is not critical since the length of the individual connecting

Bob F Burns, G3OOU, C Eng FIET MSE • g3oou@aol.com

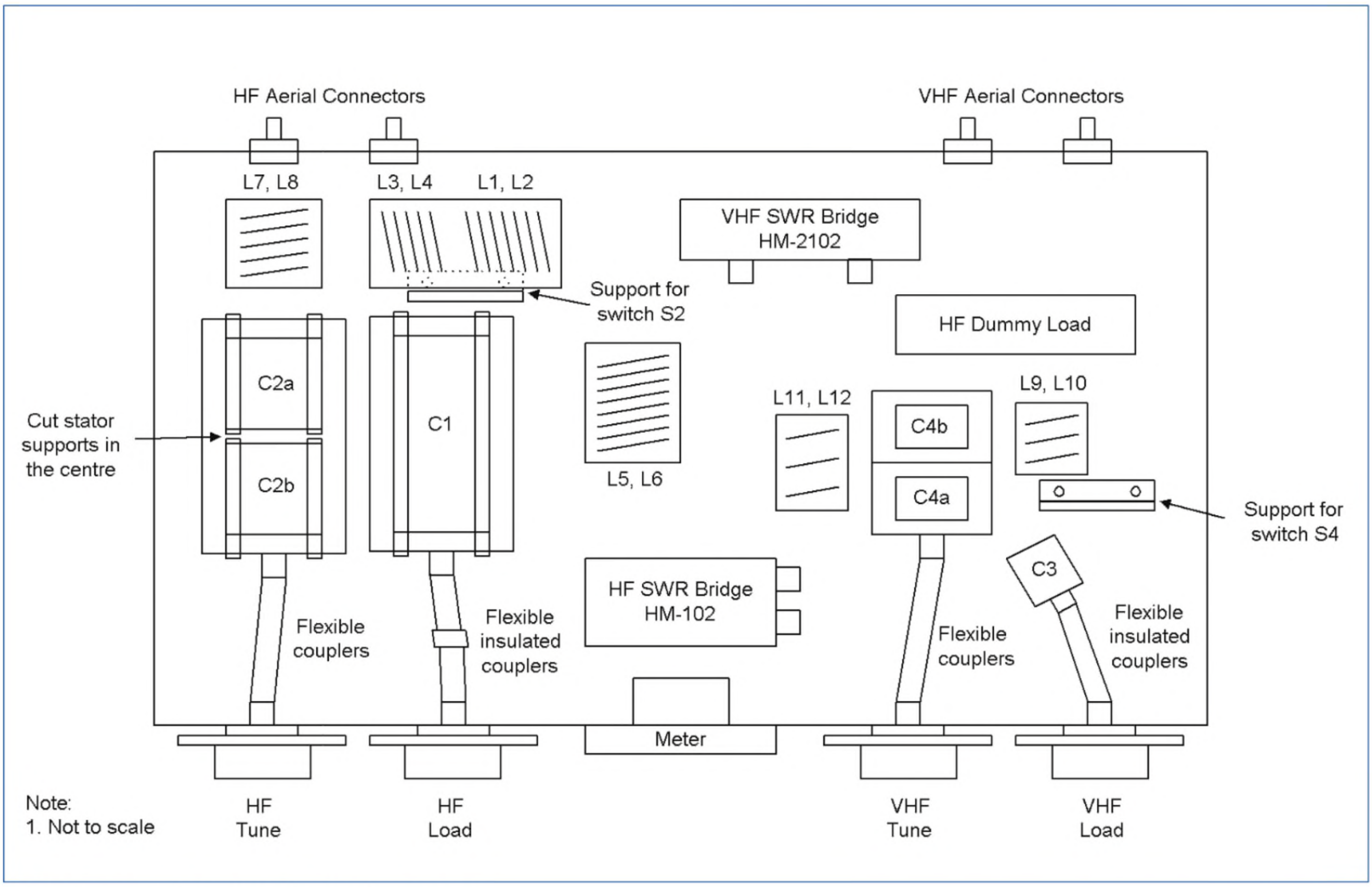

FIGURE 9: Chassis layout with circuit references.

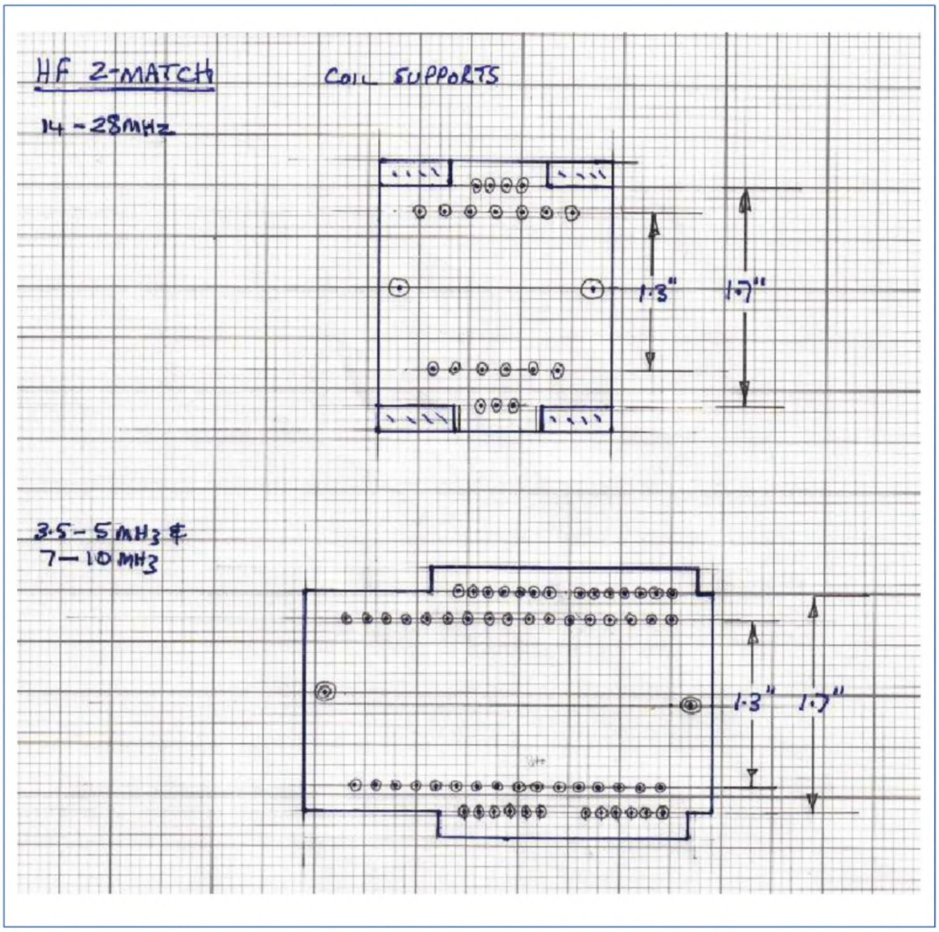

PHOTO 4: Support templates for the HF transformers L1/L2, L3/L4 and L7/L8.

wires is very short compared to a quarter wavelength at the highest frequency. The inductors should be at right angles to each other and spaced away from nearby metal as much as possible, ideally by the diameter of each, to retain their high unloaded Q.

The vertical supports for the two elevated band switches S2 and S4 and variable capacitor C3 must be made from a strong but flexible insulating material and were originally made from Perspex sheet. However, some evidence of cracking appeared after a year or two and one has been changed to 1.6mm fibreglass PC board with all of the copper removed by etching in ferric chloride. It is likely that the other two supports will need changing in due course.

RF CONNECTORS. The author has long used Belling & Lee TV coaxial connectors on HF equipment with no issues with powers up to 100W but some precautions are required for reliable operation:

- The modern plugs have a fairly weak cable clamp (compared to the original plated steel part) which collapses fairly easily under pressure so one half of a small grommet is placed over the coaxial cable centre conductor and inside the cable clamp to provide additional support
- The best socket is the surface mounting type with a robust steel clamp around the periphery

Bob F Burns, G3OOU, C Eng FIET MSE • g3oou@aol.com

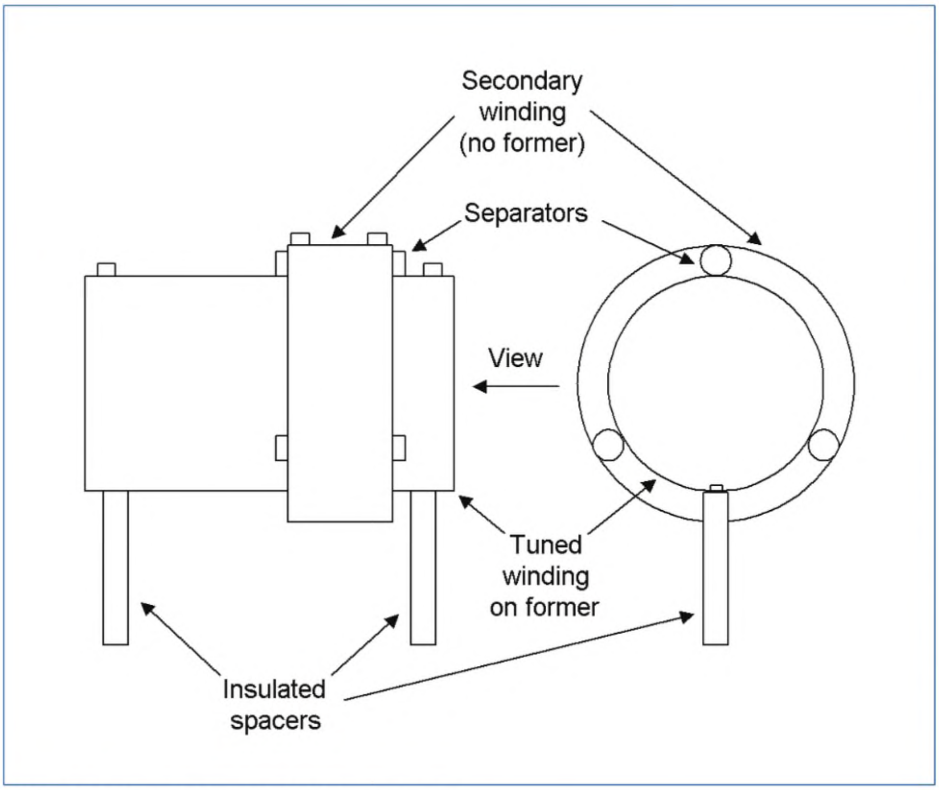

FIGURE 10: The Top Band (1.8MHz) transformer.

- To reduce the inductance of the coaxial cable braid connection fit solder tags to both retaining bolts of the socket and connect half of the braid to each tag
- A very small amount of lubrication should be applied to the section of the plug that mates with the socket to avoid the aluminium surface jamming in the socket
- 50Ω BNC connectors are used on all VHF bands.

The decision on the type of coaxial connector is left to the individual constructor.

CHASSIS LAYOUT – TOP VIEW. This layout shows the position of the major chassis mounted items and the reader should refer to Photo 2 of the interior for more detailed information.

Inductors. The Top Band tuned winding is wound on a conventional former with its secondary wound on a slightly larger former positioned concentrically over the cold end of the tuned winding. At this frequency fibreglass or ceramic formers will be fine but plastic should be avoided as it may not be stable with temperature or time.

Figure 10 shows the Top Band transformer arrangement viewed from the side and end. The separators are glued in place once the inductors have been tested and the tuning range is correct.

Photo 3 shows more details of the Top Band transformer.

All other transformers are wound on the correct diameter template and threaded through pre-drilled polystyrene or acrylic sheet and held in place with an acrylic adhesive [7]. See **Photo 4** for the mandrill drawing.

The graph paper has 2mm and 10mm spaced lines.

Constructors should note that as the wire has a tendency to expand as it unwinds from the mandrill when the tension is released a slightly smaller diameter mandrill will be required compared to the finished inner diameter of each inductor – some trial and error is necessary. Prior to use the wire should be stretched under tension in order to remove any kinks.

Top Band Inductor. **Photo 3** shows the Top Band tuned circuit and secondary winding. The left hand side shows the fibreglass switch support and the miniature brass tubing that was used to make low resistance wiring joints that may be easily taken apart for future maintenance.

30dB Coupler. This function was originally envisaged when operating QRP so an approximate –30dB sample (10mW) was considered sufficient. For use with higher power transmitters the sample probably needs to be –40dB or more below the maximum RF power. At present the sample is obtained by a simple resistive divider. The 1k5 1W resistor in **Figure 4** should be increased to at least 4k7 2W for use with 100W output power or 12k 2W for 400W. Two resistors of half the value in series may be used instead of a single resistor to improve isolation and leakage across the resistor due its self capacitance.

VHF Z-MATCH CONSTRUCTION. The close-up view in **Photo 5** shows the main components in the VHF matching circuit and the simple method of retaining the concentrically positioned inductors using strips of Perspex or acrylic. The 50/70MHz tuned circuit is at the bottom and the 144MHz tuned circuit at the top.

CALIBRATION DISKS. Each disk was marked out on a one sixteenth inch (1.6mm) thick acrylic or Perspex sheet, the centre hole drilled and the overall shape roughly cut out, slightly oversize. The cut item was then mounted onto a threaded rod with washers and nuts, held in the chuck of a small lathe [6] and the outer edge turned down to the correct size using a very sharp cutting tool. Keep the turning speed down to avoid overheating and melting the plastic material. The disks were then temporarily mounted on each Jackson Bros 4511DAF epicyclic drive [8] to mark the mounting hole positions for the retaining bolts, removed and drilled.

FINISHING. Once the metal work is completed, the front and rear panels may be finished as follows:

- Rub down the side to be painted with a well worn foam rubber abrasive sanding block. Do not use a new block as it will excessively score the panel surface.
- Wash in luke warm water and washing up liquid to remove any remaining aluminium dust, rinse well and dry.
- Degrease with white spirit, cellulose thinners etc. in a well ventilated area.
- Paint the outer surfaces and edges with a cold acid etch primer [4] and leave to dry and cure for twenty four hours. If the finish is particularly uneven it may be gently smoothed down with a fine wet and

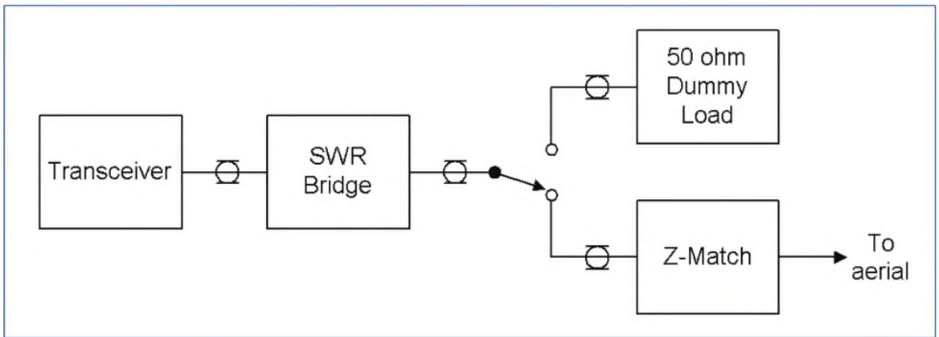

FIGURE 11: Generic block diagram.

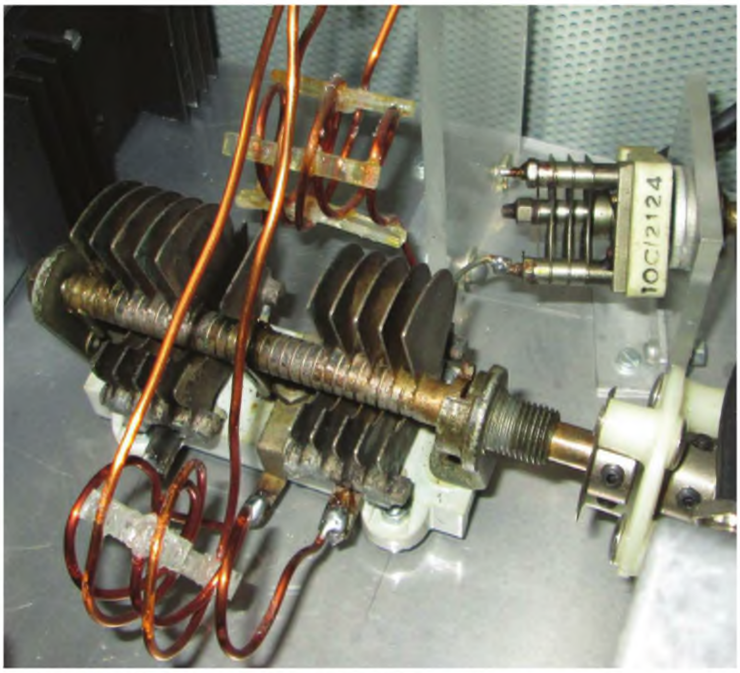

PHOTO 5: The main components in the VHF matching circuit.

dry rubbing down paper, wrapped around a rectangular block, under a running cold water tap. If too much primer is removed then bare metal will show which will require additional primer and smoothing.

- Paint with the chosen colour. The author uses Humbrol or Revell enamel modelling paint that was number 48 to match the Heathkit matt 'green' but do check in case the numbers have since changed. Several coats may be required with smoothing down of each with wet and dry paper as above.

LETTERING. Letter the panels using dry transfer lettering which is manufactured by Letraset and DECAdry and available from stationers, art and graphic design outlets. The author uses a large rounded end knitting needle to burnish the lettering down onto the painted panel. If a light colour paint has been used then black lettering is best. If, as with the author, a darker colour has been used then white lettering is best. If you make a mistake then the lettering may be very gently scraped away with a model maker's curved scalpel without damaging the paint surface and the error corrected. To ease the placement of the letters a positioning template may be drawn on drafting film and used as a guide for the lower edge of each letter or word.

There are two options for the switch position dots as Letraset no longer supply solid dots – use a lower case letter 'o' and fill it in with paint or drill a small shallow hole in the paint with a sharp drill and fill that with paint – the same colour as the lettering. The author uses the latter with a pre-drilled jig held in place in the switch mounting hole and a one sixteenth inch (1.6mm) diameter drill.

Spray the lettered surface with a fixative spray. Letraset make a suitable spray but the author had some difficulty in finding a local outlet and changed to using an acrylic spray. Note that the acrylic spray will dissolve the dry transfer lettering so the first coat should be very fine, quickly applied and left to thoroughly dry. Subsequent coats may then be applied with little risk of damage to the lettering. The author's preferred finish is matt as this does not reflect room light or day light but this choice is, of course, left to the individual constructor.

The same lettering and fixative processes are applied to the perspex/acrylic calibration disks on each variable capacitor.

A sheet of paper was carefully marked out to scale with the centre hole and the eleven calibration points spaced every 18° and marked 0 – 100.

The paper was mounted on a flat surface with masking tape, the disks correctly held in position on the paper with some more masking tape and the calibration marks and numbers 0 - 100 put in place. White dry transfer lettering was used in the same way as the front panel.

Each marked disk was then given an initial very quick coat of clear acrylic spray, allowed to dry and then a more substantial final coat.

The completed disks are mounted directly onto the front of the Jackson 4511DAF 6:1 epicyclic reduction drives with two small bolts – originally these were 8BA but may now be an equivalent metric size.

TEST AND ADJUSTMENT. Each section of each Z-Match may be tested separately commencing with the SWR bridges.

Select HF, connect a known good 50Ω load to the HF 'through' socket, apply 5-10W of RF at 29MHz and adjust the preset balance control in the HM-102 for the lowest reflected power indication on the meter. The balance control in the HM-102 is a preset trimmer capacitor.

Select VHF, connect a known good 50Ω load to the VHF 'through' socket, apply 5-10W of RF at 51MHz and adjust the preset balance control in the HM-2102 for the lowest reflected power indication on the meter. The balance control in the HM-2102 is a preset trimmer capacitor. Repeat the same test using a frequency of 145MHz. The author noted a better balance sensitivity at 145MHz compared to 51MHz so the constructor should choose the best one.

Once these adjustments are complete both SWR bridges may be closed up.

Select HF and Reflected Power, connect a multiband HF transceiver and an HF aerial to the HF Z-Match. On receive on the 1.8MHz band, find a clear channel and adjust the HF tuning capacitor for a peak in received noise. Now go to transmit and using 5 – 10watts of output power, adjust the tuning and loading controls until you have the lowest reflected power reading. Once found, record the frequency and capacitor settings for future use. If a good match cannot be found, check the wiring and coil windings in case an error

TABLE 3: Inductor details.

Inductor	Turns	Wire guage	Dimensions / Remarks
L1	6	16swg	See Photo 2 for the support jig
L2	9	16swg	L2 and L4 are a single 15 turn winding tapped at 9 turns
L3	6	16swg	
L4	6	16swg	
L5	3+3+3	18swg	Each group of 3 turns are close wound with tapping points at 3, 6 & 9 turns – see Photo 3 for more details
L6	22	16swg	Close wound
L7	6	16swg	See photo 2 for a template for the support jig
L8	3	16swg	
L9	2	16swg	1.25 inch ID, 0.375 inch wide
L10	3	16swg	0.75 inch ID, 0.25 inch wide
L11	3	16swg	0.75 inch ID, 1.25 inch wide
L12	2	16swg	1.25 inch ID, 0.25 inch wide

Bob F Burns, G3OOU, C Eng FIET MSE • g3oou@aol.com

PHOTO 6: Rear panel of the finished Z-Match unit.

in construction has been made. Repeat these tests on each HF band up to 29MHz using the shortest time 'on air' to minimise interference to other band users.

Check the forward power reading on all bands using a calibrated wattmeter and 50Ω dummy load connected to the HF 'through' socket. The readings should not change significantly on any band. Adjust the power calibration preset control in the HM-102 to obtain the correct power reading on the meter, ideally using a power that is as close to full scale as is possible.

Select VHF and Reflected Power, connect a multiband VHF transceiver and a VHF aerial to the VHF Z-Match. On receive on the 50MHz band, find a clear channel and adjust the VHF tuning capacitor for a peak in received noise – use AM or SSB but not FM in this case. Now go to transmit and using 5 – 10W of output power, adjust the VHF tuning and loading controls until you have the lowest reflected power reading. Once found, record the frequency and capacitor settings for future use. If a good match cannot be found, check the wiring and coil windings in case an error in construction has been made. Repeat these tests on each VHF band up to 145MHz using the shortest time 'on air' to minimise interference to other band users.

Check the forward power reading on all bands using a calibrated wattmeter and 50Ω dummy load connected to the VHF 'through' socket. The readings should not show major changes on any band but presets have been provided in **Figure 6** in case the frequency response is not entirely flat. Adjust each power calibration preset control to obtain the correct power reading on the meter on the respective band, ideally using a power level that is as close to full scale as possible.

In the event that a good tuning point cannot be found on one or more bands or the tuning point is too close to the end of the tuning capacitor travel it may be necessary to increase or decrease the number of turns in the respective tuned winding.

In the event that a good matching point cannot be found on one or more bands then the respective secondary winding may have to be increased or decreased.

OPERATION. The generic block diagram in **Figure 11** shows how to connect up any form of Z-Match including the one in this article.

Many years ago with CW and AM valve transmitters, the normal process for setting up an aerial matching unit was to tune the transmitter and AMU for maximum aerial current on a particular band and that was it. Solid state and valve based SSB transmitters however require the power amplifier (PA) to see the correct load impedance for best linearity and longest operational lifetime. This is best achieved with a valve PA by first loading the PA into a dummy load to obtain the correct amount of dip in anode current at the desired output power. Modern solid state PAs are normally broadband and have no tuning and loading controls.

Now, for both types of PA, reduce the output power, switch to receive, select the correct band on the Z-Match, switch from the dummy load to the Z-Match, key up the transmitter and adjust both tuning capacitors in the Z-Match for minimum reflected power. Once this has been achieved, the Z-Match is providing a close to 50Ω load to the transmitter so switch back to receive and make a note of the settings and frequency for future reference. The output power may now be increased to the desired level for normal operation.

The constructor will find that the tuning characteristic for minimum reflected power is usually a lot sharper than the changes in aerial current or forward power to the aerial.

Possible future developments

- Static discharge resistors
- Improvements to the –30dB coupler
- A 70cm line based Z-Match for use on my stub loaded HF/VHF dipole aerial [1]
- An automated Z-Match using microprocessor controlled stepper motors for tuning

COMPLETED UNIT. The finished unit, shown at the beginning, has been in operation for several years with no problems to date.

REFERENCES

[1] Stub Loaded HF/VHF Dipole, Bob F Burns G3OOU, *RadCom*, June 2015, www.qsl.net/g3oou/aerialsandfeedersforhf.html

[2] A Top Band Z-Match, R F Burns G3OOU, *RSGB Bulletin*, September 1961

[3] TO-220 resistors: BI Technologies / TT Electronics MHP50101F Resistor, 100Ω 1% 50W TO-220 or Vishay SFERNICE RTO050F100R0JTE1 RES, Thick Film, 100R, 5%, 50W, TO-220 both available from Farnell / Element 14

[4] Acid Etch Primer (grey) and a matching solvent available from Howes Models Ltd, Kidlington, Oxon.

[5] Goddards Silver Dip

[6] Seig Micro Lathe available from Axminster Power Tool Centre Ltd

[7] Acrylic adhesive – Revell Contacta Professional in a 25g container with an inbuilt applicator

[8] Jackson Bros is now part of Mainline

[9] RG142 PTFE coaxial cable available from Burklin GmbH & Co, Germany. Carriage costs make a group purchase more cost effective.

Dr Chris Barnes, GW4BZD • Chris@gw4bzd.co.uk

Examining Sporadic-E

New methods for predicting the start of the UK Sporadic-E season

INTRODUCTION. Sporadic-E, or Es is, as the name suggests, a highly variable and sporadic form of radio propagation dependent on lesser known characteristics of the Earth's ionosphere. A good and readable review of Es and related propagation suitable for radio amateurs is to be found at [1].

Some of us wait patiently in springtime for the start of this apparently random season, which seems to vary from April to even as late as early June. The question arises then, could we ever predict such a start with any more certainty. This article will attempt to show just that and explain the scientific reasoning behind it.

We are all familiar with HF sky wave propagation wherein the diurnal and solar cyclic ionisation properties of the so called F region in the ionosphere bends or, more correctly, scatter refracts radio signals back toward the Earth's surface. The F layer is a continuous region whereas with Sporadic-E radio signals bounce off much smaller clouds or volume patches of unusually ionised atmospheric gas in the lower E region (altitude range approximately 90 to 160km). Sporadic-E occasionally allows for long distance communication at VHF, usually only suited to line of site or tropospheric propagation.

Communication distances of 800–2200km can occur as a result of a single Es cloud. This variability in distance depends on a number of factors, including cloud height and density. The maximum useable frequency (MUF) also varies widely, but most commonly falls in the 27–110MHz range, which includes the amateur radio 10 6 and 4m bands. Propagation at 2m and even higher frequencies may occur in very strong Es events.

As a random and abnormal event and not the usual condition, Es can occur at almost any time; it does, however, display seasonal patterns. Because of this, Sporadic-E activity peaks predictably in the summertime in both hemispheres. In Europe and North America, the peak is most noticeable in mid-to-late June, trailing off through July and into August. Sometimes subsequent smaller peaks are seen in late autumn and around the winter solstice.

Until recently, many countries in Europe transmitted low band analogue TV that with an appropriate 'dual standard' receiver could be used as an ideal indicator of the presence of Es propagation. These days few, if any, such signals remain with the advent of UHF DVB. Still, a reasonable indicator of the probability of finding 6m Es propagation is the presence of short or very short skip on 10m. For example, a good start is to search for local 10m beacons such as, for example, but not limited to, the German CW beacon on 28.205MHz.

Signals received via Sporadic-E can be extremely strong and may range from barely perceptible in strength to overloading over very short periods. Although polarisation shift can occur, single-hop Sporadic-E signals tend to remain in the original transmitted polarisation. A long single-hop is in the region of 900–1,500 miles or 1,400–2,400 kilometres. Shorter-skip (400–800 miles or 640–1,290 kilometres) signals tend to be reflected from more than one part of the Sporadic-E layer, resulting in flutter and even phase distortion.

Sporadic-E usually affects 6m most regularly, 4m somewhat less and there can be as few as two or three good 2m openings in a season. The typical expected distances are about 600 to 1,400 miles (970 to 2,250km). However, under exceptional circumstances, a highly ionised Es cloud can propagate 6m signals down to approximately 350 miles (560km). When short-skip Es reception occurs, ie under 500 miles (800km) on 6m, there is a greater possibility that the ionised Es cloud will be capable of reflecting a signal at a much higher frequency – ie at 2m – since a sharp reflection angle (short skip) favours low frequencies, a shallower reflection angle from the same ionised cloud will favour a higher frequency [2].

At polar latitudes, Sporadic-E can sometimes accompany auroras and is then associated with disturbed magnetic conditions called Auroral-E [3].

MECHANISM OF SPORADIC-E. We are learning more about Sporadic-E year on year (see *RadCom* June 2015) but no one single mechanism fully explains all its attributes. Attempts to connect the incidence of Sporadic-E with the eleven-year sunspot cycle have, however, provided tentative correlations. There seems to be a positive correlation between sunspot maximum and Es activity in Europe. Conversely, there seems to be a negative correlation between maximum sunspot activity and Es activity in Australasia.

Thunderstorms are also known to affect Sporadic-E, see Davies and Johnson (2005) [4]. This and the link with solar behaviour suggests that the behaviour of Es clouds must be capable of atmospheric modulation from both above and below. Whitehead (1989) [5] has summarised a considerable amount of both theoretical and experimental work on Es. His findings imply that mid-latitude Sporadic-E is most likely due to a vertical shear in the horizontal east-west wind and that this theory accounts for the detailed observations of the wind and electron density profiles. Preferred heights of Sporadic-E are separated by about 6km and descending layers are often seen moving down with velocities in the range 0.6–4 ms. Sometimes Sporadic-E layers are very flat and uniform, and at other times form clouds of electrons 2–100km in size moving horizontally at 20–130ms^{-1}. Surprisingly, Whitehead also finds that Sporadic-E is probably not correlated with meteor showers even though a source of the ions involved might be meteor debris. This is because metal ions are stable in the E-layer for long periods.

Further, according to Whitehead, the major problem with purely a windshear theory of Sporadic-E is in accounting for the dramatic seasonal variation and, to a lesser extent, for the geographical and diurnal distributions.

Sporadic-E clouds are ideally shaped for radio reflection and are known to have a concave underside with an extremely high internal electron density making them difficult to track with HF radar, see From and Whitehead (1978) [6].

Davies and Johnson (2006) [7] have shown that during a thunderstorm multiple mechanisms enhance the Es layer, especially gravity waves and EMPS above Elves (upwardly propagating lightning). Sporadic-E propagation from a fixed location is known to exhibit a wax and wane effect over an approximate 40 minute or so interval. I believe a paper by Lu et al (1984) [8] may explain this elegantly. In making VHF Doppler Radar Observations of Buoyancy Waves Associated with Thunderstorms they have observed large quasi-sinusoidal wave trains with periods of about 40 minutes. Power spectra of the vertical velocity time series showed enhancements at all frequencies during thunderstorm activity, but for periods longer than 30 minutes the enhancements were larger, particularly for the mid-tropospheric range gates from 5.7 to 12.9km. I believe such wave trains periodically enhance the E layer accordingly as upwardly propagating gravity waves. Furthermore, when no thunderstorm activity was present, the vertical velocity fluctuations were small and erratic.

Some have suggested that Sporadic-E propagation cannot take place in the absence of thunderstorms but others have shown an association with jet streams. The latter is not so unreasonable, considering the work of Fritts and Nastrom (1992) **[9]** who consider Sources of Mesoscale Variability of Gravity Waves due to Frontal, Convective, and Jet Stream Excitation they conclude a major role for localised sources in energising the mesoscale motion spectrum at horizontal scales <~100km, and correspondingly greater influences for such motions at greater heights. Such heights are exactly those where the Es clouds are found.

Other earth and atmospheric scientists concur with the opinion that the ionosphere, eg F region is inevitably driven from both above and below, see for example Rishbeth (2006) **[10]**. They conclude that 'Ionospheric weather', as a part of space weather, (ie hour-to-hour and day-to-day variability of the ionospheric parameters) awaits explanation and prediction within the framework of the climatological, seasonal and solar-cycle variations. Further they give the reason for the extreme variability of the thermosphere–ionosphere system as its rapid response to external forcing from various sources, ie, the solar ionising flux, energetic charged particles and electric fields imposed via the interaction between the solar wind, magnetosphere and ionosphere, as well as coupling from below ('meteorological influences') by the upward propagating, broad spectrum, internal atmospheric waves (planetary waves, tides, gravity waves) generated in the stratosphere and troposphere. They also state that thunderstorms, typhoons, hurricanes, tornadoes and even seismological events may also have observable consequences in the ionosphere. Even the release of trace gases due to human activity have the potential to cause changes in the lower and the upper atmosphere. They summarise experimental results that have confirmed that the ionosphere is subject to meteorological control (especially for geomagnetic quiet conditions and for middle latitudes). D region aeronomy, the winter anomaly of radiowave absorption, wave-like travelling ionospheric disturbances, the non-zonality and regional peculiarities of the lower thermospheric winds, Sporadic-E occurrence and structure, spread-F events, the variability of ionospheric electron density profiles and Total Electron Content, the variability of foF2, etc., and feel that these all should be considered in connection with tropospheric and stratospheric processes.

PREDICTING THE START OF THE SPORADIC-E SEASON (6m). Following the previous thoughts, reference to weather maps, thunderstorm detectors and Jetstream mapping ought, as others have already suggested, and to some extent experimentally proved, to be useful in predicting the possibility of individual Sporadic-E events but could we ever predict when the season might commence and how long it might last?

Riggin (1986) **[11]** has studied the plasma instabilities associated with night-time Sporadic-E layers, using the Cornell University Portable Radar Interferometer (CUPRI), a 50MHz Doppler radar system. The CUPRI beam was directed over Arecibo, Puerto Rico, and concurrent electron density profiles within the CUPRI scattering volume were measured by the Arecibo Observatory's 430MHz radar. During the strongest Es event, radar echoes were received from several altitudes up to 130km. Large mean Doppler velocities (at times exceeding 250m/s) were observed during this event and the power spectra closely resembled those obtained at the magnetic equator. This led to the conclusion that the mid-latitude large-scale waves are generated by the same gradient drift instability mechanism responsible for equatorial large-scale waves and that the similar type waves can be generated at mid-latitudes with drift velocities well below the sound speed because of the very sharp plasma density gradients associated with metallic ion Sporadic-E layers.

Following from this, I have applied a little lateral thought to the problem of prediction. The buffer sitting between the ionosphere and the troposphere is the stratosphere. The winds above the equator in the upper stratosphere exhibit a peculiar pseudo cyclic variation in direction, phase and amplitude the so called Quasi-biennial oscillation (QBO). The history and development of theories of the QBO have been summarised by Lindzen (1987) **[12]**. The direction of the QBO has merely been linked with Atlantic storminess in the past and more recently discussed by the Met Office Centre for Ecology and Hydrology **[13]**. I wondered if the QBO could be used for far more detailed medium term weather trend prediction and after examining retrospective data have filed a series of patents accordingly **[14, 15]**. This disclosure does not compromise the detail. Since the weather and Sporadic-E are clearly linked and since according to Riggin [11] equatorial and mid latitude processes with regard to Sporadic-E may be linked, it was natural for me to extend this hypothesis to examine if there was any link between the QBO and the start of the Es season. The QBO is commonly recorded by meteorologists as the so called zonal wind index. The two most common QBO zonal wind indices refer to equivalent pressure heights of 50mb and 30mb and data for these is available from NOAA **[16, 17]**. The sign of the index indicates the direction of the zonal wind and the numeric value assigned indicates the descent rate.

So, is there any firmer evidence that the QBO and Sporadic-E could be linked? There are several references in the scientific literature to the appearance of so called time series wave behaviour in Sporadic-E, ranging from the 40 minute wax and wane effect, through the diurnal tide effect (there are even some references to a tri-urnal (8h) effect) to longer Planetary wave periods of 2, 5, 10 and 16 days as, for example, reported by Haldoupis et al (2004) **[18]**. One paper, Pancheva et al (2003) **[19]** observes a seven day period and another a five day period, see Tsunoda et al (1998) **[20]**. The Pancheva paper is important for it establishes a 7-day periodicity in foEs directly with concurrent variations over a large distance in the mesospheric neutral wind measured with atmospheric radars in Saskatoon, Canada, and in Sheffield, UK and provides a new physical explanation for the observed relation between Sporadic-E layers and planetary waves.

The QBO direction and descent rate is also known to affect the entire global circulation at 50mb, see Holton and Tan (1980) **[21]**, both Southern and Northern Polar Vortices, Baldwin et al (2012) and Calvo et al (2009) **[22,23]**, Jet stream and storm tracks, see Tinsley (1988) **[24]**, and to modulate the length of certain Planetary wave periods, see for example Sato et al (1994) **[25]**, Mitchell et al (1999) **[26]**, Sridharan et al (2003)**[27]**, Kodera (1993) **[28]**, Hibbins **[29]** and, finally, Cheng and Huang (1999) **[30]** whose study provides illustrative support for the mechanism of the QBO modulation of planetary wave propagation and the associated effects in the residual meridional circulation.

Considering all of this data, we now have a scientific basis for the hypothesis presented by this work.

EXPERIMENTAL METHOD. The initial data given is for North Wales. The experimental date data simply comprises retrospective date entries in my amateur radio log dating back to 1992 ie approximately 2 solar cycles. Since that date, I have been a keen 6m operator and have, in the past, often checked the bands on a methodical basis to try and establish the presence of Es. One can assume that, retrospectively, I may often, but not necessarily have always, caught the very start date of the Es season because until this present study that was not my specific intention. One cannot guarantee that one will always be in the operating shack 24/7, thus any such data can be subject to error. Nevertheless, it was decided to use these past first observed Es dates from previous years as a first attempt at 'start' date data. The zonal wind data was obtained from www.cpc.ncep.noaa.gov/data/indices/qbo.u50.index [16], and were the values of the zonal wind index in the month of March preceding each year's Es season.

An attempt was made to correlate the onset of the Es season each year with the value of the 50mb zonal wind index in April of each same year. Initially a linear correlation was attempted but the correlation factor was poor. The best fit is obtained using a cubic equation. Data plotted only represents the Es seasons in which I was active between 1992 and 2013. The former and the latter dates are inclusive. 2014 data has not been included in the model.

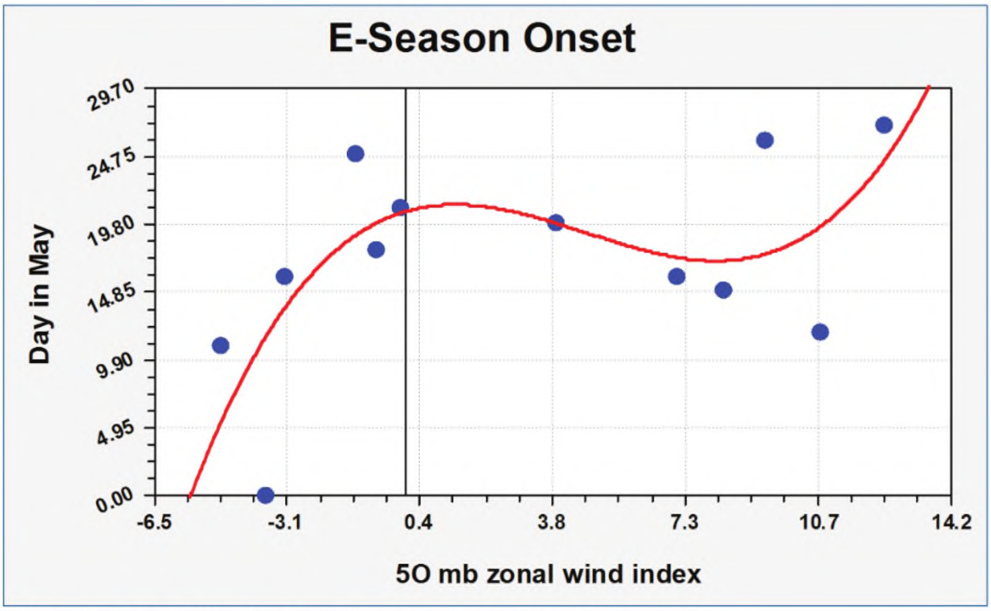

FIGURE 1: The initial result of data collected by the author in North Wales.

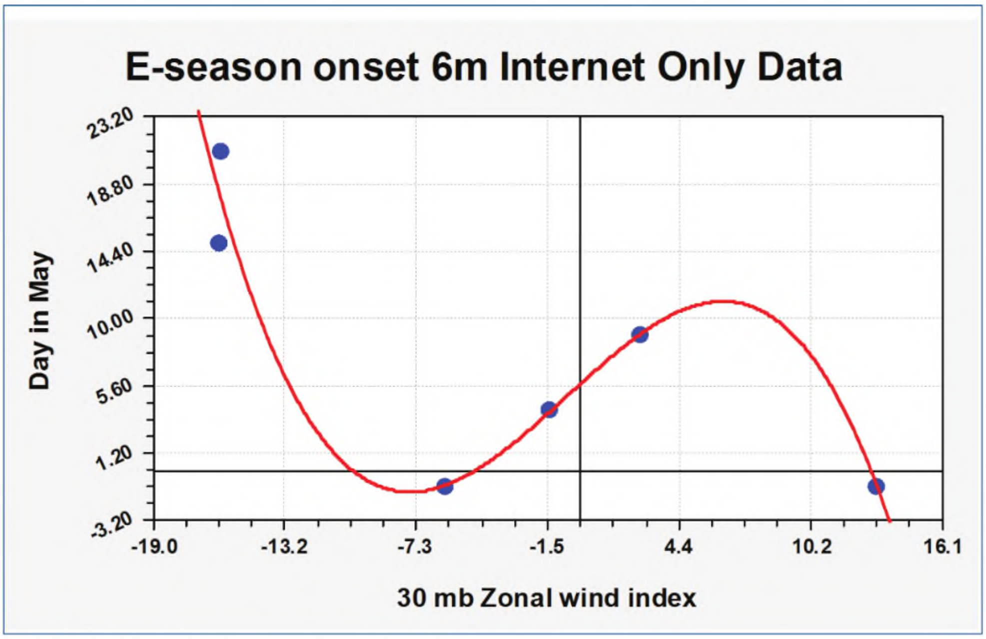

FIGURE 2: Refined results using internet only data.

INITIAL RESULTS. The initial results are shown in **Figure 1**.

The value of the 50mb zonal wind index for April 2014 was given on the NOAA website as 9.72. When this value is plugged into the curvefit model using the above cubic fit a start date of May 14.85 is returned. Significant variation can be seen between some of the data points and the curve predicted. It is suggested here that particularly for the points in error lying above the data plot, these may have been generated with higher values on occasions the author was simply not in the shack at about the right time in order to catch the earliest Es opening of the season. Clearly with the model in this state it is not sufficient to prove the hypothesis but does offer a tantalising taste of what might be possible. The best fit points seem to predict the start of the season to within a day but the worst fit ones can be out by up to ± several days.

REFINING THE MODEL. The main question is can this sort of model be refined to be worthwhile? It would be ideal if, for example, the prediction could be made with more notice. Due to the way in which the zonal winds descend this is not a problem. Data from zonal winds higher in the atmosphere, the so called 30mb QBO offers predictably of Es April or May onset dates from as early as January. Due to phase variations in the descent rate, the shape of the new plot will not be expected to mirror the above plot but it may also be cubic in general form.

The first subsequent question is can the data input be refined to make it more reliable? The notion of using retrospective start date data acquired from Internet sources seems reasonable in that a large number of amateur radio operators will have contributed thereby increasing the chances of coming up with a correct start date for the Es season in any given year.

A second subsequent question is can an algorithm generated by date data from the internet by refined by making a compilation of data from the present author's log?

REFINED RESULTS. The refined result using January 30mb zonal wind data and internet only Es start dates is shown in **Figure 2**. This time the data is a near perfect fit to the cubic model, with a near perfect regression order =0.974. The phase is shifted with respect to the in initial result above for the 50mb zonal wind.

The validity of the model was tested by fitting years not available in the internet data and comparing them to my data. In cases where my observed start data was equal to or less than the predicted date this too was then adopted into the model. My data with start dates beyond those predicted by the model were rejected on the basis that I had simply not been in the operating shack at the right time to catch the appropriate start date.

The compilation data file and its best cubic fit are shown in **Table 1** and in **Figure 3**.

TABLE 1: Compilation data file.

Index	Day Number	Year
-13.99	5	1992
9.62	5	1993
8.37	7	1995
-5.8	-1	1996
0.74	10	1998
1.4	11	1999
4.62	11	2000
-15.02	12	2001
4.63	14	2002
-4.84	1	2004
-1.4	7	2004
-0.46	5	2005
-18.9	23	2006
2.6	9	2007
-12.43	4	2008
10.71	2	2009
-16.02	18	2010
9.18	9	2011
-16.09	15	2012
-6.07	-1	2013
13.13	-2	2014

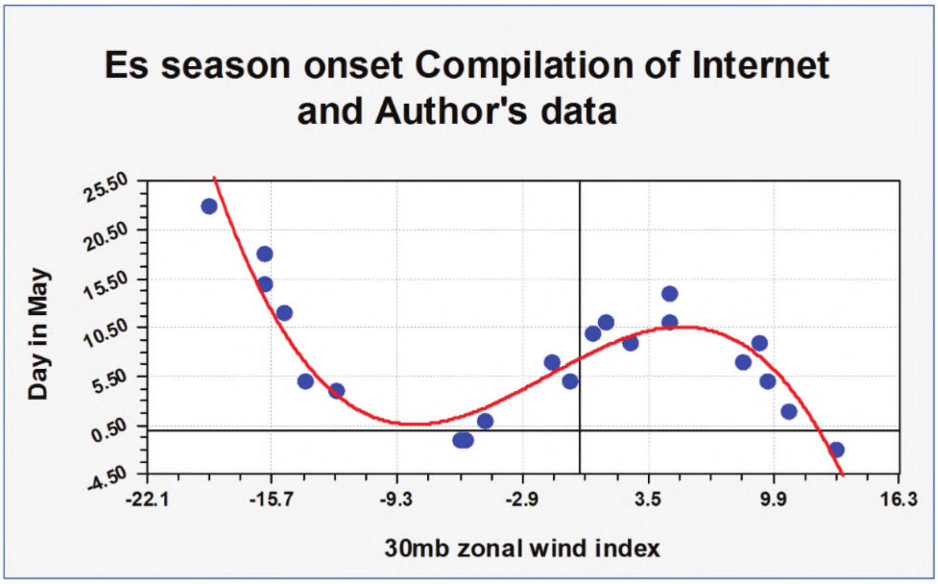

FIGURE 3: Best cubic fit data.

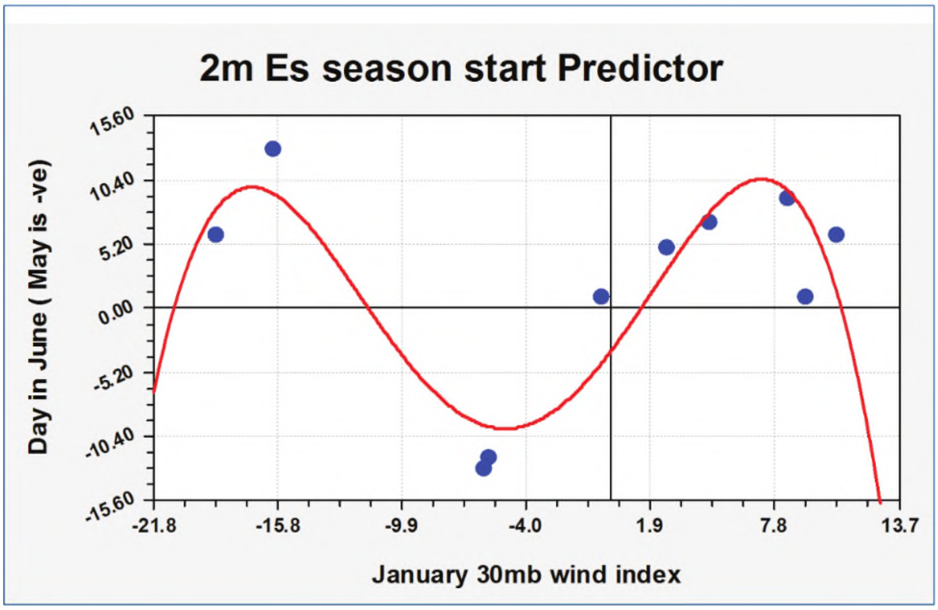

FIGURE 4: 2m predictions based on internet only data.

The correlation coefficient for this data set is .93 and the worst case predictability for any year's Sporadic-E season start date is within 2.5 days. Given the sensitivity to geographic position in the UK that I have noted when using similar modelling for weather trend prediction this is quite impressive.

2 METRES. As the Es season progresses, the openings become more intense and there may be propagation as high as 144MHz (2m). Most 2m openings occur in June, although some occur earlier. The same approach has been taken to model available 2m data. I have a poor 2m location and simple antenna and rarely experience 2m Sporadic-E so, in this case, reliance has been placed on internet data from a variety of sources. Since some openings start in May, days in April are represented by negative values on the ordinate axis in **Figure 4**.

The regression factor of .88 is somewhat lower than that for the 6m predictor giving a potential margin of uncertainty of about 5 days. As such the predictor is less useable than the 6m predictor but given the number of separate geographic sources taken to compile the data and the very local geographic sensitivity of Es propagation in general then this is perhaps not surprising.

DISCUSSION. We have learned here that through a combination of atmospheric science and lateral thinking it has been possible to remove some of the mystery from the enigmatic phenomenon of Sporadic-E. It has, perhaps become a bit less sporadic and a bit more predictable!

Having such a method at our disposal will have time saving implications for ardent Es hunters of the future and may well be useful for climate and space weather researchers to boot.

PREDICTING SPORADIC-E. In the UK and Europe, it is generally accepted that the main Sporadic-E or Es season starts in April or May, peaks in June or July and is all but over by late August. Reed (1997) **[31]** has offered an explanation for different shaped activity distributions in Sporadic-E openings in terms of X-ray solar flux.

Occasionally we see an additional peak or peaks in Sporadic-E activity in late autumn and again around the mid-winter period, which might coincide with the main southern hemisphere peak.

Following the method developed for predicting the start of season, I decided to explore if the state of the QBO (equatorial zonal wind) could also be used to predict the length of the main season.

EXPERIMENTAL. This time data was much harder to come by. Reed's data [31] for 6m suggested that, at least at his QTH, 1996 activity in August was significantly lower than that for 1994 and 1995. My own log certainly concurs that 1996 was an early ending season.

Since internet data appears scarce in defining the end of the 'main' season, I relied entirely on data from my own log that covers some but not all of the 6m seasons from 1992 to 2013. I have defined the 'main' season length in days from when Sporadic-E was first worked in April or May through to the last contact found in the log but excluding any contacts in late October, November or December on the basis that according to the data of Reed [31], these are distinctly separate peaks.

RESULTS. The season lengths were plotted against the corresponding year's March 50mb zonal wind indices. The results which correlate best according to a cubic function and are shown in **Figure 5**.

This time the regression factor is only of the order of .7, so not brilliant, and nowhere near as good as for using this type of method to predict the onset of the Es season and meaning that any estimate could be out by up to ±13 days. However, given that the whole season can vary from about 70-130 days in length any improved estimate on this is welcome. The result is shown in Figure 5.

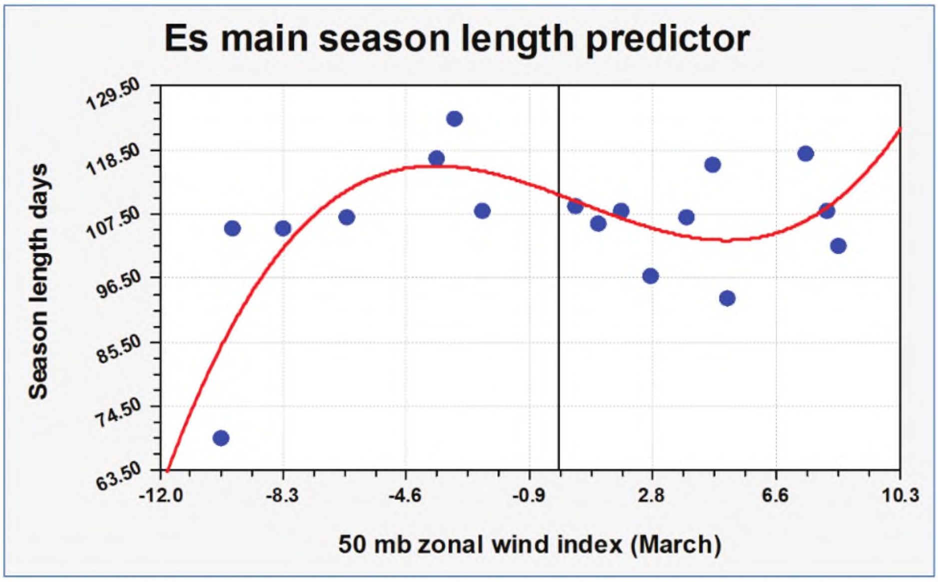

FIGURE 5: Season lengths were plotted against the corresponding year's March 50mb zonal wind indices.

DISCUSSION. On the basis of his 1990s data, Reed [31] has suggested changes in solar X-ray flux as being an important factor in determining the shape of the Es season intensity-duration distribution function. I have no data between 2008 and 2012 but the data for 2007, which had low sunspot numbers, has a reasonably low season length of 97 days but not the shortest. Clearly there are other factors at work. This is because Es and the atmosphere in general depends on driving from both above and below.

Most certainly the solar cycle influences the QBO, see Liu et al (2010) **[32]** and Nastrom and Belmont (1976) **[33]** and the QBO and storm tracks, see Tinsely (1988) **[34]**. Possibly other planets perturb the Earth-Sun magnetic field as well, see Dudok de Wit and Watermann (2009) **[35]**.

However, solar influence on our atmosphere is only half the story. We must also consider cosmic rays as well, see Tinsley et al (2012) **[36]**. High energy galactic cosmic rays can not only have an influence on the ionosphere direct but also possibly on cloud nucleation in the troposphere, see Pierce (2011) **[37]** and Tinsely and Deen (1991) **[38]**. Both could thus be relevant to the behaviour of Sporadic-E.

It is thus very instructive to plot the duration of the main 6m Es season against percentage deviation from an 'average' GCR (Galactic Cosmic Ray) input to the planet, see **Figure 6**.

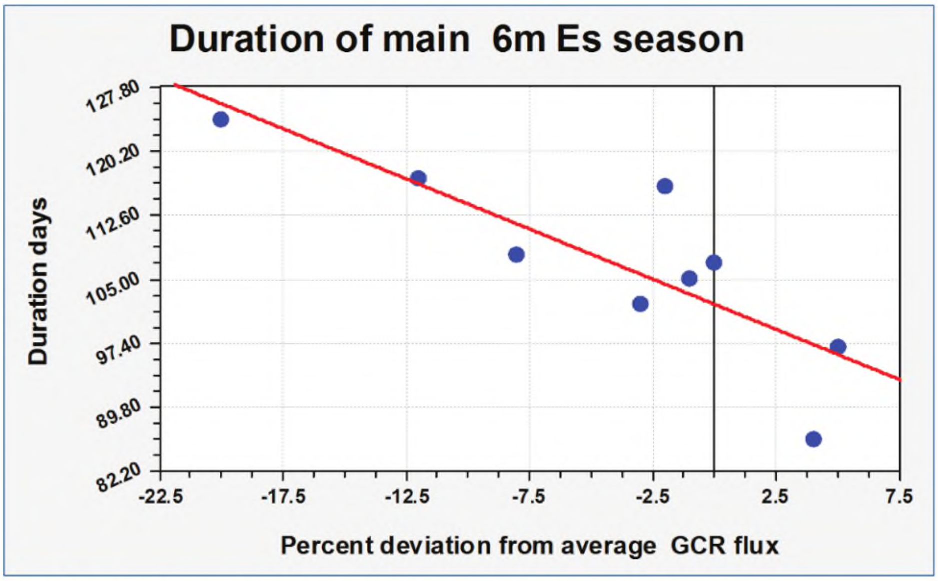

FIGURE 6: Cosmic rays can possibly influence cloud nucleation in the troposphere.

The GCR data are courtesy of the Oulu Cosmic Ray Station in Finland (http://cosmicrays.oulu.fi/). The linear regression factor is .83 and an even higher correlation coefficient can be obtained by switching to a quadratic fit. In any event, the duration of the Es season can be predicted well by this method.

Although the GCR flux varies hourly and on a day by day basis, it also varies more dramatically over longer timescales of years and so might probably be able to be used predictively for Es seasons as an adjunct to or possibly prove more effective than the zonal wind method.

Thunderstorms are, of course, very relevant to Sporadic-E and Schlegel et al (2001) **[39]** have found that lightning frequency is anti-correlated with cosmic ray flux. Thus accordingly the present hypothesis would suggest, the more cosmic ray flux, the less lightning and hence the less Sporadic-E. Since this effect seems to determine the duration of the season it is more than likely countered by the effect of both meteor injection and any high speed solar wind streams at the start of the season which can enhance thunderstorms for up to 40 days, see Scott 2014 **[40]**.

CAN WE PREDICT SPECIFIC OPENING DATES? There have been several publications in recent years linking Sporadic-E openings to thunderstorms. So, if we know where the thunderstorms are, we might be able to predict the likely path of an opening. But could we ever predict more precisely on which days to listen for Es once the season has started or after any subsequent opening, at least know the days with highest probability of finding an opening.

In the past, people have suggested that the aftermath of certain meteor showers may increase the probability of Es openings on specific dates. However, the metal ions that meteors inject tend to be very long lived in the ionosphere so perhaps we need an alternative hypothesis. Planetary waves were first proposed as relevant to metal ion Es layers as early as 1997, see Clemesha et al (1997) **[41]**.

Previously, we saw how a strong solar wind stream could enhance Es for up to 40 days. We might ask the question, if this is the case, why is there not just one continual Es opening for the entire season. Indeed, the facts are there are probably almost continual openings somewhere in the Northern Hemisphere sometime in the summer months. It is the much localised nature of Es clouds in time and space that limits us. Then because of this we need to know just what puts Es clouds in a particular place at a particular time. The best hypothesis we have is the planetary wave hypothesis. This tends to suggest that there should be repetitions in Es openings at intervals of two or three times a day, see Fytterer et al (2013) **[42]** and according to the normal Rosby wave interludes of 2,5,7,10 and 16 days, see Haldoupis, C., Pancheva, D. and Mitchell, N.J., 2004 **[43]**. Because there can be non-linear interactions between planetary tides and planetary waves, see for example but not exclusively Kamalabadi et al (1997) **[44]**, we might also potentially expect Es openings with these Rosby wave periodicities ±1 day and ±1.5 days. There are two ways of checking this.

First, we can check the scientific literature and examine what has been discovered and published. Secondly, we can examine archive data of real openings and QSOs. I have examined my own log for 6m data and has examined multiple internet sources for 2m data.

EXPERIMENTAL. The number of instances of a particular number of days gap (between 1-20 days) between openings from the UK has been examined for both 6m and 2m and converted into a statistic. At the height of the Sporadic-E season across some 20 years of data the results are very informative. The *minimum* probability of finding a 2m opening is 11-12 days after a first opening or after subsequent openings. For 6m the *minimum* probability is also at day 12 but *also in the period days 17-20.*

So at least we now know when **not** to expect an Es opening.

The maximum probabilities for 2m Sporadic-E openings is shown in **Table 2**, while **Table 3** shows the results for 6m Sporadic-E.

TABLE 2: Maximum probabilities for 2m Es.

2 metres

Rank	Day (s)	Probability
1	1	0.14
2	4	0.11
3	7	0.11
4	10	0.11
5	2,3,8	0.07
6	9,13,18	0.05
7	5,14,17,19,20	0.036
8	6,15	0.018
9	11,12,16	0

TABLE 3: Maximum probabilities for 6m Es.

6 metres

Rank	Day (s)	Probability
1	5	0.16
2	2	0.14
3	1	0.127
4	3	0.11
5	9,10	0.08
6	6	0.064
7	4,7,16	0.05
8	8	0.032
9	11,14,15	0.016
10	12,17-20	0

DISCUSSION. The day ranking orders are different for each band. *For 2m, the highest probability of finding another opening is a day after the first.* Presumably this is because the much higher ionisation levels required are able to persist better the first 24 hours. The Rosby wave periods of 7 and 10 days also feature quite strongly and overall there are combined odds of about 7/10 of finding another opening sometime within the first week but at first sight and from this statistic alone it would seem we could never say this with any more certainty.

It is instructive to look at the 6m results. Here, the common Rosby wave periods feature more strongly. There is better than a 6/10 chance of having another opening in the first 5 days and almost an 8/10 chance of finding another opening within the first week after a first or subsequent opening during the season.

Voiculescu et al (1999) **[45]** have examined a large database of mid-latitude E region coherent backscatter, obtained with a 50MHz Doppler system and used it to investigate the long-term variability in echo occurrence. They found the backscatter to be dominated by pronounced quasi-periodic variations with periods in the range from about 2 to 9 days that persisted for time intervals from about 10 to maybe more than 20 days and which have no relation to geomagnetic activity. The most commonly observed periods appeared in two preferred bands, namely a 2 to 3 day and the 4 to 6 day band. Using concurrent ionosonde data they found that variations in backscatter were exactly in-phase with similar periodicities in the occurrence of relatively strong Sporadic-E layers. Their findings support the present hypothesis that planetary waves are responsible for longer term periodicity in Es. They also concluded there is a close relation between planetary waves and the well-known, but not well understood, seasonal Es dependence, which I expanded upon earlier in this article. From the results above it is evident that 4-6 day band is relevant to both 6m and 2m openings but that both timescale bands are relevant to 6m openings.

The work in the present article strongly supports the notion that Sporadic-E may, in many ways, be more predictable than we ever thought. We now know when a season might start, how long its main part is likely to be and the days with highest probability to listen for openings on various bands. Nevertheless, on those days we should still look for evidence of triggers particularly thunderstorms towards one or other end of the intended propagation path. I have also noted that small patches of Jetstream flowing roughly orthogonal to the proposed path are also a good pointer. An excellent Jetstream online mapping facility to use for this purpose is the one at the California Weather Server **[46]**.

In the final part of the article I will ask the question can we predict years in which a late autumn blip in Es activity will occur and is there such a thing as mid-winter Es in the UK or is what we hear really F2 propagation?

PREDICTING LATE AUTUMN SPORADIC-E. In order to try and understand autumn and possible winter Es propagation, we need to revisit the mechanism of Sporadic-E.

No one single hypothesis completely explains the behaviour of Sporadic-E. This does not mean to say that existing hypotheses are incorrect, it is more likely that we need to combine various facets of each to get nearer to the true picture.

Although meteors are probably not relevant to individual Sporadic-E openings they are a very important source of metal ions at E layer height. Wind shear is equally important. Haldoupis et al (2012) **[47]** have shown that mid-latitude Sporadic-E layers form when metallic ions of meteoric origin in the lower thermosphere are converged vertically in a wind shear. Further they found that the occurrence and strength of Sporadic-E follow a pronounced seasonal dependence marked by a conspicuous summer maximum. Something known, of course, by radio amateurs for some five or six decades, and also known since the early years of ionosonde studies, the cause of this summer peak has remained a mystery as it cannot be accounted for by the windshear theory of Es formation alone. Further Haldoupis et al [47] showed that the marked seasonal dependence of Sporadic-E correlated well with the annual variation of sporadic meteor deposition in the upper atmosphere.

Perhaps the key paper on meteor rates is that of Singer et al (2004) **[48]** that studied meteor rates per se at the Arctic Circle without specific reference to Sporadic-E. However, when one looks at the distribution curves for 2002-2004 the number of meteors per hour across a year more or less mirrors but somewhat precedes the likelihood of UK /European/ Northern Hemisphere Es with a pronounced summer peak. For meteors this is between day 165 and 190, possibly 30-40 days earlier than the Es peak. It is interesting to note that meteoric material in the ionopshere has a long lifetime of this order before falling to the troposphere where it can act as cloud nucleating centres, see for example Bowen (1955) **[49]**, given this there is possibly no wonder Haldoupis et al [47] were able to reach their conclusion. There would appear to be two smaller sub-peaks in meteor rate some 30 days before the late autumn and mid-winter period.

We are all familiar with the fact that meteor showers are very regular in nature so why then are autumn and winter Es openings not so consistently regular.
In fact, close inspection of the data for 2002-2004 does show slight year on year variation. Whether it is possible to use this variation in known meteor showers to account for the large observed year on year absence or presence of October/ November Es openings remains to be seen. Kopp (1997) **[50]** has certainly shown that metal ions are very abundant at Sporadic-E layer height with mean total column density of the ionised metals is within $4.4 \pm 1.2 \times 109\ cm^{-2}$ in even in periods without special meteor shower activity. They also showed the column density to increase by 1 order of magnitude during the Perseid meteor shower of 12 August 1976. Since the Perseids precede the late autumn Es 'blip' by about 80 days and meteoric deposit's lifetime in the upper atmosphere is about half this period, I feel it may be unlikely that they are causative in this respect.

Wright (1967) **[51]** was perhaps one of the first to propose an understanding of Es similar to that we have today. He made standard measurements of Sporadic-E blanketing frequencies (fbEs, assumed to indicate peak ion densities) during November 1965 from three temperate latitude stations. His understanding predicts two important properties of Sporadic-E: (a) that major events consist predominantly of slowly-recombining monatomic ions, probably of meteoric origin, and (b) that these ions converge and accumulate in thin layers through combined effects of the geomagnetic field and the profile of horizontal winds. His data seemed to prove both facets of Es were prerequisite. Again the hypothesis of a meteoric origin for the ions suggested that major events of fbEs might correlate with the increased meteoric mass arriving during large showers. Wright

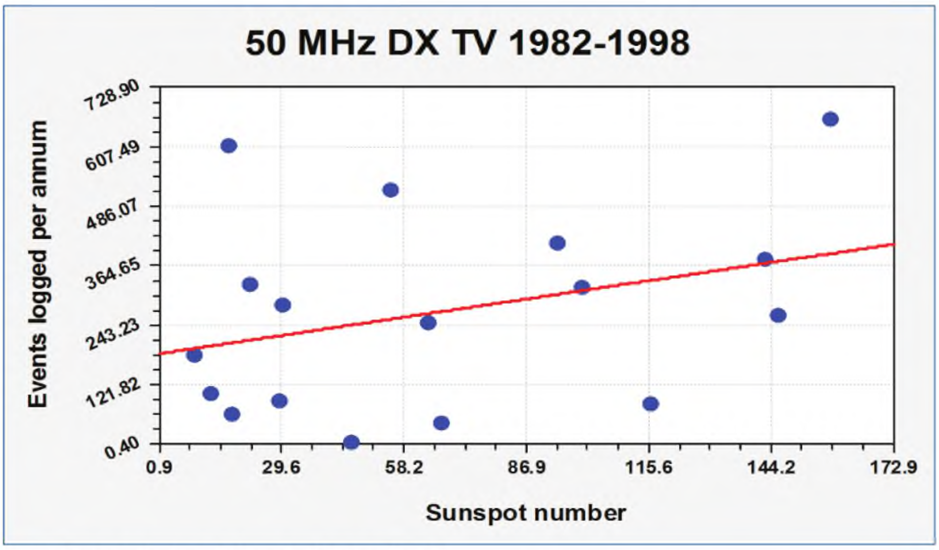

FIGURE 7: Analysis of data collected by G4FBZ.

[50] presented some evidence of this correlation for the November 1965 Leonid meteor shower. The Leonid shower is regarded as both bright and fast **[52]**. I feel that given the lifetime of meteoric material it is possible this shower may be sufficient to account for mid-winter Es openings although these tend to be more a North American than a European feature.

One question remains, how does Es break up from thin continuous layers to become more like apparently sporadic or randomly moving lens shaped patches. Moreover, could this mechanism be crucial in understanding why we sometimes have late autumn and winter Es and other times do not. We only need to look at a smooth pond or calm sea to perceive an answer. The surface of which can become very perturbed as a result of wind and waves. The atmosphere is literally full of tides and waves on all sorts of timescales from seconds to many days. Some waves for instance such as the acoustic gravity waves (AGW) above thunderstorms have very dramatic effects and propagate up to E layer height, this has been both observed by both atmospheric scientists, see Kazimirovski **[53]** and also as proposed by radio amateurs, see for example Grassmann et al **[54]**. So maybe thunderstorms provide sufficient wind shear energy to break the Es layers into patches and their repetition is linked with planetary waves, see earlier. There is additional evidence that Es are influenced by other types of gravity waves. For instance, SM7GVF has found a link between Es and volcanic activity **[55]**. Volcanoes generate strong upwardly moving infrasound of, in some cases, up to 10 million watts acoustic power, see for example, but not exclusively, Johnson (2013) **[56]**. Es is enhanced during solar eclipses and the proposed mechanism is the effect of temperature gradient on wind shear, see Chen et al (2010) **[57]**.

Given this, we can now formulate additional hypotheses about what might influence the presence of otherwise of late season Es openings. Although these lesser mechanisms such as volcanoes and eclipses are academically interesting, thunderstorms remain the single most common and documented feature to do with Es. Let us ask ourselves if there is anything that could control the seasonal occurrence of thunderstorms, because if so this would also control Es and our chances of seeing late season openings.

DATA AND EXPERIMENTAL. When one searches online for amateur radio references to Es openings outside the usual May-August season, references are indeed very scarce. Before we can fully formulate a hypothesis we must try and acquire sufficient data to examine which years have exhibited good late season Es. One such useful reference is the '6 and 10 report' [58], which concluded that Es was the controlling factor for DX on 6m in October 1998 whereas F2 was the controlling factor for 10m. Additionally, M6PCZ refers to some very short skip on 10m in October 2010 but concludes it was backscatter rather than Es. He does not mention whether this is tropospheric or ionospheric propagation but another possibility is that it was tropospheric ducting, see **[59]**. My data suggests that late autumn Es were prevalent in the following years: 2003, 2004 and 2007.

A huge amount of data for propagation in the 40-70MHz band has been gathered by DX TV enthusiast William Kitching, G4FBZ during the years 1992-1998 inclusive **[60]**. The data, re-evaluated by me in **Figure 7**, is whole year data so it has not been possible to separate out the late season Es peak. However, it is instructional in that it only shows a weak correlation with solar cycle, suggesting that only a small fraction of what was received was F2 propagation.

The months/years with autumn openings that Kitching **[60]** specifically refers to as being possibly Es or a mix of Es and F propagation are November 1988 and October/ November 1989. Interestingly, 1988 features in the 6/10 report above also and the two years 1988 and 1989 have the lowest ever cosmic ray counts in the last 50 years or so.

HYPOTHESIS. From the behaviour observed above it is possible to formulate a simple hypothesis, namely that; in years with increased cosmic ray activity there is certainly an early end to the main Es season, see earlier.

Thus the hypothesis being presently proposed is that low cosmic ray counts together with an appropriate bright, fast meteor shower some thirty days earlier favour late autumn Sporadic-E openings. The cosmic ray connection being because cosmic rays and thunderstorms are actually anti-correlated, see U. V. Shamansky and Vladimir A. Kovalenko (2003) **[61]** and Kozlov et al (2007) **[62]**.

The anti-correlation is perhaps somewhat surprising given that Svensmark and Friss-Christensen 1997 **[63]** published in the journal *Atmospheric, Solar and Terrestrial Physics* an indication that cloud cover varies in cycle with cosmic ray intensities suggesting a close cause-and-effect-relationship. Because cosmic rays are anti-correlated with the 11-year sunspot cycle, this predicts that cloud cover is modulated by solar activity in a non-direct way. The two are not at odds because of the way in which cosmic rays influence the global electric field and atmospheric conductivity however. I also have another suggestion, that is that increased cloud cover will tend to cause global cooling which ought to reduce storm intensity generally and vice versa.

RESULTS. The results shown, **Table 4**, are a compilation my own data and those from the references above and appear to be in support of the hypothesis.

It can be clearly seen that there are no late season openings observed in years when the cosmic ray flux is above 7% over average.

UK MID–WINTER ES? Again data is very scarce and hard to come by. My only experiences of mid-winter propagation were in 2000 and 2001 respectively and were to the USA and Canada at times of very high solar activity. I have always assumed this was, therefore, F2 propagation. However, these years represent years when the cosmic ray flux was -3% and -5% below average respectively and thus since there would appear to be an element of discrepancy I would welcome hearing from anyone who has logged shorter, European contacts at this time of year that did not occur during tropospheric lift conditions. It is also interesting to note that activity from the Leonid meteor shower (November) peaks approximately every 33 years, see Chandra et al (2001), [64] and that the year 2000 was only 1 year after such a peak.

TABLE 4: Compilation of data.

Year	Cosmic Ray Count percent from average	Months	Es
1988	-15%	oct/nov	Yes
1989	-15%	oct/nov	Yes
1992	-5%	sep	Yes
1997	7%		None
2002	-5%	sep	Yes
2003	-6%	nov	Yes
2004	-12%	nov	Yes
2007	5%	oct	Yes
2009	10%		None
2010	7%		None

OVERALL CONCLUSIONS. This article has shown us that Sporadic-E as a useful DX mode for VHF radio amateur operators is perhaps a little less 'sporadic' and a little more predictable than any of us would have ever thought. Moreover, it has given us a clearer picture of mechanism Sporadic-E and has established links between the various and previously 'competing' theories of Es.

We can see Es clouds as:

- Localised offshoots of Es layers containing highly conductive metal ion interiors and radio reflective concavely curved lower surfaces
- Meteors as a long lived 30-40 day metal ion source
- Patchy Es clouds arising because of coalescence and propulsion by wind shear which is modulated at multiple levels in time and space by AGW from thunderstorms, and planetary waves and tides

We can see the start of the 6m Es season as:

- Predictable to within a few days in more than a month
- Predictable by using an algorithm connected to the behaviour of the QBO (zonal equatorial winds)
- This being the link between energy inputs from 'above' and 'below' and modulator of many atmospheric features world-wide

We can see the start of the 2m Es season as similarly predictable.

We can see that once the season has started or that once a strong opening has occurred that there are higher probabilities of finding openings on some days than others according to planetary wave hypothesis advance here but not withstanding the presence of strong thunderstorms along possible propagation paths. Probability of a re-occurrence is greatest on the first day after a 2m opening and on the 5th day after a 6 metre opening. The 6m behaviour is most closely in line with the observation of Tsunoda et al [20]. Probability of re-occurrence is second greatest on the 4th, 7th and 10th days after 2m openings and on the 2nd,1st and 3rd days after 6m openings in rank order, all these, lengthwise, are either Rosby wave periods or Planetary wave periods modulated by planetary tides and would therefore appear to confirm the new hypothesis proposed here. Finite probability of Es repeat openings on the second, fourth and tenth days after the start of a season or any subsequent opening is consistent with the observations of Karami et al (2012) **[65]** using a digital ionosonde for Es over Tehran in July 2007 but interestingly no 16 day periodicity is found here which is contrary to the observations of Karami.

We can predict the end of the main Es season either by means of a QBO algorithm or by means of a GCR algorithm again to within a relatively small number of days.

We can use the Oulu GCR monitor to predict the likelihood of late autumn Es that only seem to occur for a comic ray count of 5% or more below average but conceivably may be also influenced by the quality of meteor showers some 30 days earlier.

We only remain somewhat uncertain about mid- winter Es which, at the height of the solar cycle could conceivably be hard to distinguish from F2 propagation. An appeal for more data from other operators might resolve this situation.

FURTHER POSSIBILITIES. Increased predictability of Es propagation may conceivably have advantages for other uses of the radio spectrum such as for example military and emergency international communications. Because of the intimate connection of Es with both troposphere and ionosphere there may even be implications for climate and weather forecasting. Troposphere and ionosphere are also thought to be linked to the lithosphere via the global electric circuit and via the earth's magnetic field. Thus there may even, remote as it may seem, be implications for volcanism and earthquake forecasting.

REFERENCES

1: Collection of articles on Sporadic-E: www.df5ai.net/Material/articles.html

2: http://en.wikipedia.org/wiki/Sporadic_E_propagation

3: www.dtic.mil/dtic/tr/fulltext/u2/a265059.pdf

4: Lightning-induced intensification of the ionospheric Sporadic-E layer, C J Davis & C G Johnson, *Nature* 435, 799-801 (9 June 2005) | doi:10.1038/nature03638, Abstract at www.nature.com/nature/journal/v435/n7043/abs/nature03638.html

5: Recent work on mid-latitude and equatorial Sporadic-E, *Journal of Atmospheric and Terrestrial Physics*, Volume 51, Issue 5, May 1989, Pages 401–424 Abstract at: www.sciencedirect.com/science/article/pii/0021916989901220

6: On the peculiar shape of Sporadic-E clouds, Journal of Atmospheric and Terrestrial Physics olume 40, Issue 9, September 1978, Pages 1025–1028 Abstract at: www.sciencedirect.com/science/article/pii/0021916978900065

7: The location of lightning affecting the ionospheric Sporadic-E layer as evidence for multiple enhancement mechanisms, C J Davies and C G Johnson (2006) *Geophysical Research Letters* > Vol 33 Issue 7 Abstract at : http://onlinelibrary.wiley.com/doi/10.1029/2005GL025294/abstract

8: VHF Doppler Radar Observations of Buoyancy Waves Associated with Thunderstorms, Daren Lu, T E VanZandt and W L Clark, J. Atmos. Sci., 41, 272–282. Abstract at: http://journals.ametsoc.org/doi/abs/10.1175/1520-0469(1984)041%3C0272%3AVDROOB%3E2.0.CO%3B2

9: Sources of Mesoscale Variability of Gravity Waves. Part II: Frontal, Convective, and Jet Stream Excitation. Fritts, David C, Gregory D Nastrom, 1992: J. Atmos. Sci., 49, 111–127.doi: http://dx.doi.org/10.1175/1520-0469(1992)049<0111:SOMVOG>2.0.CO;2. Abstract at http://journals.ametsoc.org/doi/abs/10.1175/1520-0469(1992)049%3C0111:SOMVOG%3E2.0.CO%3B2

10: F-region links with the lower atmosphere? H Rishbeth - *Journal of Atmospheric and Solar-terrestrial Physics*, 2006 – Elsevier. Abstract at www.sciencedirect.com/science/article/pii/S1364682605002567

11: Radar studies of long-wavelength waves associated with mid-latitude Sporadic-E layers, D Riggin, W E Swartz, J Providakes, D T Farley, *Journal of Geophysical Research*: Space Physics (1978–2012) > Vol 91 Issue A7. Abstract at http://onlinelibrary.wiley.com/doi/10.1029/JA091iA07p08011/abstract?deniedAccessCustomisedMessage=&userIsAuthenticated=false

12: A Theory of the Quasi-Biennial Oscillation, Lindzen, Richard S, James R Holton, 1968, J. Atmos. Sci., 25, 1095–1107.doi http://dx.doi.org/10.1175/1520-0469(1968)025<1095:ATOTQB>2.0.CO;2.

13: Report of the CEH, UK Met Office 2014, www.metoffice.gov.uk/media/pdf/1/2/Recent_Storms_Briefing_Final_SLR_20140211.pdf

14: UK Patent application number GB1403127.2

15: UK Patent application number GB1404039.8

16: www.cpc.ncep.noaa.gov/data/indices/qbo.u50.index

17: www.cpc.ncep.noaa.gov/data/indices/qbo.u30.index

18: A study of tidal and planetary wave periodicities present in mid-latitude Sporadic-E layers, Christos Haldoupis1, Dora Pancheva and N J Mitchell, *Journal of Geophysical Research: Space Physics*, Volume 109, Issue A2, February 2004. Abstract at http://onlinelibrary.wiley.com/doi/10.1029/2003JA010253/abstract

19: Evidence of a role for modulated atmospheric tides in the dependence of Sporadic-E layers on planetary waves, *Journal of Geophysical Research: Space Physics* 2003. Abstract at http://onlinelibrary.wiley.com/doi/10.1029/2002JA009788/abstract

20: Quasi-periodic radar echoes from mid-latitude Sporadic-E and role of the 5-day planetary wave, *Geophysical Research Letters*, Roland T. Tsunoda, Mamoru Yamamoto, Kiyoshi Igarashi, Klemens Hocke and Shoichiro Fukao, Volume 25, Issue 7, pages, 951–954, 1 April 1998. Abstract at http://onlinelibrary.wiley.com/doi/10.1029/98GL00663/full

21: The Influence of the Equatorial Quasi-Biennial Oscillation on the Global Circulation at 50mb, James R Holton and Hsiu-Chi Tan, J. Atmos. Sci., 37, 2200–2208. Abstract at http://journals.ametsoc.org/doi/abs/10.1175/1520-0469(1980)037%3C2200:TIOTEQ%3E2.0.CO;2

22: Quasi-biennial modulation of the southern hemisphere stratospheric polar vortex, Mark P Baldwin and Timothy J Dunkerton, *Geophysical Research Letters*, Volume 25, Issue 17, pages 3343–3346, 1 September 1998. Abstract at http://onlinelibrary.wiley.com/doi/10.1029/98GL02445/full

23: Nonlinearity of the combined warm ENSO and QBO effects on the Northern Hemisphere polar vortex in MAECHAM5 simulations, Natalia Calvo, Marco A Giorgetta, Ricardo Garcia-Herrera and Elisa Manzini, *Journal of Geophysical Research: Atmospheres*, Volume 114, Issue D13, 16 , July 2009. Abstract at http://onlinelibrary.wiley.com/doi/10.1029/2008JD011445/abstract

24: The solar cycle and the QBO influences on the latitude of storm tracks in the North Atlantic, Brian A Tinsley, *Geophysical Research Letters*, Volume 15, Issue 5, pages 409–412, May 1988. Abstract at http://onlinelibrary.wiley.com/doi/10.1029/GL015i005p00409/abstract?deniedAccessCustomisedMessage=&userIsAuthenticated=false

25: 'Short Period Disturbances in the Equatorial lower Stratosphere, K Sato, F Hasegawa, I Hirota - J. Meteorol. Soc. Jpn, 1994 - www-aos.eps.su-tokyo.ac.jp Full paper at www-aos.eps.s.u-tokyo.ac.jp/~kaoru/CV/PDFs/SatoHasegawaHirotaJMSJ1994.pdf

26: The 16- day planetary wave in the Mesosphere, by NJ Mitchel, DOI: 10.1007/s00585-999-1447-9; Print ISSN: 0992-7689; Online ISSN: 1432-0576; Publisher: Springer-Verlag; Additional Links. 1. Department of Physics, The University of Wales, Aberystwyth, Ceredigion, SY23 3BZ, UK; 2. Find at http://link.springer.com/article/10.1007/s00585-999-1447-9#page-1

27: QBO influences on the variability of planetary waves in the equatorial mesopause region, S Sridharan1, S Gurubaran1, and R Rajaram1, Earth Planets Space, 55, 687–696, 2003, Full version at www.terrapub.co.jp/journals/EPS/pdf/2003/5511/55110687.pdf?origin=publication_detail

28: Quasi-decadal modulation of the influence of the equatorial quasi-biennial oscillation on the north polar stratospheric temperatures, *Journal of Geophysical Research: Atmospheres,* Volume 98, Issue D4, pages 7245–7250, 20 April 1993. Abstract at http://onlinelibrary.wiley.com/doi/10.1029/92JD02930/abstract?deniedAccessCustomisedMessage=&userIsAuthenticated=false

29: Quasi-biennial oscillation influence on long-period planetary waves in the Antarctic upper mesosphere, R E Hibbins, M J Jarvis and E A K Ford, Journal of Geophysical Research: Atmospheres, Volume 114, Issue D9, 16 May, 2009. Full paper at http://onlinelibrary.wiley.com/doi/10.1029/2008JD011174/full

30: Modulation of Planetary Wave Propagation by the Tropical QBO, Chen and Whang, 1999. Full paper at: http://cmsr.iap.ac.cn/upload/File/cw/1999-1-QBO-CAP.pdf

31: A Review of 50MHz Sporadic-E in 1996, Issue 53 *Six News*, May 1997, by Steve Reed, G0AEV, http://www.uksmg.org/content/es96.htm

32: The Influence of the 11-Year Sunspot Cycle on the Atmospheric Circulation during Winter,Liu Yi, LU Chun-Hui, *Chinese Journal of Geophysics* Vol.53, No.3, 2010, pp: 354~364. Full paper at: www.agu.org/wps/ChineseJGeo/53/03/ly.pdf

33: Nastrom, G.D. and Belmont, A.D. (1976). The influence of long-period dynamo region winds on the surface geomagnetic field elements. *Journal of Geophysical Research* 81. doi: 10.1029/JA081i025p04800. issn: 0148-0227. Abstract at http://earthref.org/ERR/25806/

34: The solar cycle and the QBO influences on the latitude of storm tracks in the North Atlantic, Brian A. Tinsley, *Geophysical Research Letters*, Volume 15, Issue 5, pages 409–412, May 1988. Abstract at http://onlinelibrary.wiley.com/doi/10.1029/GL015i005p00409/abstract

35: Solar forcing of the terrestrial atmosphere, Thierry Dudok de Wit, Jürgen Watermann, C R. Geoscience xxx (2009) xxx–xxx, External geophysics, climate and environment

(Climate). Abstract at: http://lpc2e.cnrs-orleans.fr/~ddwit/soleil/DdW_solar_forcing_CRGeo2009.pdf

36: Solar Variability Influences on Weather and Climate Possible Connections Through Cosmic Ray Fluxes and Storm Intensification Brian A Tinsley Center for Space Sciences, University of Texas at Dallas, Richardson, Texas, Journal of Geophysical Research, Vol. 94, No. D12, Pages 14,783-14,792, October 20, 1989. Full paper at http://gacc.nifc.gov/sacc/predictive/SOLAR_WEATHER-CLIMATE_STUDIES/GCR%20GEC-Solar%20Variability%20influences%20on%20Weather%20and%20Climate%20GCR%20Tinsley%201989Oct.pdf

37: Cosmic rays and clouds: Potential mechanisms, Jeffrey Pierce, Filed under: Climate modelling Climate Science Sun-earth connections group @ 26 September 2011 - See more at: www.realclimate.org/index.php/archives/2011/09/cosmic-rays-and-clouds-potential-mechanisms/#ITEM-8796-0

38: Apparent Tropospheric Response to MeV-GeV Particle Flux Variations' A Connection Via Electrofreezing of Supercooled Water in High-Level Clouds? Brain A Tinsley and Glenn W Deen, *Journal of Geophysical Research*, Vol. 96, No. D12, Pages 22,283-22,296, December 20, 1991. Full paper at http://gacc.nifc.gov/sacc/predictive/SOLAR_WEATHER-CLIMATE_STUDIES/GEC-Tropospheric%20Response%20to%20MeV-GeV%20Flux%20Variations%20on%20Electrofreezing%20of%20supercooled%20water%20Tinsley%201991.pdf

39: *Journal of Atmospheric and Solar-Terrestrial Physics* Volume 63, Issue 16, November 2001, Pages 1705–1713 Thunderstorms, lightning and solar activity - Middle Europe www.sciencedirect.com/science/article/pii/S1364682601000530

40: Evidence for solar wind modulation of lightning, C J Scott et al 2014 Environ. Res. Lett. 9 055004 doi:10.1088/1748-9326/9/5/055004. Full paper at http://iopscience.iop.org/1748-9326/9/5/055004/article

41: Wave-associated sporadic neutral layers in the upper atmosphere, B R Clemesha, P P Batista & D. M. Simonich, Rev. Bras. Geof. vol 15 no 3 São Paulo Nov. 1997. Full paper at www.scielo.br/scielo.php?pid=S0102-261X1997000300003&script=sci_arttext

42: T. Fytterer, C Arras, and C Jacobi, Mitteil. Inst. f. Meteorol. Univ. Leipzig. Full paper at www.uni-leipzig.de/~jacobi/docs/Fytterer_2013_LIM_8h-Es.pdf

43: A study of tidal and planetary wave periodicities present in mid-latitude Sporadic-E layers. Journal of Geophysical Research, 109 (A2). Haldoupis, C, Pancheva, D and Mitchell, N. J., 2004. Full paper at http://onlinelibrary.wiley.com/doi/10.1029/2003JA010253/full

44: Evidence for nonlinear coupling of planetary waves and tides in the Antarctic mesopause F Kamalabadi J M Forbes N M Makarov and Yu I Portnyagin, Journal of Geophysical Research, Vol 102, No. D4, Pages 4437-4446, February 27, 1997. Full paper at http://onlinelibrary.wiley.com/doi/10.1029/96JD01996/pdf

45: Evidence for planetary wave effects on mid-latitude backscatter and Sporadic-E layer occurrence, Mirela Voiculescu, Christos Haldoupis, Kristian Schlegel, Geophysical Research Letters - Geophys Res Lett 01/1999; 26:1105-1108. DOI:10.1029/1999GL900172. Abstract at www.researchgate.net/publication/252960685_Evidence_for_planetary_wave_effects_on_midlatitude_backscatter_and_sporadic_E_layer_occurrence

46: California weather server, 300mb Jet stream mapping, http://squall.sfsu.edu/crws/jetstream.html

47: An explanation for the seasonal dependence of mid-latitude Sporadic-E layers C. Haldoupis, D Pancheva, W Singer, C Meek, and J MacDougall, *Journal of Geophysical Research*, Vol. 112, A06315, doi:10.1029/2007JA012322, 2007. Full paper at http://onlinelibrary.wiley.com/doi/10.1029/2007JA012322/pdf

48: Diurnal and annual variations of meteor rates at the arctic circle, W Singer, U von Zahn, and J Weiß, Atmos. Chem. Phys., 4, 1355–1363, 200 www.atmos-chem-phys.net/4/1355/2004/acp-4-1355-2004.pdf

49: E. G. Bowen (1955), 'The Relation between rainfall and meteor showers' Commonwealth Scientific and Industrial Research Organization, *Journal of Meteorology*, 13, 142-148. Full paper at www.atmos.washington.edu/~dennis/BowenRainMeteors_1956.pdf

50: On the abundance of metal ions in the lower ionosphere, Ernest Kopp, *Journal of Geophysical Research: Space Physics*, Volume 102, Issue A5 Pages 9497–9842. Abstract at http://onlinelibrary.wiley.com/doi/10.1002/jgra.v102.A5/issuetoc

51: Sporadic-E as an indicator of wind structure in the lower ionosphere and the influx of meteors, J.W. Wright, *Journal of Geophysical Research*, Volume 72, Issue 19, pages 4821–4829, 1 October 1967 Abstract at http://onlinelibrary.wiley.com/doi/10.1029/JZ072i019p04821/abstract;jsessionid=D4705BC17EADE8C8B181407A0788F9F2.f02t04?,deniedAccessCustomisedMessage=&userIsAuthenticated=false

52: Wikipedia List of Meteor Showers http://en.wikipedia.org/wiki/List_of_meteor_showers

53: Coupling from below as a source of ionospheric variability: a review, E S Kazimirovsky, *Annals of Geophysics*, Vol 45, No 1 (2002), Abstract at www.annalsofgeophysics.eu/index.php/annals/article/viewArticle/3482

54: Thunderstorm effects on Sporadic-E propagation in 144MHz by Volker Grassmann (DF5AI), Sabine Cremer (DL1DBC), Udo Langenohl (DK5YA), Allard Munters (PE1NWL), Gabriel Sampol (EA6VQ), Joachim Kraft (DL8HCZ) http://df5ai.net/ArticlesDL/Thunderstorm/ThunderstormEffectsDUBUS.pdf

55: http://sm7gvf.dyndns.org/sm7gvf/sm4gvf/Openings.html

56: Comparison of some volcano infrasounds, Jeffrey Johnson Volcano Acoustics Workshop IAVCEI Kagoshima 2013. Article at https://vhub.org/resources/2801/download/Johnson_volcano_infrasound_comparisons.pdf

57: Gravity waves and spread Es observed during the solar eclipse of 22 July 2009, Gang Chen, Zhengyu Zhao, Yuannong Zhang, Guobin Yang, Chen Zhou, Shuo Huang, Ting Li, Ning Li andHengqing Sun, *Journal of Geophysical Research: Space Physics*, Volume 116, Issue A9. Full paper at http://onlinelibrary.wiley.com/doi/10.1029/2011JA016720/full

58: Sporadic-E (Es) as the control for 50MHz DX, *The Six Ten Report* October 1998. http://homepages.force9.net/explore/6and10/articles/50eslink.htm

59: Definition of tropospheric ducting at http://www.radio-electronics.com/info/propagation/tropospheric/tropospheric-propagation.php

60: DX TV at the height of Sunspot Cycle 22, William F Kitching at: www.g4fbz.net/dxtv/sunspot22/dxtv.htm

61: Influence of cosmic rays on atmospheric-electrical characteristics bottom layers of an atmosphere, U V Shamansky and Vladimir A. Kovalenko, SPIE Proceedings | Volume 5027 | Atmospheric Physics (2003). Abstract at http://proceedings.spiedigitallibrary.org/proceeding.aspx?articleid=757432

62: Relationship between variations in thunderstorm very-low-frequency radio noise and variations in the solar wind density (1979–1994), V I Kozlov, R R Karimov, V A Mullayarov, *Bulletin of the Russian Academy of Sciences: Physics*, July 2007, Volume 71, Issue 7, pp 997-999. Abstract at http://link.springer.com/article/10.3103%2FS1062873807070313#page-1

63: Variation of cosmic ray flux and global cloud coverage, *Journal of Atmospheric and Solar-Terrestrial Physics*, Vol. 59, No. 11, pp. 122&1232, 1997. Full paper at http://kbar.sitecore.dtu.dk/upload/institutter/space/forskning/05_afdelinger/sun-climate/full_text_publications/svensmark_96_variations%20of.pdf

64: Sporadic-E associated with the Leonid meteor shower event of November 1998 over low and equatorial latitudes, H. Chandra, S Sharma, C V Devasia, K S V Subbarao, R Sridharan, J H Sastri, and J V S V Rao, *Annales Geophysicae* (2001) 19: 59–69. Full paper at http://hal.archives-ouvertes.fr/docs/00/31/67/45/PDF/angeo-19-59-2001.pdf

65: Karami, K, S Ghader, A A Bidokhti, M Joghataei, A Neyestani, and A Mohammadabadi (2012), Planetary and tidal wave-type oscillations in the ionospheric Sporadic-E layers over Tehran region, J. Geophys. Res., 117, A04313, doi:10.1029/2011JA017466. Full article at http://onlinelibrary.wiley.com/doi/10.1029/2011JA017466/full

Steve Hunt, G3TXQ • www.steve@karinya.net

High performance common-mode chokes

There can't be many components used by radio amateurs that are more misunderstood than the humble common-mode choke. Many amateurs still haven't even heard of it and even those who have can't agree on its name: is it a common-mode choke, an RF choke, a 1:1 current balun or a 1:1 Guanella balun? Since these are all alternative names for essentially the same device – the name changes mostly with the application – the best answer is probably: 'Any or all of the above'.

I shall generally refer to it as a common-mode choke (CM choke for short), and although very similar chokes can be used for control cables, phone lines etc, the scope of this article will be limited to chokes used in typical HF antenna systems.

This article is an attempt to shed some light on this misunderstood component, covering:

- What a CM choke does
- Why and where we might need one
- What properties it should have
- How to build a good one; and
- How to measure its performance.

But first we need to understand what 'common-mode current' is, and why we usually want to prevent it.

PHOTO 1: A 7-turn broadband common-mode choke.

COMMON-MODE CURRENT.

Figure 1 shows a generator connected to a load impedance ZL via a 2-wire transmission line. One side of the generator is connected to ground, but the load is completely 'floating'.

The basic concept of an electrical circuit tells us that the 'outgoing' current Ia and the 'return' current Ib are in fact the same current, flowing around the loop. There are no alternative paths for that current to take. Because Ia and Ib are flowing along the two legs of the transmission line in opposite directions, there is a phase difference of 180° between them.

Equal and opposite currents in the two conductors of a transmission line are called differential-mode currents. Since the two conductors are very close together, the external fields from the two opposing currents cancel out and the line does not radiate. These are the defining features of differential-mode currents and of a balanced transmission line.

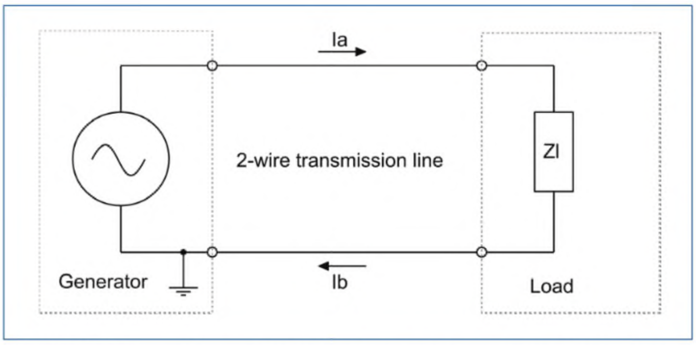

FIGURE 1: Balanced transmission line from a generator to a 'floating' load.

Suppose we now change the conditions at the load by introducing a path to ground, Zc, from the upper leg of the transmission line as shown in **Figure 2**. There are now two different paths that the return current can take. As well as the normal return current along the lower leg of the line, a new current Ic can now flow back to the generator via Zc and earth. Notice that Ic flows into Zc and then down to earth at the load end; and since currents flow in closed loops, that same current Ic will also emerge from the earth terminal at the generator as shown in Figure 2.

Ic is what we refer to as the common-mode current. Any current, Ic, that takes this alternative return path must result in the transmission line currents Ia and Ib being unequal – in other words, the transmission line is no longer balanced. To some extent, this is always the situation in real life.

To distinguish more clearly between differential-mode and common-mode currents that are coexisting on the same transmission line, it is often convenient to think of the unequal currents Ia and Ib as the superposition of a 'pure' differential-mode signal and a separate

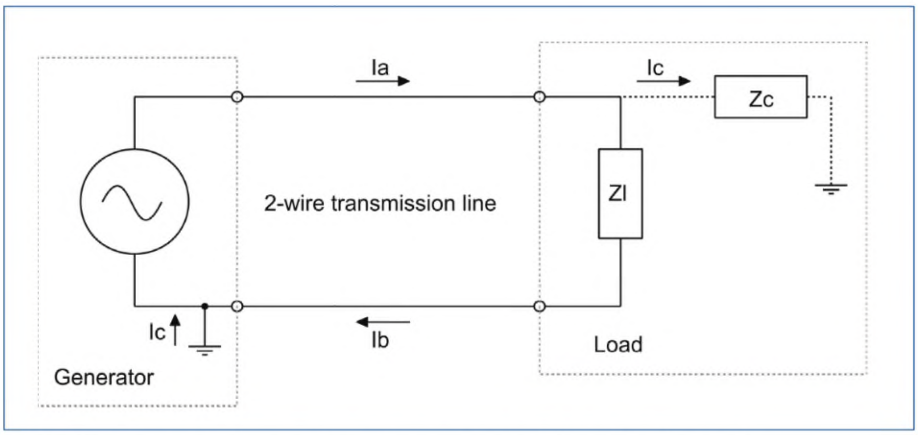

FIGURE 2: Common-mode current Ic creates an unwanted alternative return path.

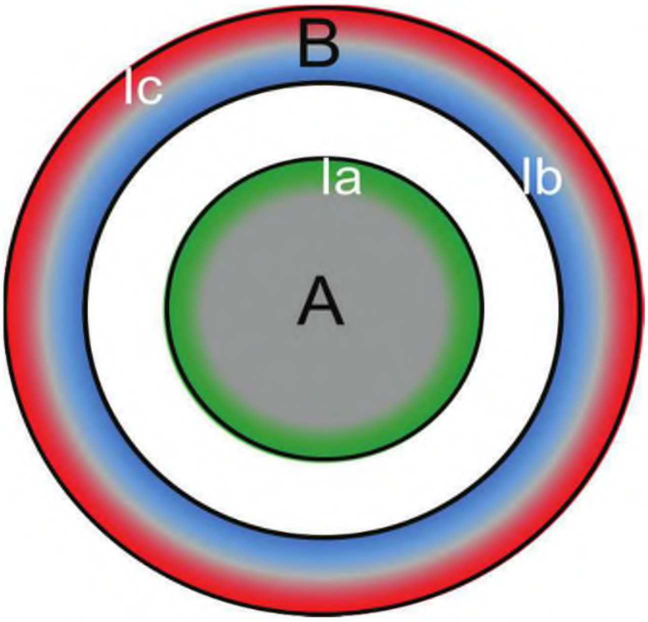

FIGURE 3: Skin Effect makes coax behave as a THREE-conductor transmission line.

common-mode signal. The common-mode current Ic is simply equal to (Ia-Ib). A little more algebra then shows that the differential-mode (balanced) currents in Figure 2 must each be equal to (Ia+Ib)/2.

If all that sounds strange and unfamiliar, it shouldn't, because Figures 1 and 2 also show some basic principles of UK domestic mains supplies. The upper leg of the transmission line is the 'Live' conductor and the lower line leg is Neutral. Figure 1 shows the normal situation where all the current returns in the Neutral leg – in other words, the two-conductor mains cable is intended to function as differential-mode transmission line. Figure 2 then shows a fault condition that allows a 'leakage current' Ic to flow directly from Live to ground rather than returning via Neutral.

For safety, we typically employ a Residual Current Device (RCD) to detect that leakage current by continuously monitoring for unequal Live and Neutral currents. Now that we are transmission line experts, we see that the RCD is really a common-mode current detector!

A defining feature of common-mode current in both mains and RF systems is that common-mode currents do not cancel out. Common-mode currents carried by a multiple-conductor line will always reinforce each other so that, regardless of the actual number of conductors, the cable behaves as if it were a single wire… and in RF systems, that means common-mode current will cause radiation. In order to return via the ground terminal at the generator, the common-mode current flowing through Zc in Figure 2 will flow along any conductors it can find that lead towards ground. This makes unwanted common-mode currents a prolific source of both radiated and conducted interference.

FUNNY STUFF, COAX! When we use coax for our transmission line, the two wires of Figure 1 and Figure 2 become the centre conductor and the shield (**Figure 3**). But because the centre conductor is totally enclosed by the shield, the electric and magnetic fields from the two conductors are extremely tightly coupled together, and physics then demands that the currents on the centre conductor and the inside of the shield are equal and opposite. Unlike the parallel-wire line in Figures 1 and 2, the interior of a coaxial transmission line will only support differential-mode currents.

Something called the Skin Effect means that RF currents flow only along the surfaces of conductors and never through the thickness. More accurately, the current density flowing along a conductor is much higher at the surface than within its bulk; for example at 10MHz in a solid copper conductor the current density at a depth of just 20μm has fallen to 37% of its value at the surface. This means that in a coaxial line the transmission-line current is flowing almost exclusively on the outside surface of the inner conductor (Ia, shaded green in Figure 3) and on the inner surface of the braid (Ib, shaded blue).

Because RF current does not flow through the thickness of the shield, the interior of a coaxial cable is completely 'private' from the outside world – and that is what gives coax its unique tolerance to the way it is installed. Bend it, bury it, soak it in water, pass it through walls and metal bulkheads, or even wind the cable around a magnetic core – none of those actions makes any difference to the pure differential-mode currents in that private interior world. At first sight, therefore, we might think that coaxial line cannot possibly carry common-mode current… but unfortunately we'd be wrong!

The Skin Effect is a very important concept that unlocks many mysteries, but not all of its consequences are welcome. Because the shield has two surfaces, an outside as well as an inside, a completely separate current (Ic, shaded red in Figure 3) can flow along the outside surface.

Let me repeat that: the current, Ic, on the outside surface of the shield is completely independent of Ib on the inside surface. The two currents are completely separate and do not interact in any way. So, in fact, a coaxial cable is a 'three-conductor line' with a third independent conductor on its outside surface! This is hard to grasp for anyone who is new to RF engineering, but the Skin Effect is a dependable fact and so are all its consequences.

Comparing coax (Figure 3) with parallel-wire line (Figures 1 and 2), we now see that each of them can support both differential-mode and common-mode currents at the same time, but that they achieve it in different ways. The parallel line requires the two modes to share the same two conductors; but coax does it differently, by keeping the two modes completely separate – the pure differential mode on the inside and the common mode on the outside. We can always picture coax as a completely balanced internal pipeline for delivering RF power, overlaid by an entirely separate outside conductor that behaves as a single large-diameter wire. Because that's exactly what coax is. Once we grasp this key characteristic of coaxial cable, the solutions to many antenna common-mode problems become much more obvious.

Now we are ready to consider some practical engineering.

WHAT ARE CM CHOKES AND WHY DO WE NEED THEM? Quite simply, a common-mode choke suppresses or 'blocks' the common-mode current. And in doing so, it forces the currents at its output terminals to be balanced – equal in magnitude and opposite in phase – no matter how unbalanced the load or source to which it is connected may be. Because of this useful property, it frequently finds application interfacing balanced systems to unbalanced systems; no surprise then that it often gets called a balun!

Baluns in general come in many different types. CM chokes are the type that force current balance at their output terminals, so they are also sometimes called 'current baluns'. But there are also completely different types of balun that force voltage balance instead. Some baluns also perform an impedance matching function (for example 4:1 or 9:1) but this is not an essential part of what baluns do. Because our CM choke enforces current balance but does not perform an impedance matching function, within the wider family of baluns it can legitimately be called a '1:1 current balun'. And because Guanella first identified these properties it's also legitimate to call it a '1:1 Guanella balun'.

We will now focus on two typical amateur applications where we might need a CM choke: firstly, connecting a balanced dipole or beam antenna to unbalanced coaxial cable; and secondly, connecting the balanced feedline from a multiband doublet to an unbalanced tuner.

DIPOLE TO COAX. **Figure 4** shows a detailed view of the connection between a half-wave dipole and its coaxial feedline, but with no balun.

The centre conductor of the coax is connected to the right-hand leg of the dipole and the shield to the left-hand leg. We have seen that the pure differential mode inside the shield means that the current flowing on the centre conductor of the coax (A) must be of equal magnitude and opposite sign to the current flowing along the inside surface of the braid. However, on emerging from the open end of the shield, that current from the inside of the shield is forced to divide itself between two possible paths: into the left-hand dipole leg (B) or back along the outside surface of the braid (C) as the separate common-mode current.

Kirchhoff's Current Law tells us that (B+C) must equal the inside braid current, which is a differential-mode current equal and opposite to A. So if there is any common-mode current (C) at all, it must mean that the currents (A) and (B) in the dipole are unbalanced. That is why we need a balun – to block that common-mode current and force the dipole into a better state of balance.

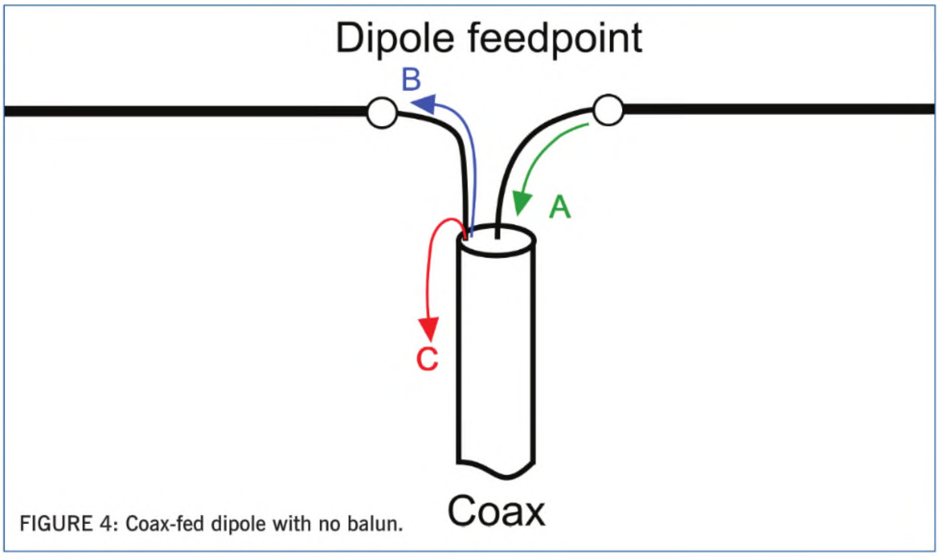

FIGURE 4: Coax-fed dipole with no balun.

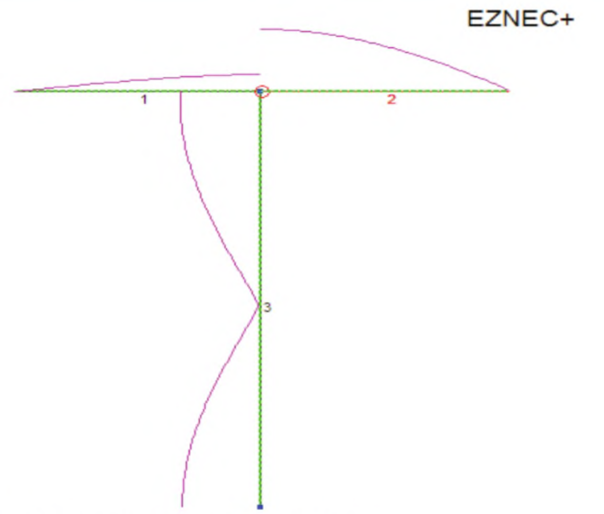

FIGURE 5: NEC model of a severely unbalanced coaxial feed.

The amount of common-mode current that flows back along the outside surface of the braid, compared to that flowing into the left-hand dipole leg, will depend on the relative impedances of those two different current paths. The impedance of the 'wanted' path into the antenna will be one-half of the dipole's feedpoint impedance, ie something in the region of 20-40Ω.

However, the impedance of the common-mode path impedance at the feedpoint could easily be quite similar, or even lower, depending on the combination of the coax length, its routing and its grounding. If the impedances are roughly equal, then about half of the current will be 'robbed' from the dipole and will flow down the outside of the coax instead. If the common-mode impedance is lower still, it's possible for current (C) to be much greater than (B) – resulting in gross imbalance of the dipole and severe radiation from the feedline.

Figure 5 shows a computer model of just such a situation, and the severely unbalanced current distribution that will result. Green wires 1 and 2 represent the two legs of a 20m dipole erected 36ft above ground; green wire 3 represents the outside of the coax shield, which is connected to the left-hand dipole leg. This coax shield is well grounded at the bottom end in the 'shack' (not shown).

The source of RF in this computer model is exactly where it is in real life: at the top of the feedline where the transmission-line currents emerge from the internal privacy of the coax. Then the mauve lines in Figure 5 indicate the magnitudes of the currents along the three wires. Because the length of the coax is close to a half-wavelength, the impedance of the common-mode path as seen at the feedpoint is very low, so most of the current that should have been flowing into the left-hand leg of the dipole is instead flowing back along the outside of the coax!

Does it matter? Well, yes it does – the coax shield is acting as a third radiating wire, inadvertently turning our dipole into a 'tripole'! And because the coax shield at the shack end is carrying a high surface current, it will radiate just like any antenna element; so we can expect RF feedback in the transmitter and also RF current flowing back along the domestic mains wiring, creating a strong possibility of interference to other nearby equipment. Of equal concern, during reception that unwanted 'third antenna wire' can pick up noise from the mains, and from other equipment in the shack, the house and the general surroundings, all of which then flows up the outside of the coax to the feedpoint and is injected into the signal path. This can raise the receiver noise level by large amounts (often above S9) and is a frequent cause of complaints about "my noisy QTH". Thirdly, the unequal currents flowing into the two dipole legs will distort the radiation pattern; whilst that

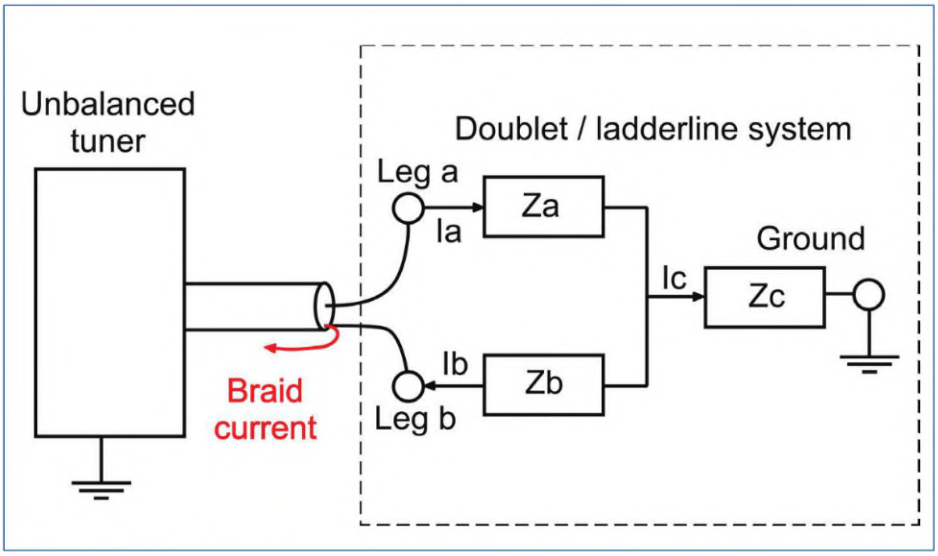

FIGURE 6: Three-terminal representation of a partly unbalanced doublet/ladderline system, as seen from the shack.

might not worry us unduly when using a dipole, it can be a serious problem when using a beam.

Ideally we want the common-mode current (C) in Figure 4 to be zero so that the currents (A) and (B) are equal and the dipole's balance is retained. We can achieve that by deliberately inserting a large impedance in the path of the common-mode current, forcing the dipole back towards its ideal balanced condition… and that is the role of the CM choke.

When we force a change towards a more ideal situation, it will also force a change in the voltages and currents at the feedpoint itself. Therefore you can expect the VSWR to change as well. This is completely normal – that's what almost always happens when you change from one antenna to another. And that is what you just did: the CM choke has literally changed the whole antenna, from the malfunctioning 'tripole' of Figure 5 into a properly functioning dipole that you have now.

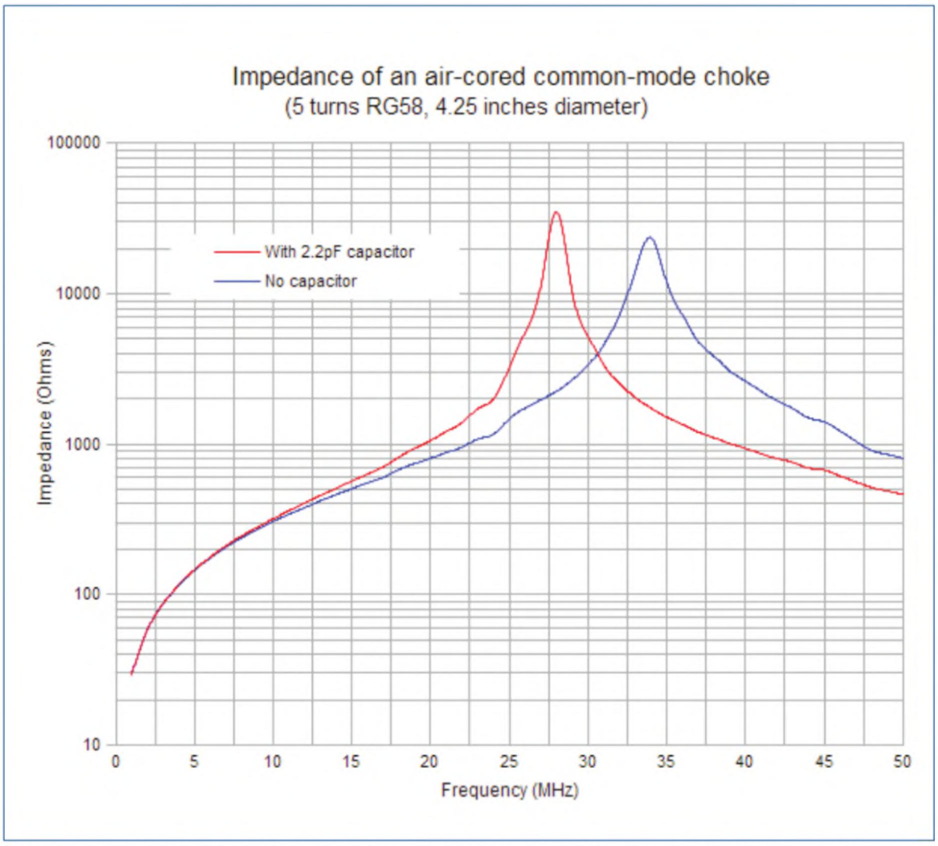

FIGURE 7: Air-cored chokes have a narrow impedance peak, and are easily de-tuned by small amounts of stray capacitance.

DOUBLET – LADDERLINE – UNBALANCED TUNER. Next, let's look at the challenges of connecting an unbalanced tuner to a multiband doublet antenna fed with ladderline, for example a G5RV. **Figure 6** represents the system as viewed at the shack end.

The components within the dotted rectangle are the equivalent circuit of the antenna system. If the antenna were in free space, the equivalent circuit would have been a simple two-terminal network representing only the two connections to the legs of the ladderline. However, no terrestrial antenna system can be completely independent of local ground, so a real-life representation requires the three-terminal network shown in Figure 6, the three terminals now being Leg a, Leg b and Ground.

If the doublet and ladderline were installed perfectly symmetrically with respect to ground, then of course we could expect that Za = Zb. However, in real-world installations this is never the case. My own doublet/ladderline installation looks quite symmetrical but measurements showed that to be far from true. The measured values showed significant differences in the magnitudes of the three impedances Za, Zb and Zc, which were respectively 80Ω, 109Ω and 114Ω. But the differences in the vector (R + jX) impedance values were even more dramatic:
Za = (15.1+j79)Ω,
Zb = (1.6-j109)Ω
and Zc= (30.7+j110)Ω.

So as well as the doublet's feedpoint impedances Za and Zb being highly asymmetrical, there was also quite a low common-mode impedance Zc to ground. You probably shouldn't assume that your installation would be any better!

We have already seen that the ladderline currents Ia and Ib should be as well-balanced as possible, to reduce the common-mode component Ic that is mostly responsible for radiation from the ladderline and noise pick-up during reception. If we connect an unbalanced tuner directly to the ladderline as shown in Figure 6, this will destroy any system balance that might otherwise have existed because one of the two terminals (Leg b) is shorted directly to ground at the transmitter. It's clear that we must do something to prevent this.

As in the dipole/coax case, the common-mode current can be found flowing on the outside of the coax, so the best way to block it is by placing a CM choke at the transition between the coax and the ladderline. The high impedance of the CM choke then forces the external shield current towards zero, so that Ia and Ib are forced towards balance.

Steve Hunt, G3TXQ • www.steve@karinya.net

FOLLOW THE CURRENT! Notice that in both the dipole/coax and the doublet/ladderline examples we are concerned primarily with currents rather than voltages. In both cases it is unwanted common-mode current that we are aiming to suppress, and also differential-mode currents that we are aiming to establish on the ladderline. This need to focus on currents is true in nearly all antenna balun applications that we come across, indicating that a current balun or CM current choke is nearly always the appropriate choice.

A voltage balun is almost always the wrong choice because it fails to address the real problem. If I had used a voltage balun at terminals a and b of my own doublet/ladderline system, it would have forced equal voltages across the two unequal impedances Za and Zb, and thereby guaranteed that the currents Ia and Ib would be unequal – so a voltage balun would have done exactly the opposite of what was needed! (Interestingly, this doesn't prevent many tuner manufacturers from incorporating a 4:1 voltage balun, which makes one wonder how well they are keeping up with the state of the art.)

WHAT MAKES A GOOD CM CHOKE? A good CM choke will present a very high impedance to unwanted common-mode currents across its entire range of operating frequencies, without having any significant effect on its ability to deliver the desired differential-mode power to the antenna system. Which leads to the question: how high a common-mode (CM) impedance do we need? And the answer, of course, is: "It depends!"

In the dipole/coax case (assuming the feedpoint impedance is around 50Ω) we could easily achieve a reasonable current balance with a CM impedance as low as 250Ω. From that very limited point of view, 500Ω has often been presented as a value to aim for. But that isn't the whole story, for two important reasons.

First, in the multiband doublet/ladderline case the feedpoint impedance is likely to be very high on some bands. To achieve the same degree of balance as the easy 50Ω case, the CM impedance will need to be higher still – possibly several thousand ohms.

The second consideration is power dissipation in the choke. If the CM impedance is not sufficiently high, the very high voltages present on the ladderline on some bands can still manage to drive enough common-mode current through the choke that losses in any core material can lead to overheating. Assuming UK power limits, and a duty cycle of 50% or less, a CM impedance of 4000Ω or more should ensure safe choke operation and is a realistic design aim.

There will certainly be some cases where a lower CM impedance will be good enough, so we don't have to be so particular about the type of CM choke. But usually we only discover that in hindsight. For reliable performance – to get it right first time – we still need to aim for a high CM impedance like 4000Ω.

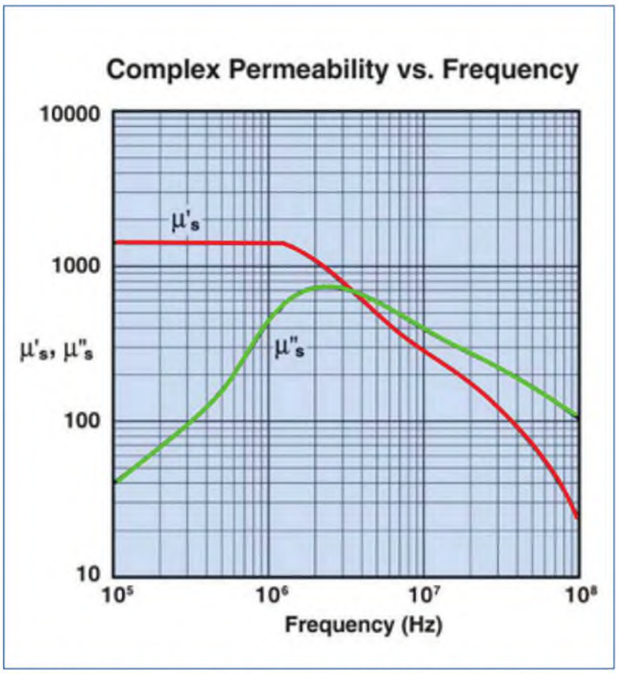

FIGURE 8: μ'S affects inductance while μ''S affects the loss resistance.

AIR-CORED CHOKES – RARELY A GOOD CHOICE. A commonly recommended method for making a CM choke is to take some extra length of coax and simply form it into a multi-turn coil. As I hope you'll understand, making the coax into a coil will obviously not affect differential-mode currents flowing inside the coax. In the outside world, making a coil will have some of the desired effect of impeding the common-mode current flowing along the outside surface of the shield. But the performance will rarely be as good as we might expect.

Figure 7 shows the CM impedance of a typical 'coiled-coax' choke comprising 5 turns of RG-58 on a 110mm (4.25-inch) diameter. Some very impressive CM impedances can be achieved in this way, as shown by the blue trace on the chart which reaches a peak value of over 25,000Ω. This high peak impedance is the result of the coil's inductance combining with the stray capacitance between the turns to form a high-Q parallel tuned circuit. Looking across a wider range of frequencies, at lower frequencies the choke behaves like an inductor, so increasing the frequency increases the impedance. Then as we come close to the self-resonant frequency (SRF) the impedance peaks sharply. As we go beyond the SRF the impedance falls sharply away again, and continues to fall because the choke is no longer behaving like an inductor; the dominant component is now the stray capacitance.

Impressive though the peak impedance is, this type of choke has several weaknesses. The high-Q nature of the choke means it only delivers high impedance over a relatively narrow range of frequencies; and secondly, any small change in stray capacitance can shift the self-resonant frequency dramatically, as shown in the red trace in Figure 7 where a 2.2pF capacitor has been placed in parallel with the choke to represent a small change in the layout of the turns. Even such a small change in capacitance has detuned the SRF by 17%. Because the performance can be seriously affected by such small details, different constructors following the same design may well end up with significantly different results.

There is a further problem with air-cored chokes which is even more important but not often appreciated. Because of their low-loss characteristics, the common-mode impedance that these air-cored chokes can deliver is almost entirely reactive (inductive below the SRF, or capacitive above it)… and any reactance can be partly or even completely cancelled out by another reactance of opposite sign. So if a reactive choke is inserted into a common-mode path which, in the absence of the choke, is reactive and of opposite sign, it is perfectly possible for the choke to reduce the net impedance, allowing the CM current to become even worse!

By way of example, a computer model of a 20m dipole erected 30ft over average ground and fed with RG213 showed a common-mode path impedance back along the coax shield of (28-j200)Ω; the CM impedance is capacitive because the feedline is just under a half-wave long. If we now insert a choke at the feedpoint that has a reactance of +j200Ω and very little resistance, the reactances will cancel and will reduce the net CM path impedance to 28Ω!

That said, air-cored CM chokes can sometimes be useful in non-demanding cases, especially if you restrict them to monoband applications and try to make sure that their self-resonant frequency is close to the operating frequency. (But then, please don't spoil it all by taping the coil of coax directly onto a metal boom!)

FERRITE CHOKES FOR BROADBAND PERFORMANCE. Clearly, for multiband applications it would be preferable if the choke maintained a high CM impedance across a much wider bandwidth, and also if its impedance was predominantly resistive because, unlike reactance, resistance can't be cancelled out. Fortunately, the properties of some ferrite materials allow us to approach this ideal.

If we wind a CM choke using a high permeability core material such as ferrite, we can achieve a high CM impedance with relatively few turns, which makes the choke easier to wind and also keeps the inter-winding stray capacitance to acceptable levels. However, it's the complex nature of a ferrite's permeability that proves to be its most useful attribute.

Figure 8 shows a plot of permeability against frequency published by manufacturer Fair-Rite for a core made from their Type 31 ferrite material. The red line represents permeability as most folk envisage it – the magnetic property of the ferrite that magnifies the inductance of a coil wound around it. This aspect of the permeability is given the symbol μ'S (pronounced "mu-dash-S"). Notice that μ'S is frequency dependent; its value is constant at low frequencies but for this particular material the value falls rapidly above 1.3MHz.

But because this ferrite material is 'lossy' it also generates an equivalent resistance in any coil wound round it, and this property is reflected in the green line. Fair-Rite give this resistive property the symbol μ''S (mu-double-dash-S). Notice that μ''S rises with frequency before falling again, but that μ''S is always more important than μ''S at frequencies above 3.5MHz. We might therefore expect that a choke wound around this Type 31 material will be more resistive than reactive over a wide frequency range from 3.5MHz upwards, and we'd be right!

Note that the use of a lossy ferrite material is NOT a bad thing. The ferrite does not introduce any loss into the differential-mode signal path. It only affects the common-mode path, where we can put that loss to very good use! The resistive loss in the core (due to μ''S) is what we have to thank for delivering a dependably high impedance across a broad bandwidth.

But now another warning: DO NOT use iron dust toroids for common-mode chokes! Their low permeability produces very poor chokes that have very low impedance in the HF range. (See the chart at the end of this article… and here again, we have to wonder about the level of knowledge among some suppliers to the amateur market.)

HOW DO WE BUILD A GOOD CM CHOKE? So at last we come to the practical details – but I make no apology for keeping you waiting. Unless you understand the technical background of what a CM choke is for, and what qualities make a good one, you are much less likely to get good results.

The key point is that the highest performing CM chokes use ferrite cores. One simple construction technique is to slip ferrite beads over a transmission line. That works, and the choke's impedance is pretty much proportional to the number of beads used; but if instead we wind the transmission line around a ferrite toroid we can benefit from the so-called 'N-squared' effect whereby the impedance increases as the square of the number of turns, reducing the number of turns needed for a particular level of impedance. A multi-turn choke is also cheaper, lighter and smaller than a long string of beads; it also allows more design freedom to control the self resonant frequency.

Commonly-available ferrite toroids come in diameters up to 61mm (2.4 inches) with an inside diameter of 25mm (1.0 inches) so practical considerations mean the transmission line used for the winding is often small diameter coax (RG-58 size or smaller). As an alternative to coax, you can sometimes use a bifilar pair of parallel wires; the choice between the two is determined by the application. For example, if the choke is to be used at the feedpoint of a coax-fed, nominally 50Ω antenna, we would prefer to wind the choke with 50Ω coax so that it doesn't introduce an unwanted impedance transformation. On the other hand, a choke used at the output of a tuner has no such requirement because any unwanted impedance transformation can be tuned out, so we can wind it with a transmission line of any characteristic impedance

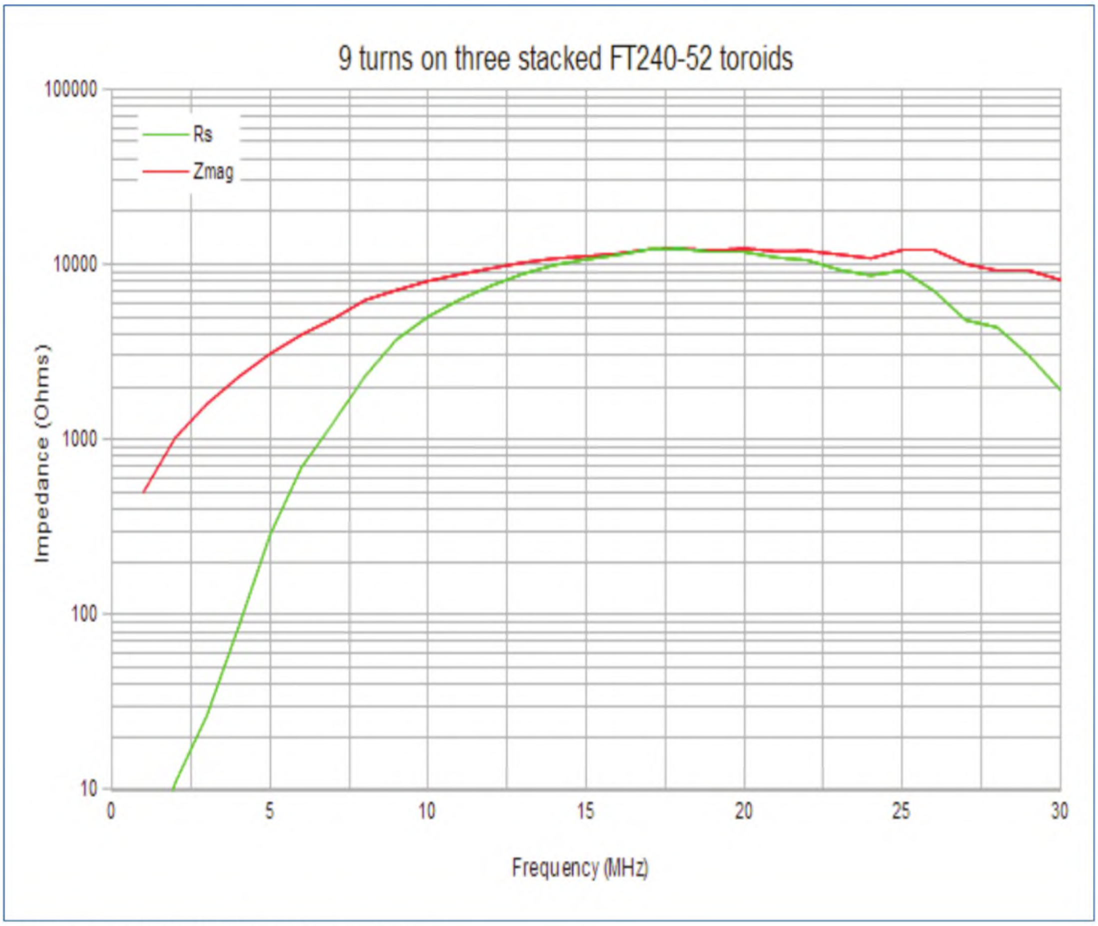

FIGURE 9: Optimised CM choke for 6-30MHz.

within reason. We would likely choose a bifilar pair of well insulated wires for this application because they can withstand higher differential-mode voltages than small diameter coax.

Photo 1 shows how a typical toroidal choke is wound. This one comprises 7 turns of coax on two stacked 61mm diameter toroidal cores. Plastic tie-wraps have been used to secure the ends of the coax. The crossover at the 4th turn is not essential and it has no major impact on the choke's performance; it's mostly a way of making the two ends of the coax emerge on opposite sides of the toroid, which can be handy in some installations. Every pass of the coax through the centre of the toroid – including the crossover – counts as one turn.

How the coax ends are terminated will depend on the application. The choke is often placed in a box with a coax connector at one end and a terminal pair at the other. It's important in this case that the box is plastic. Using a metal box can significantly alter the stray capacitance and change the choke's performance, and if you ground both ends of the coax to the metal box, the choke will stop working altogether! Plastic boxes are cheaper and better for this application, so why bother with metal?

Figure 9 shows the sort of CM choking impedance that can be achieved using these construction techniques. This choke is an optimized design using 9 turns of coax on three stacked FT240-52 toroids. It achieves the design goal of at least 4,000Ω impedance from 6MHz to 30MHz, and the impedance is above 10,000Ω from 13MHz to 27MHz.

The green trace indicates that the choke impedance is predominantly resistive over a large part of this bandwidth, and from 10MHz to 28MHz it achieves 4000Ω on resistance alone.

By careful choice of the ferrite mix, number of turns, and the number of toroids in the core stack, it is possible to produce a CM choke for most HF applications. **Figure 10** illustrates the performance of a number of useful designs, and the chart format allows easy comparison of the various options.

The CM impedance in Figure 10 is represented by the coloured bars. Dark green is the highest impedance (>8kΩ) and red the lowest (>500Ω). Within these multi-coloured bars, the black line shows the frequency range over which the choke is predominantly resistive.

By way of comparison, a ferrite bead choke, an iron dust choke and an air-cored coiled-coax choke have been included at the bottom of the chart. Notice the very modest performance of the bead choke, the abysmal performance of the iron dust choke, and the very narrowband performance of the coiled-coax choke!

All the results in this chart were obtained using RG-58 for the windings, and using the cross-over winding arrangement shown in the lead photograph. Using a smaller diameter coax, a bifilar winding, or not using the cross-over will change the results somewhat, but with these fairly wideband chokes the effects are not major.

TYPES AND SOURCES OF FERRITE PARTS. Throughout this article I have used the popular amateur designations for the ferrite parts; for example FT240-43 indicates a Ferrite Toroid with an outside diameter of 2.40 inches, made from the Fair-Rite type 43 grade of ferrite. Two points to note here:

- Those particular grades of ferrite are manufactured by only one company, Fair-Rite in the USA. The grades or 'mixes' that are most useful are 31, 43, 52 and 61. Other manufacturers may produce similar materials but their properties will be different (meaning: you're on your own!).

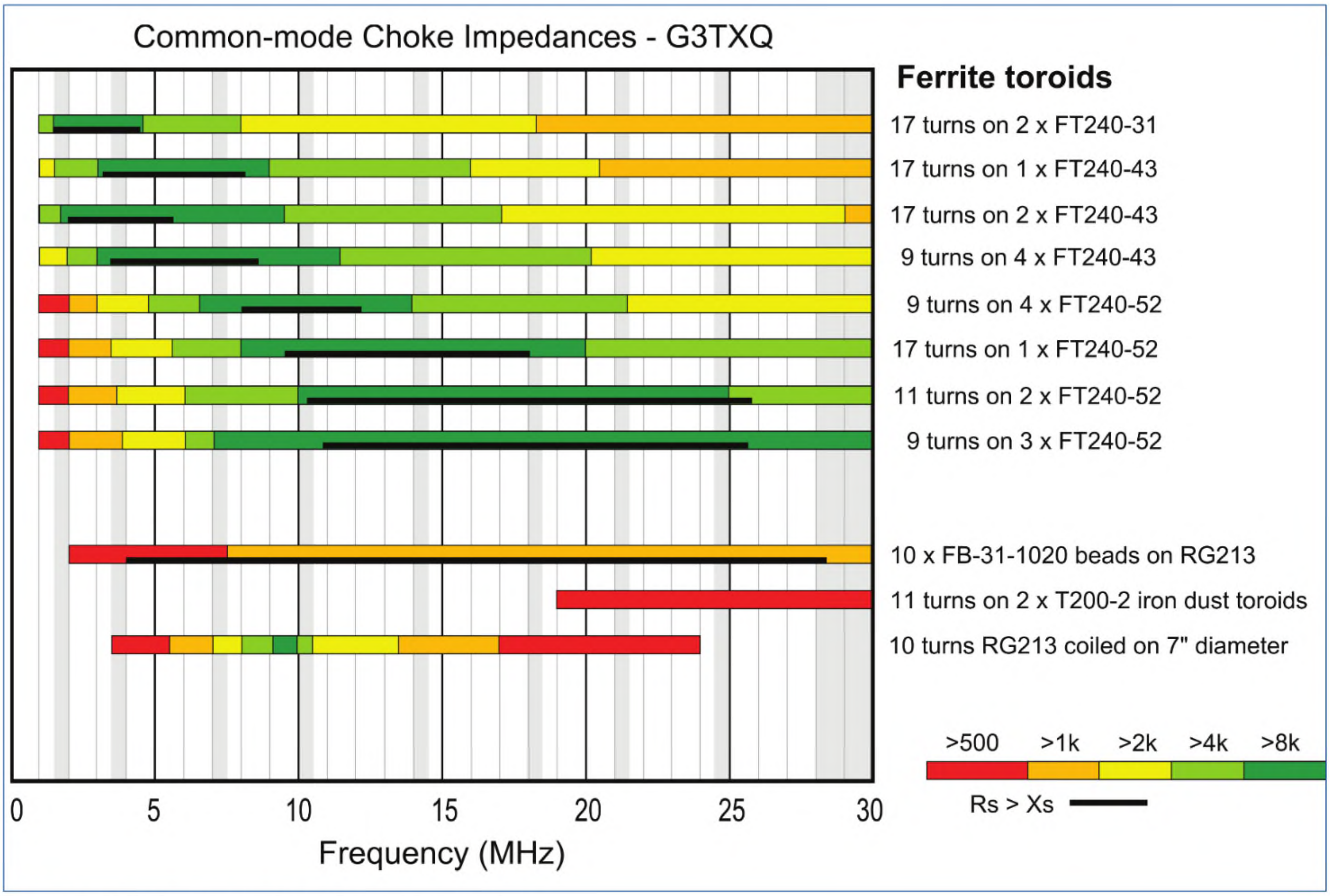

Figure 10: G3TXQ's recommendations for good ferrite chokes

- Fair-Rite do not use the 'FT240-43' style of part numbering. These numbers are added by resellers, primarily to the amateur market. Fair-Rite and their main dealers use the original part numbers, which are as follows:
  - 'FT240-31' (Fair-Rite part number 2631803802)
  - 'FT240-43' (Fair-Rite part number 2643803802)
  - 'FT240-52' (Fair-Rite part number 5952003801).

Note that the 3rd and 4th digits are the grade of material – 31, 43 or 52.

You can order Fair-Rite toroids from a number of suppliers serving the UK. Recommended suppliers include Farnell (www.farnell.com), Mouser Electronics (based in the USA but with a dedicated UK website http://uk.mouser.com and excellent shipping arrangements) and a number of amateur dealers (search on eBay for the FT- number).

By all means shop around for the best prices, but always check the total cost including shipping. Ferrites are heavy and fragile, which makes them genuinely expensive to ship, so take advantage of 'free shipping' offers wherever you can.

G3TXQ CHOKE CHART. The chart in **Figure 10** shows my recommendations for a range of high-performance ferrite chokes, between them covering all of the HF amateur bands. Be warned that the last three are examples that you should not follow!

Finally, my website includes a performance chart similar to Figure 10, but which includes a different range of choke designs (www.karinya.net/g3txq/chokes). It's worth taking a look from time to time because I add new designs as I make further measurements. The website also includes more detail about why reactive chokes can be undesirable.

Appendix: How to measure CM choke impedance

My early attempts at choke impedance measurement used a single-port vector impedance analyser (AIM4170) with the choke directly connected from the measurement port to ground. However, it's not ideal: very high choke impedances are outside the range where the analyser can be expected to be accurate. Despite careful calibration to the measurement plane, the analyser always added the equivalent of a few pF of parallel capacitance; this significantly shifts the self-resonant-frequency of higher-Q chokes.

More accurate results can be obtained by measuring the attenuation that the choke introduces when placed between a signal source and a load. So, for instance we could place the choke in series between a signal generator and an RF voltmeter; then, knowing the generator output and the RF voltmeter reading, we could deduce something about the choke's impedance. However this simple scalar measurement will not tell us anything about the choke's complex impedance ($R \pm jX$). As we have seen throughout this article, it is vital to know both the resistance and the reactance for a complete understanding of how well it will perform.

Fortunately, a 2-port vector network analyser (VNA) can measure both the magnitude and the phase of the attenuation introduced by the choke, and that allows us to fully determine the choke's complex impedance. I use an Array Solutions VNA2180 in the arrangement shown in **Figure 11**. This jig typically adds the equivalent of 0.2pF or less of parallel capacitance.

The ports of the VNA are connected to the test jig via two short lengths of coax – long enough that the choke is physically well-isolated from anything that could cause stray coupling and affect the measurements. The test jig comprises two BNC sockets mounted on a small piece of PCB material; crocodile clips soldered to the BNC centre pins allow the choke to be connected in line. A 50Ω resistor on the jig ensures that the impedance 'seen' by Port A of the VNA never becomes extreme.

The VNA is first calibrated with the two coax leads removed from the jig and connected back to back through a BNC double-female adapter. Then they are re-connected to the jig, the choke clipped between terminals A and B, and a VNA measurement scan made between the required frequencies. The resulting S21 amplitude and phase data is then transferred to a spreadsheet to calculate the choke's complex impedance, and produce the plots shown throughout this article.

Figure 12 shows the significantly different results that are obtained on a high-Q choke when using the one-port reflective measurement of an analyser like the AIM4170 compared to the two-port transmissive measurement of the VNA2180. Incidentally, this choke design is taken from the *ARRL Antenna Book* where the self-resonant frequency is stated as 14.3MHz, indicating an even greater error caused by uncorrected stray capacitance.

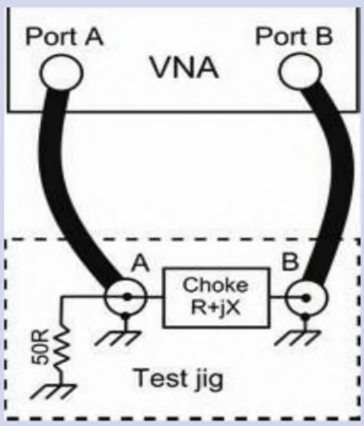

FIGURE 11: How to measure complex impedance using a two-port VNA.

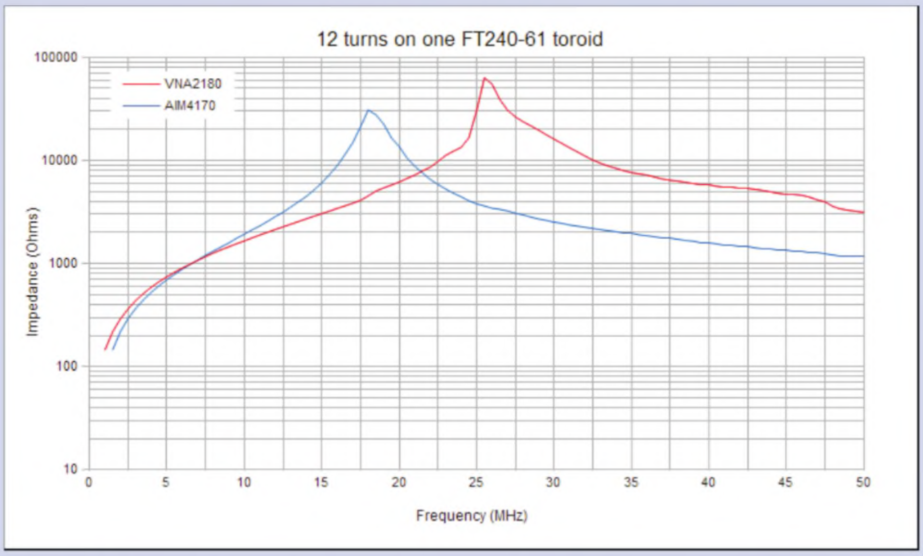

FIGURE 12: Effect of measurement method on the apparent resonant frequency. The higher measurement, made as described here, is the more correct value.

Peter Chadwick, G3RZP • g8on@btinternet.com

Screening

Screening is used to stop stages interacting and oscillating or to stop unwanted radiation

INTRODUCTION. Screening – also known as shielding – is used in most radio equipment, for a number of reasons. It can be provided to stop stages interacting and oscillating, or to stop unwanted radiation (this is especially so in transmitters) or prevent unwanted pick up of signals. Many years ago, a man came into the shop where I worked part time with a radio that he said 'squealed'. He said he cleaned the dirt out of it and there was a lot of loose flaking red paint on the valves which he'd removed and now it 'squealed' and 'whistled'. Of course, said valves all had metallised envelopes for screening, and without it, oscillation ensued. Some metallizing seemed more prone to come off than others, which was probably why he managed it so easily!

WHAT DOES SCREENING DO?

Screening prevents the ingress or egress of either a magnetic or electric field or sometimes, an electromagnetic field. Depending on the frequency, type of field and the required attenuation determines the form of the screen, its thickness and its material. Because the discussion here involves frequency, obviously fixed (DC) fields are excluded from consideration.

In general, LF fields are either magnetic or electric, emanating from a current carrying inductor as a magnetic field or from a high voltage AC point as an electric field. The reason why they are not electromagnetic (E-M) fields is that an E-M field has the electric and magnetic fields in phase and at 90 degree polarisation: this is not achieved until some distance from the radiator, and for shorter distances, the radiation is in the near field.

The near magnetic field extends to a distance of $\lambda/2\pi$ (where λ is the wavelength) from the radiator, and from the Biot-Savart law, decays according to an inverse cube law **[1]**. The same applies to the electric field, and quite obviously, in any equipment, this will apply to internal fields up to the range 50 – 150MHz.

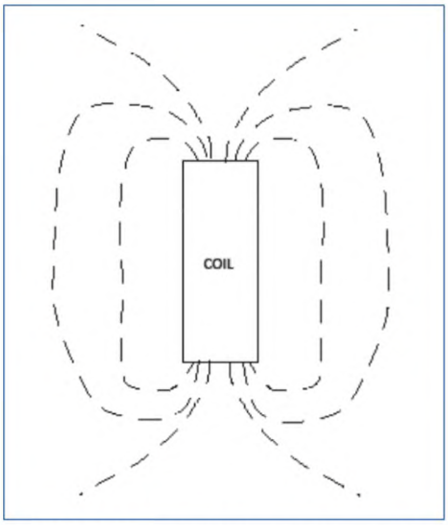

FIGURE 1: Magnetic field surrounding a coil carrying a current.

LOW FREQUENCY MAGNETIC SCREENING. Consider **Figure 1**, where there is a coil with AC flowing through it. Magnetic field lines are produced: some flow round and back to the coil, while some leak away – strictly, they eventually get back to the coil, but in the meantime, have weakened so much that they can be considered to have 'escaped'. These magnetic fields can induce currents into conductors (which can include a stream of electrons in a CRT!) leading to feedback and other ills. Incidentally, other conductors can include a chassis!

At low frequencies, below about 10 to 20kHz, screening the coil with a box of material of low magnetic reluctance – or high μ (high permeability) – is very effective. **Figure 2** shows the magnetic field flowing in and confined to the low reluctance material – this is because the box has a lower reluctance than air. Very high μ material, such as 'Mumetal' (a nickel – iron alloy with a μ of around 70,000) allows thinner shields, but is much more expensive than mild steel and can also easily lose some of its μ value under conditions of shock and vibration, whereon it needs to be re-annealed, a process requiring precise temperature control in a hydrogen atmosphere. This applies after working the material mechanically. The box has to be thick enough to confine the magnetic field, and the required thickness is related to the μ of the material and the amount of attenuation required.

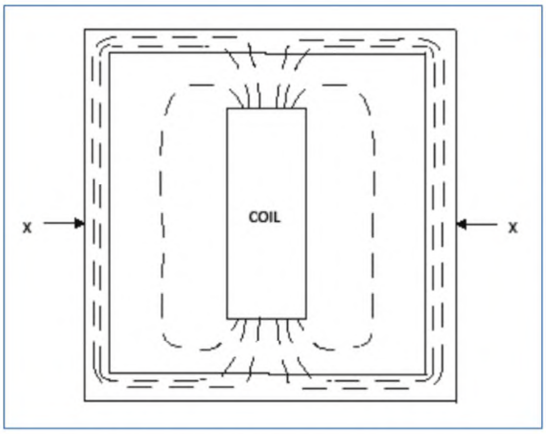

FIGURE 2: Magnetic screening by a low reluctance enclosure.

For a closed screening can the attenuation A in terms of 20log H_0/H_i dB (where H_0 is the magnetic field strength outside the screen and H_i is the field strength inside the screen):

$$A = 4/3\ (\mu d/D)$$

where

μ is relative permeability,
d is material thickness and
D is the screening can diameter

There should be no seam or break in the shield along the plane XX, as this would increase the reluctance and decrease the screen effectiveness.

So, for those not conversant with magnetic circuits and reluctance (which is the magnetic analogy to resistance), **Figure 3** shows an electrical analogy for the use of low reluctance screening. R1 is the internal resistance of the EMF of the battery, while the low resistances R2 and R3 reduce the voltage across them because they are low in comparison

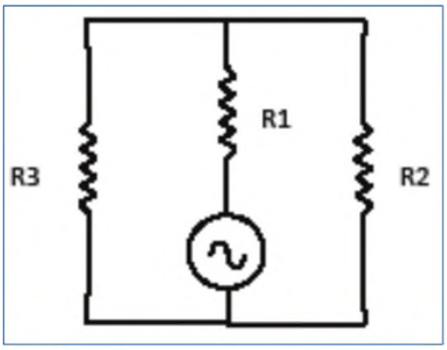

FIGURE 3: Electrical analogy to a low reluctance magnetic screen.

Peter Chadwick, G3RZP • g8on@btinternet.com

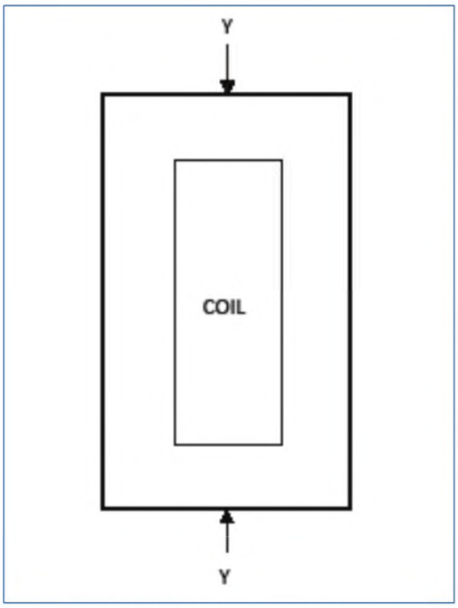

FIGURE 4: Magnetic screening by a low resistance enclosure.

with R1. R2 and R3 correspond to the 'magnetic resistance' or reluctance of the shield: R1 is the reluctance between the coil and the shield.

As the frequency increases, the effectiveness of the shielding falls because of skin resistance. This is an effect where the current in a conductor flows on the surface as the frequency increases. The depth to which the current penetrates to where it is approximately 37% (1/e) of its value at the surface is the skin depth and is given by:

$\delta = (2.6/\sqrt{FMHz})\sqrt{(\mu_{r-1})}\ \rho/\rho_c)$ thousandths of an inch

where

μ_r is the relative permeability of the material,

ρ is the relative resistivity of the conductor at the applicable temperature, and

ρ_c is the resistivity of copper at 20°C = 4.379 $\mu\Omega$/inch.

As Mumetal has appreciable permeability and resistivity, the skin depth decreases with frequency. This means that the effectiveness of a Mumetal screen of a given thickness is inversely proportional to frequency, as more skin depths are required to attenuate the current to a given level. In general, a screen needs at least 10 skin depths to give about 87dB attenuation between the current on the surface of one side and the current on the surface of the other side.

Because the effect of the high permeability material is to concentrate the lines of flux and thus the strength of the field, it is equivalent to increasing the number of turns in the coil, and increases the inductance.

HIGH FREQUENCY MAGNETIC SCREENING. At higher frequencies, a different technique is used. A low resistance screen of conductive material surrounds the coil, and in this is induced, by transformer action, a current, see **Figure 4**. This current produces its own magnetic field which opposes that of the coil: although the induced current is much smaller than the coil current, the field produced by the coil at the screen is lower than immediately adjacent to the coil, and so the induced magnetic field substantially cancels that of the coil.

The induced current in the screen also reflects back into the coil, effectively reducing the field strength for a given current, which leads to a reduction the inductance – as opposed to effect of the high permeability screen. It also leads to a reduction Q, because the screen looks like a short circuited single turn, and that has some resistance. By transformer action, this is reflected into the coil as an added series resistance, which is why the screen should not be too close to the coil, although if a high permeability iron dust or ferrite 'pot core' surrounds the coil, the effect of the close shield is markedly reduced because there is little external field in the first place.

Because the induced currents circulate round the inside of the can, it is important that no seam is along the axis Y-Y because that would introduce resistance to the induced current and thus the cancellation effect. Again, the screen thickness needs to be such that the current on the outside of the screen is attenuated enough to give the desired attenuation – which is why making screening boxes for coils from PCB material with 0.001 inch thick copper is not very effective on 160m where the skin depth for copper is almost 0.002 inches!

Note that so far, no mention has been made of earthing the screen, and indeed, for pure magnetic screening, that is not necessary, although in practice, the capacitance that will necessarily exist between the coil and the screen will lead to the screen being some voltage above zero if it is not earthed.

ELECTRIC FIELD SCREENING. Electric field screening is somewhat less demanding, in that provided the field is not strong enough to produce large currents in the screen, the screen can be very thin. The principle may be seen in **Figure 5**.

An object at high voltage V, such as a PA valve anode top cap, has a series of lines of electric force radiating from it to earth.

At least in theory, screening could be provided in a manner analogous to Figure 2 by the use of a very high permittivity insulated screening box, but the difficulty is that the permittivity needed is extremely high, more than is practically available. So the method analogous to Figure 4 is used, and the lines of electric field are confined by being earthed – see **Figure 6**.

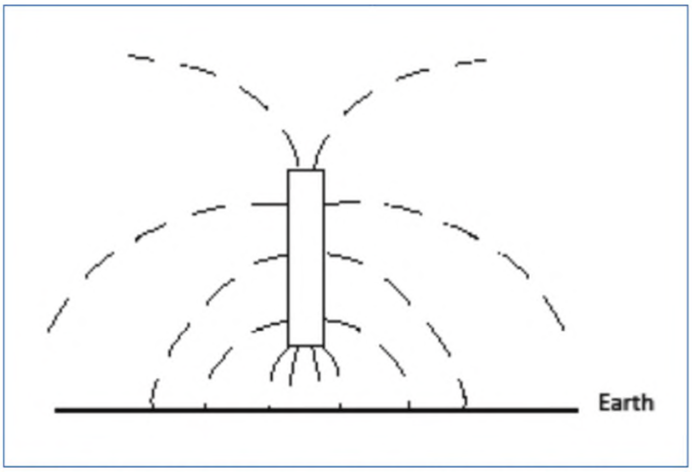

FIGURE 5: Electric field around an unscreened high voltage point.

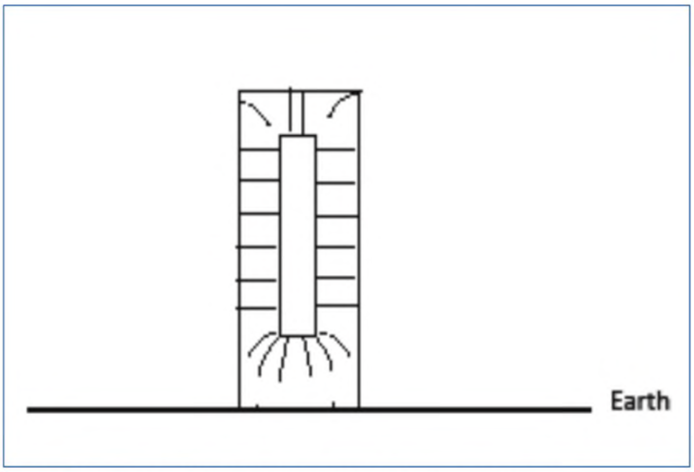

FIGURE 6: Electric field around a screened high voltage point.

May 2015 • RadCom Plus
Peter Chadwick, G3RZP • g8on@btinternet.com

The screen does not necessarily have to be continuous, but can be in the form of a cage or a grid, as in a tetrode valve, or in a Faraday screen, which provides electric, but not magnetic, screening between two coils, as in **Figure 7**. Examples of such screens could be found between PA and antenna coils in late 1940s VHF R/T equipment by Marconi, and also in the 1953 *ARRL Handbook*, where such a screen is shown between the aerial coupling coil and the first tuned circuit in converters for 20, 15 and 10 metres.

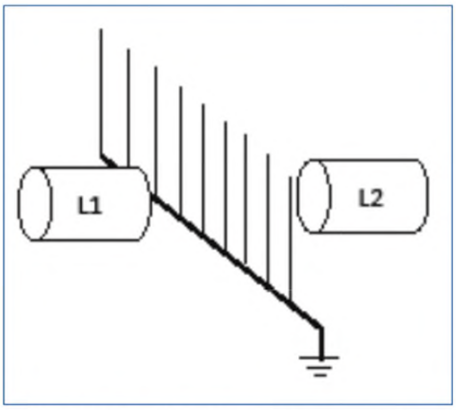

FIGURE 7: Electric field screening between two magnetically coupled coils.

A popular variant when TVI became a problem in the 1950s was to use a 'screened link' winding on an ATU to prevent capacitive coupling of harmonics: this was made of coax. See **Figure 8**.

Another place where electric field screening may be found is in mains transformers, where it can take the form of single turn of foil with the ends isolated from each other such that it does not form a shorted turn: this helps to prevent the electric field from common mode mains borne noise getting into the power supply.

Although holes in screens will allow more leakage than solid metal, holes small in comparison with the wavelength are effective: at SHF and above breaks in screening for ventilation are provided by the 'waveguide beyond cut off' technique. In any wave guide operating below a certain critical cut off frequency, the attenuation is constant per unit length, and if the wavelength is more than about seven times $\pi D/2$ (where D is the diameter of the waveguide), attenuation will be proportional to length. Thus a multiplicity of small holes for ventilation will have less deleterious effect on the screening factor than a big hole of the same area – a point to note when deciding on the size of holes provided for cooling purposes. Regrettably, however, the resistance to air flow is greater. Long slots allow much more leakage, tending to act as a slot antenna.

In cases where a very high attenuation is required, such as in signal generators, a common approach is the use of a box within a box with the two boxes connected at one point, as in **Figure 9**.

In a similar way, double screened coax cable can be found: the single layer of braid in 'normal' coax is not a very good screen, especially at lower frequencies where the skin depth is greater. The cheaper coax available has very loose braid and in some cases, attempts to make up for this with a wrap of thin foil. Any corrosion of the foil – which will almost certainly happen over time with cheap cable – drastically reduces the screening effectiveness.

Of course, screening can be compromised if leads enter the screened area without filtering, and in the days when harmonic radiation was the major difficulty in causing interference to TV, it was quite common to use elaborate filtering on screened power leads within the transmitter enclosure. The use of a gasket where lids are screwed onto boxes is also common where very high levels of screening are required. Such gaskets are commonly of a wire braid like material enclosing compressible rubber core, or of a metallically loaded rubberlike material offering high conductivity when compressed.

In short, screening below around 20kHz is best done with a high mu material: plain mild steel can often do the job, depending on how much screening is needed: if, as is usual, the screen is also intended to provide some screening of the electric field, steps will be needed to prevent corrosion in any joints leading to increased resistivity and reluctance. At frequencies above about 20kHz, a highly conductive material such as copper or aluminium works well, provided no seams or push fit contact is made in the axis of the coil, and the material is thick enough to provide the required attenuation at the frequency in question. Screening against an electric field can be done with very thin material unless the power is high enough to produce a current in the shield, but the connection to earth needs to be one of low resistance. So just because there's a piece of printed circuit board material between coils, don't assume that they are necessarily screened!Simple really!

But it does explain why coax cables leak at LF…

REFERENCE

[1] ECC Report 69: www.erodocdb.dk/Docs/doc98/official/pdf/REP069.PDF

This article was first published in the VMARS magazine, Signal.

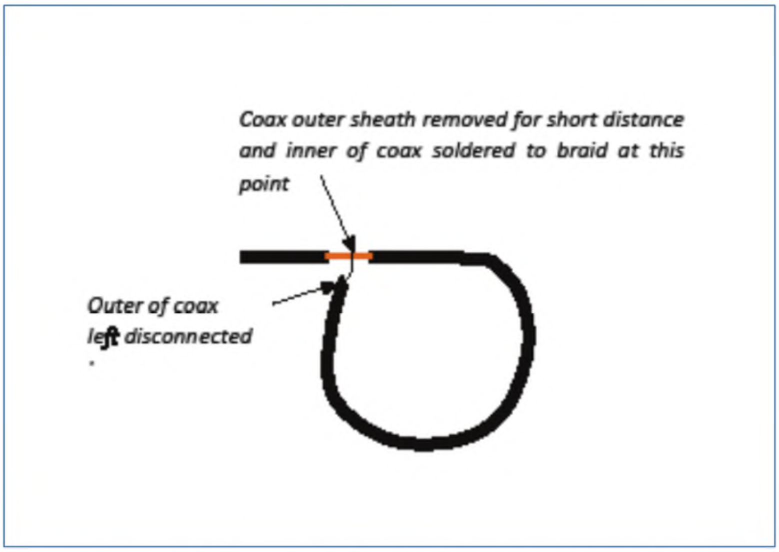

FIGURE 8: A 'screened link' or 'Faraday screened link', popular at one time for preventing capacitive coupling of harmonics to the antenna.

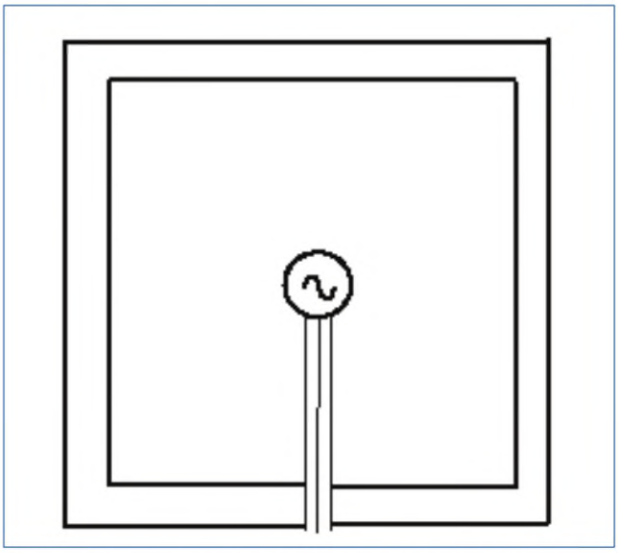

FIGURE 9: Double screening as used in signal generators.

RSGB shop

FROM P&P FREE OVER £30

E&OE **All prices shown plus p&p**

NEW

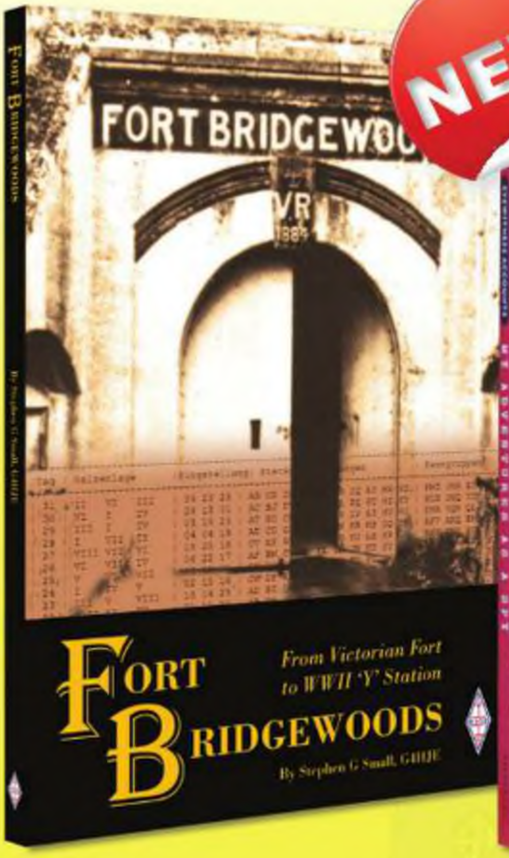

ONLY £10.19 RSGB Members' Price

25% OFF ONLY £6.74 RSGB Members' Price

Fort Bridgewoods

From Victorian Fort to WWII 'Y' Station

By Stephen G Small, G4HJE

This is the story of a Victorian Fort that was obsolete before the last stone was laid yet in the early twentieth century became one of the most secret places in the realm. It was here that the developing science of radio became a vital weapon of espionage and war. Without the painstaking work of the expert civilian intercept operators, Bletchley Park may well have failed to break the Enigma code and the vital Allied intelligence advantage may have been lost.

Fort Bridgewoods - From Victorian Fort to WWII Y Station sets out this fascinating story from its building to its final closure in 1968. The early role as Fleet protection in the late 19th Century and even its WWI activities are detailed along with the significant characters involved in its history. Readers will find much about the highly secret WWII activity as a 'Y' Station that became one of the most important signal gathering stations in Britain's 'Enigma Code' breaking operation. This book is packed with information and readers will find that the radios and equipment used are covered in detail from the early Marconi equipment to the DST-100 receiver, designed specifically for wireless interception work through to the familiar HRO sets used later in the war and are even details of the Hallicrafters and RCA receivers used.

Whilst the World slipped slowly into the abyss of a Second World War the operators of Fort Bridgewoods skillfully developed the science of signals intelligence and were intercepting both the secret diplomatic and military radio traffic. Without Fort Bridgewoods, the vital early 'breaks' of the Enigma code would certainly not have happened. *Fort Bridgewoods - From Victorian Fort to WWII Y Station* describes all of this and provides an insight into the operational work of this 'Y' Station and its part in WWII. If you are interested in the radio interception technology of WWII and its pioneers, this book is a revelation.

Size: 174x240mm, 144 pages, ISBN: 9781 9101 9309 9
Non Members' Price: £11.99
RSGB Members' Price: £10.19

Eyewitness Accounts

My Adventures as a Spy

By Sir Robert Baden-Powell 6

Many will be aware of Lord Baden-Powell as the founder of the scout movement and some may even be aware of him as national hero following the defence of Mafeking or even his elevation through the British honours system. This book is one of the many books he wrote in his lifetime and it highlights his service as intelligence officer for the Mediterranean for the Director of Military Intelligence. Written in 1915, and including Baden-Powell's thoughts on German espionage before and in the first years of the First World War, *Eyewitness Accounts - My Adventures as a Spy* describes such techniques as how to convey secret information using drawings of butterfly wings, how to quickly disguise yourself, how to safely produce plans of fortresses, observe troops and how to get past sentries.

In true scouting style this book is a cracking yarn of Robert Baden-Powell time as a young Army officer, was stationed in Malta and his many of adventures, travelling to investigate fortifications throughout the Mediterranean. Baden-Powell's love of adventure is evident in this book with much covered from disguising yourself to how to enter a fort unseen there are an array of tales, tips and techniques for the budding spy. Often defending espionage as being both useful and honourable, the book is packed with short sections explaining the world spycraft and much more. There are a large number of illustrative pictures included and a number of sketches by Baden-Powell, some of which even show how he modified sketches of fortifications to resemble subjects such as insects, stained glass windows, etc.

Written by one of the great figures of the Edwardian age this book is of its age and is funny, patriotic, historical, fascinating and even pompous but above all it is great read and recommended for absolutely everyone.

Size: 210x297, 128 pages, ISBN: 9781 4456 3610 8
Non Members' Price: £8.99
RSGB Members' Price: £6.74 (25% off)

Brian Flynn, GM8BJF • brian.flynn@tiscali.co.uk

A versatile PLL PC board design

For applications from HF to microwaves

INTRODUCTION. This article presents a versatile PCB design that can be used to provide accurate, stable frequency sources in the frequency range from a few MHz to 4GHz, depending on the components used, with a power output of about +10dBm. It was originally conceived for microwave applications to replace VHF crystal oscillators that were then multiplied up to the required output frequency, and a number of well-established designs have been published and have served us well, for example [1]. A number of factors have started to change this, namely, the reduced availability and increasing cost of good quality VHF overtone crystals, the requirement for more accurate frequency setting and the ability to easily change the output frequency when there are changes to our spectrum allocations. These factors start to make the phase locked loop (PLL) approach to frequency generation more attractive.

There are some aspects of using PLLs that are not so attractive, such as their phase noise performance and their complexity, but in many situations these are outweighed by their advantages. An additional factor is that there are now a number integrated PLL solutions from manufacturers such as Analog Devices (AD) and TI.

The object of this article is to present a versatile PCB design that can be used to provide accurate, stable frequency sources in the frequency range from a few MHz to 4GHz, depending on programming and components used, that gives a power output of around +10dBm.

PLL INTEGRATED CIRCUIT ARCHITECTURE. **Figure 1** shows a simplified block diagram of a typical PLL integrated circuit. It consists of:

- A reference divider and latch, the R counter/latch, to divide the reference frequency to the desired phase detector frequency
- An N divider/latch to divide the VCO frequency to the phase detector frequency
- A phase detector
- A charge pump.

The VCO and the reference oscillators are external to the integrated circuit. Both of the divider/latches are programmed via a three wire SPI serial data bus. This is used to keep the pin-count on the package to a reasonable level.

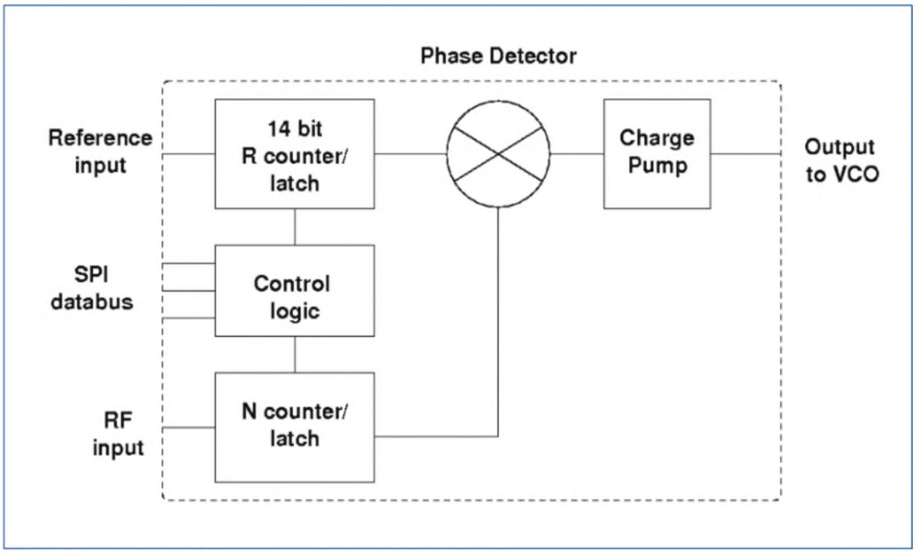

FIGURE 1: Simplified block diagram of a typical PLL chip.

To build up a complete PLL system with one of these chips, a VCO a reference frequency oscillator, a PLL filter along with some well regulated power supply rails at various voltages must be added as a minimum. It is also necessary to provide some means of programming the R and N counter registers to set the output frequency. This can be done with a Microchip PIC microcontroller. The overall block diagram will then be as shown in **Figure 2**.

DETAILED CIRCUIT DESIGN. The overall circuit is shown in **Figure 3**. The design was for an LO for a 2304MHz transverter and the LO was to run on 2160MHz. The PLL chip used is an ADF4113 from Analog Devices. To service the PLL chip three different regulated supplies are required: separate 5V digital and analogue rails and around 8V for a MMIC output amplifier. In addition to the regulators a PIC, a packaged VCO and a reference oscillator are required. The whole PCB is powered from a nominal 12 volt rail.

OBTAINING THE PCB DESIGN. The PCB design files can be downloaded from [2]. The design was done with a package called *Target*. A trial version of the software, which is adequate for this design, can be downloaded as freeware from the publisher's website [3]. Loading the design file into *Target* will allow you to preview and edit the design. The design file can be sent to your favourite PCB house to get it made. It is possible output Gerber files from *Target*, but many PCB houses will accept *Target* files. I have used two manufacturers: PCB-Pool [4] and Jackaltac [5]. Both of these take *Target* files. The latter is a service aimed at hobbyists and is

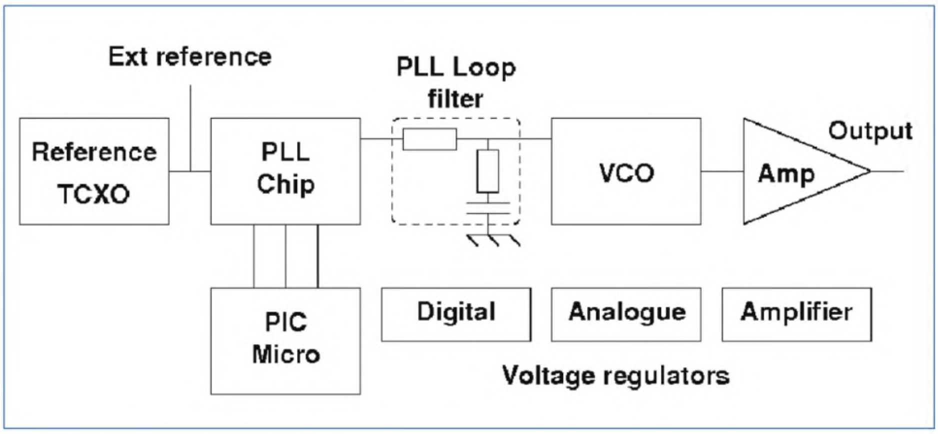

FIGURE 2: Overall PLL block diagram.

a low-cost no-frills service. It is possible to panel up the design and get a number of boards made at the one time to spread the cost either with friends or other projects. The components are all surface mount apart from the PIC, the reference oscillator and the connectors. The ICs are in TSSOP packages and are pretty straight forward to solder – compared to some other devices, anyway!

PROGRAMMING FREQUENCIES INTO THE PIC MICROCONTROLLER. The PCB is designed to take VCOs in a 16-QFN package. This package is widely used for VCOs and it pretty standard. The first step is to obtain a VCO that covers your desired frequency range. The tuning voltage output by the ADF411X chips is 0 – 5V. The next step is to decide on the four register latch values that must be programmed into the ADF411X to set it to your desired frequency. For this use the software available from AD called *Integer-N Software* **[6]**. This can be downloaded from their website and installed in the usual way. It provides a GUI which allows you to specify the reference frequency and the output (VCO) frequency and computes the register values to program into the PIC. The AD website is an extensive resource and provides a wealth of information on the design of PLLs.

PIC PROGRAM. The assembler code for programming the PIC can be down loaded from [2]. This code was written by John, GM8OTI and is well commented. Find the section containing the different register values and edit to enter the values calculated previously. An eight pin DIL packaged PIC was used in the PCB design to allow it to be plugged in and out of the PCB. It is recommended that the PIC is plugged in and out of the PCB. Although I preferred to remove the PIC for programming, the board layout does include a pin header K1 for in circuit serial programming (ISCP), which may be used if desired (with a suitable adapter lead).

PLL FILTER DESIGN. To choose the values of the components in the PLL filter download the program ADIsimPLL from the AD website [6]. This allows you to choose the type of filter you want to use and will give you component values. Tracking is provided on the PCB for different filter orders. The software allows you set different filter bandwidths to optimise the phase noise behaviour.

PHASE NOISE. **Figure 6** shows a plot of phase noise versus frequency of a PLL at a frequency of 1987.2MHz (multiply times 5 to 9936MHz for a 432MHz IF on the 10GHz narrowband segment). The response

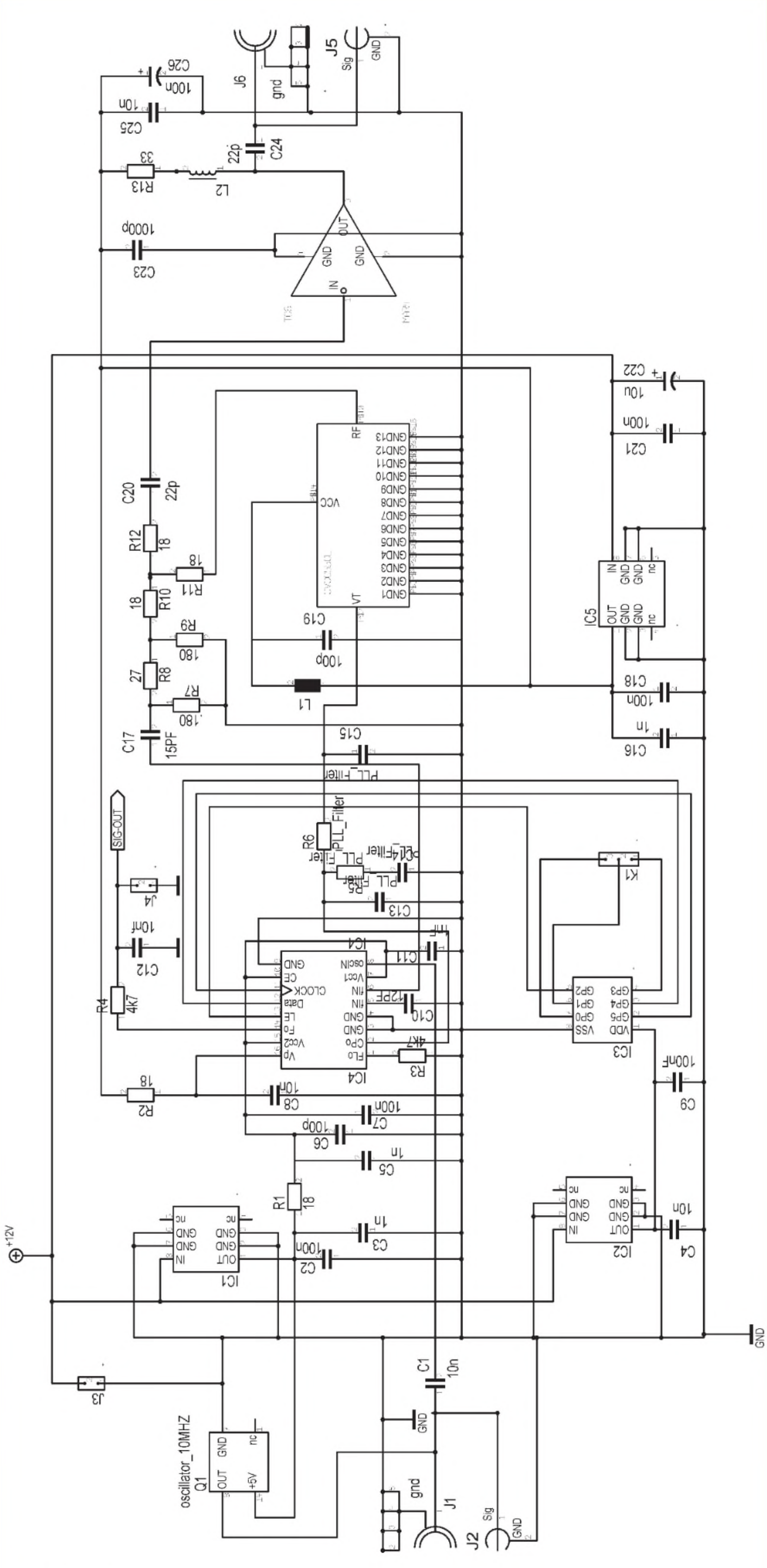

FIGURE 3: PLL circuit diagram.

May 2015 • RadCom Plus
Brian Flynn, GM8BJF • brian.flynn@tiscali.co.uk

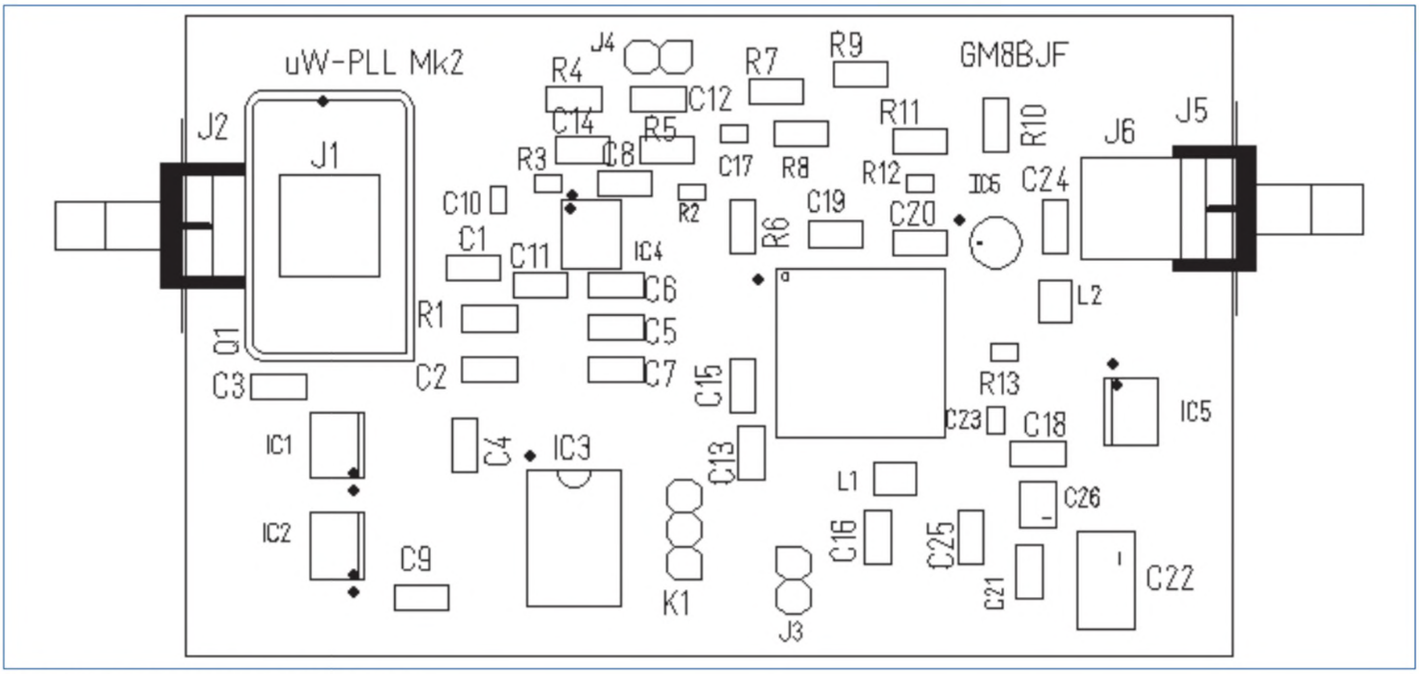

FIGURE 4: PCB layout component placement.

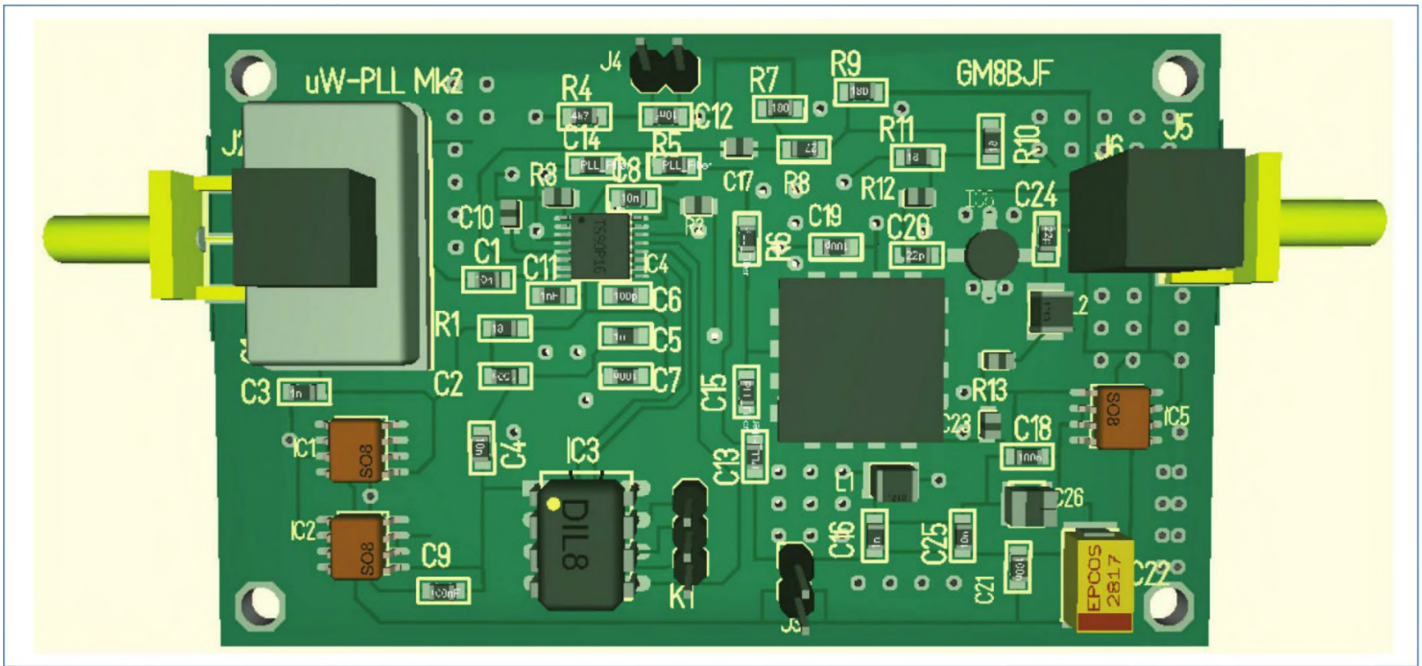

FIGURE 5: Overview of PCB.

TABLE 1: A list of some of the different synthesiser parts that share the same pinout.

Device	Maximum frequency	Synthesiser type
ADF4110	550MHz	Integer-N
ADF4111	1200MHz	Integer-N
ADF4112	3000MHz	Integer-N
ADF4113	4000MHz	Integer-N
ADF4116	550MHz	Integer-N
ADF4117	1200MHz	Integer-N
ADF4118	3000MHz	Integer-N
ADF4153A	4000MHz	Fractional-N
ADF4154	4000MHz	Fractional-N
LMX2306	550MHz	Integer-N
LMX2316	1200MHz	Integer-N
LMX2326	3000MHz	Integer-N

of the loop filter can be seen. Below about 10kHz the PLL is correcting the phase noise of the VCO, whoich would otherwise rise to high levels as the frequency reduces.

PCB DESIGN OPTIONS. The PCB has been laid out to be as flexible as possible. Different forms of connector can be used, either through-hole types or edge mount. Connectors can be SMA, SMB or SMC. The Reference oscillator can be omitted and the reference fed externally on a connector. The IC pinout is very standard across a considerable range of both integer-N and fractional-N PLL chips covering a wide range of frequencies from both AD and other manufacturers. The list in **Table 1** shows some of those available, but is not exhaustive. The components list is in **Table 2**.

PARTS AVAILABILITY. All of the parts are readily available from most suppliers with the possible exception of the VCO. These are available from Digi-key [7], who carry an extensive range and they are often available

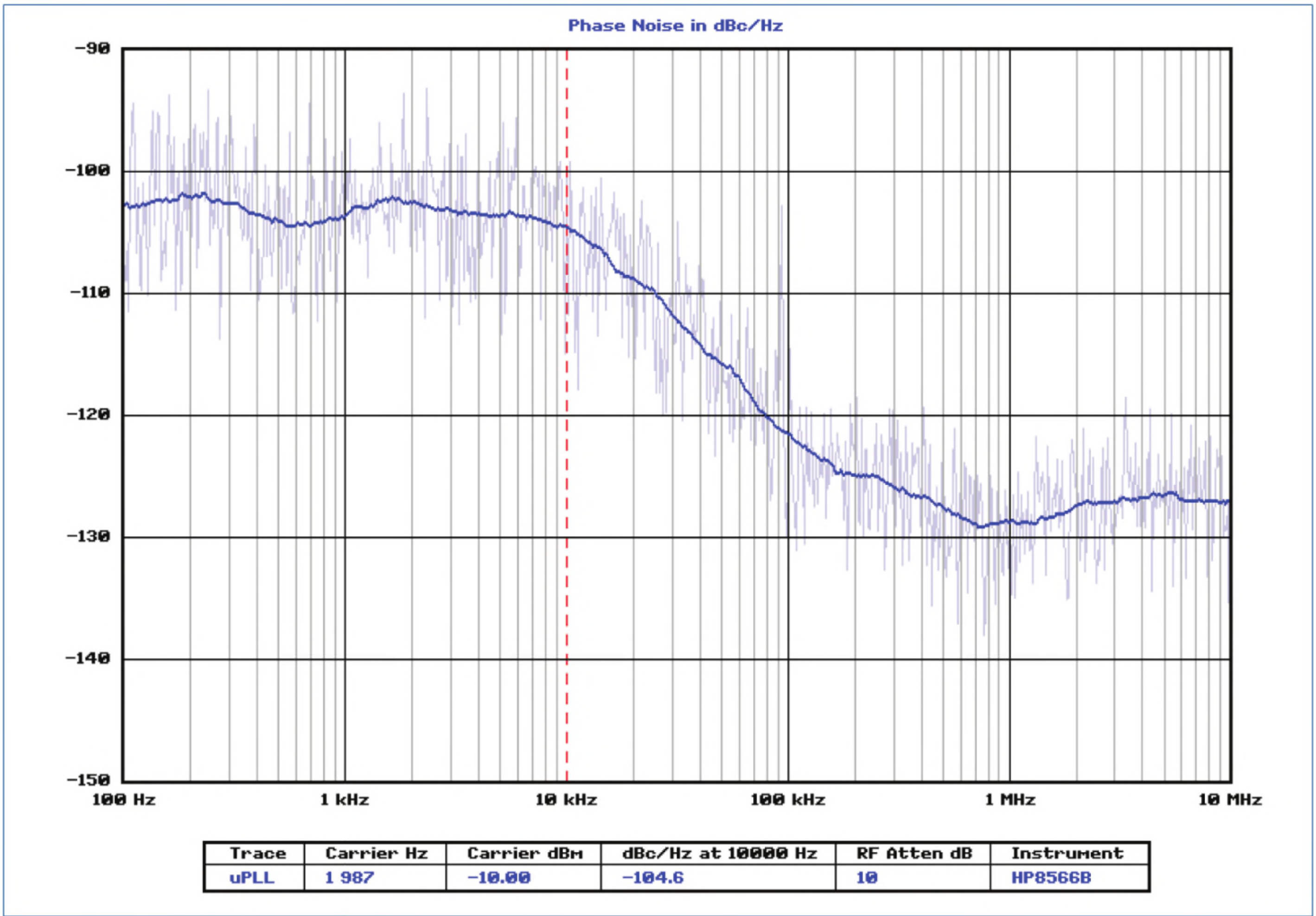

FIGURE 6: Phase noise plot made using the KE5FX GPIB utilities.

from sellers on the usual online auction sites – just watch the tuning voltage range and the power supply voltage.

CONCLUSIONS. This article has presented the design of a flexible PCB layout for a PLL that can be configured for operation at frequencies in the range from a few MHz to 4GHz. The author has used it for an oscillator for a GPS locked 20.480MHz reference for and FT-736R as well as LO for microwave applications at 880, 2160 and 2556MHz. The design files are made available others to use as-is or to modify to their own requirements.

WEBSEARCH

[1] Microwave signal source, Sam Jewell, G4DDK, *RadCom*, September 2008
[2] http://myweb.tiscali.co.uk/gm8bjf/uWPLL
[3] http://ibfriedrich.com/index.htm
[4] www.pcb-pool.com/ppuk/
[5] www.jackaltac.com/
[6] www.analog.com/en/index.html
[7] www.digikey.co.uk

TABLE 2: Component listing.

C1	10n	0805	J1	.	SMA-EINBAUBUCHSE
C2	100n	0805	J2	.	SMB_EDGE
C3	1n	0805	J3	.	1X02
C4	10n	0805	J4	.	1X02
C5	1n	0805	J5	.	SMB_EDGE
C6	100p	0805	J6	.	SMA-EINBAUBUCHSE
C7	100n	0805	K1	.	1X03
C8	10n	0805	L1	.	1210
C9	100nF	0805	L2	.	1210
C10	12pF	0805	Q1	oscillator_10MHZ	OSZILLATOR
C11	1nF	0805	R1	18	0805
C12	10nf	0805	R2	18	0805
C13	PLL_Filter	0805	R3	4k7	0805
C14	PLL_Filter	0805	R4	4k7	0805
C15	PLL_Filter	0805	R5	PLL_Filter	0805
C16	1n	0805	R6	PLL_Filter	0805
C17	15pF	0805	R7	.180	0805
C18	100n	0805	R8	27	0805
C19	100p	0805	R9	180	0805
C20	22p	0805	R10	18	0805
C21	100n	0805	R11	18	0805
C22	10µF	2817_ELKO	R12	18	0805
C23	1000p	0805	R13	33	0805
C24	22p	0805	X1	CVCO55CL(#1)	CVCO55CL(#1)
C25	10n	0805			
C26	100n	1411_ELKO			
IC1	.	SO8_SOT96-1	IC4	IC4	TSSOP16
IC2	.	SO8_SOT96-1	IC5	.	SO8_SOT96-1
IC3	.	DIL8	IC6	MAR4	MAR4SM(#2)

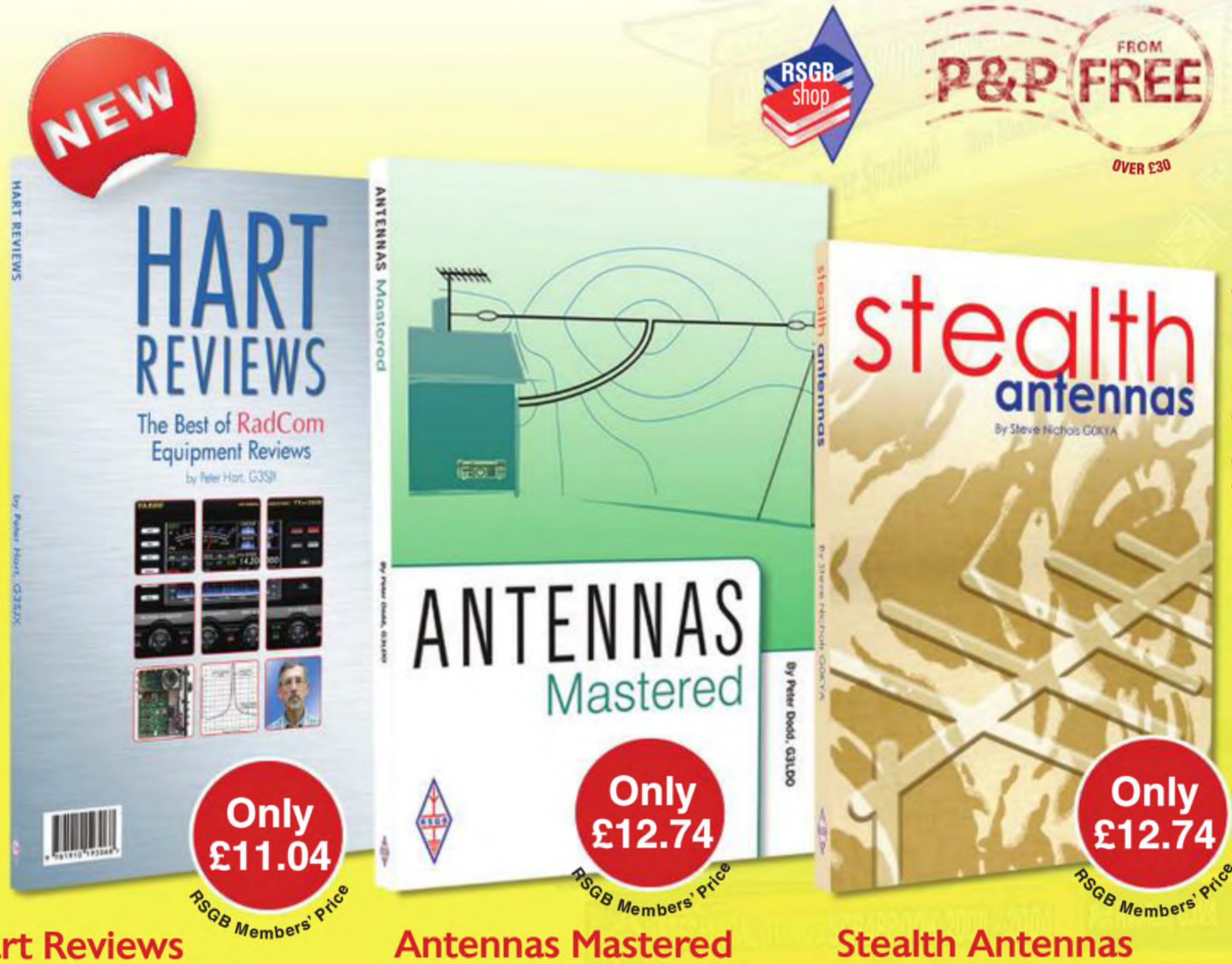

E&OE **All prices shown plus p&p**

Hart Reviews

The Best of RadCom Equipment Reviews

By Peter Hart, G3SJX

For 35 years Peter has been writing amateur radio equipment reviews for the RSGB's journal *RadCom*. These have simply been some of the best equipment reviews published anywhere. These reviews are real world testing of performance and analytical reporting of how amateur radio antennas, radios, amplifiers, etc. really work. *Hart Reviews -The Best of RadCom Equipment Reviews* builds on Peter's first book that covered his first 25 years of his reviews and collects together reviews that have been published in *RadCom* since 2004. From the Acom to Yaesu you find much represented here including Kenwood, Icom, Elecraft and even the mighty Hilberling PT-8000A. SDR radios are not forgotten and you will find Flex, Elad, SoftRock and others included. Antennas and Amplifiers reviews from suppliers as diverse as Butternut, Alphin and Linear Amp also get the same Peter Hart treatment.

Size: 210x297mm, 192 pages,
ISBN: 9781 9101 9306 8
Non Members' Price: £12.99
RSGB Members' Price: £11.04

Antennas Mastered

By Peter Dodd, G3LDO

Peter Dodd, G3LDO has long been acknowledged as one of the leading experts on antennas in the world. For over a decade he has been the regular antenna columnist ofl *RadCom*. This book brings together in a scrapbook format his work from this regular column and a collection of other antenna articles from over the years.

Antennas Mastered is packed with everything imaginable connected with antennas. Readers will find practical solutions that cover all bands, antenna types, ATUs, Meters, Software and much besides. Peter's intention in writing the 'Antennas' column was, as he stated ,"The main purpose of this column is to address problems readers may have installing and adjusting antennas from suburban sites that may be regarded as a challenge; although any antenna subject that is considered to be of interest to readers will be discussed or described". This has held true over the years and readers will be staggered by the breadth of material covered in over 280 A4 pages of antenna gold.

Also contained within the *Antennas Mastered* pages you will find several standalone articles written for *RadCom*.

Size 210x297mm, 288 pages,
ISBN: 9781 9101 9303 7
Non Members' Price: £14.99
RSGB Members' Price: £12.74

Stealth Antennas

By Steve Nichols, G0KYA

The first edition of *Stealth Antennas* quickly became the 'must have' antenna book. This brand new second edition has been expanded and updated and now provides even more.

From using house rain gutters and drain pipes, or a magnetic loop in the loft, through to a tuned loop around the window frame, *Stealth Antennas* provides a wide range of ingenious antenna solutions. Designs include magnetic loops, tuned wire loops, and even reviews of a number of commercially-made stealth antennas. There are two completely new chapters covering Receive Antennas and Top Band Antennas. *Stealth Antennas* does not neglect VHF/UHF antennas. While easier to conceal because of their small size compared with HF antennas, what are the effects of mounting a VHF antenna in the loft? Roof tile absorption is discussed, as are the effects of detuning caused by copper water pipes or house wiring.

Stealth Antennas has dozens of original and ingenious ideas for antennas and should persuade anyone with an amateur radio licence that they can work the world without a beam, tower and linear amplifier.

Size 174x240mm, 224 pages
ISBN: 9781 9101 9305 1
Non Members' Price: £14.99
RSGB Members' Price: £12.74

Radio Society of Great Britain www.rsgbshop.org
3 Abbey Court, Priory Business Park, Bedford, MK44 3WH. Tel: 01234 832 700 Fax: 01234 831 496